NUMERICAL AND EXPERIMENTAL ANALYSIS OF PHOTOVOLTAIC PANEL COOLING

BY

ABDUL SUBHAN

A Thesis Presented to the
DEANSHIP OF GRADUATE STUDIES

KING FAHD UNIVERSITY OF PETROLEUM & MINERALS

DHAHRAN, SAUDI ARABIA

In Partial Fulfillment of the
Requirements for the Degree of

MASTER OF SCIENCE

In

MECHANICAL ENGINEERING

MAY 2012

KING FAHD UNIVERSITY OF PETROLEUM & MINERALS

DHAHRAN- 31261, SAUDI ARABIA

DEANSHIP OF GRADUATE STUDIES

This thesis, written by **ABDUL SUBHAN** under the direction of his thesis advisor and approved by his thesis committee, has been presented and accepted by the Dean of Graduate Studies, in partial fulfillment of the requirements for the degree of **MASTER OF SCIENCE IN MECHANICAL ENGINEERING.**

Dr. Haitham M. S. Bahaidarah
(Advisor)

13/10/2012

Dr. Amro M. Al- Qutub
Department Chairman

10/10/2012

Dr. P. Gandhidasan
(Member)

Dr. Salam A. Zummo
Dean of Graduate Studies

Oct 8th 2012

Dr. Wael H. Ahmed
(Member)

13/10/12

Date

© Abdul Subhan

2012

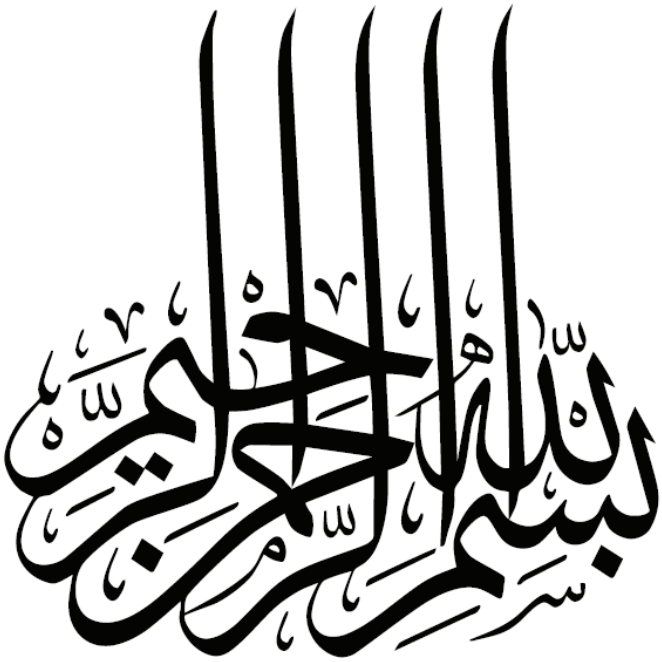

This Work is dedicated

to

My parents, brothers and

sister for their dua, constant support and encouragement

throughout my life

ACKNOWLEDGEMENTS

All praise belongs to Almighty ALLAH (S.W.T.) for bestowing me with health, knowledge and patience to carry out this work and complete my M.S. successfully at King Fahd University of Petroleum and Minerals, Dhahran. I am happy to have had a chance to glorify his name in the sincerest way through this small accomplishment and ask him to accept my efforts.

Acknowledgement is due to King Fahd University of Petroleum and Minerals for providing me financial support and good academic environment during the course of my study. Special thanks is also due to the Center of Excellence for Scientific Research Collaboration with M.I.T and to the Deanship of Scientific Research (DSR) for funding this work.

My deep gratitude and appreciation goes to my thesis advisor Dr. Haitham M. Ba-Haidarah for his constant help, guidance and motivation during the course of my study. His priceless suggestions made this work interesting and challenging for me. I also wish to express my deep appreciation to Dr. Gandhidasan for his constant help, guidance and encouragement during my study. I am greatly indebted to Dr. Gandhidasan for the valuable time he spent throughout my thesis work and also for always being supportive and helping me during difficult times. Sincere thanks to Dr. Wael H. Ahmed for his interest, cooperation and constructive criticism. I would also like to acknowledge all the Mechanical Engineering faculty members with whom I took courses during my M.S. especially Dr.Yilbas and Dr. Zubair who helped me a lot, guided me and encouraged me

during my coursework and related research. Special thanks to Engr. Karam for helping me carry out the experimental work.

Thanks to Mr.Hasan Baig for his constant help and valuable inputs to my work. I am grateful to Mr.Usama Siddiqui for helping me to EES software during my M.S. Thesis. Special thanks to a close friend, Mirza Hamed, whom I always considered my brother, for his moral support and making my stay at KFUPM, memorable.

Thanks are also due to all the graduate students and faculty with whom I interacted during my Masters namely Asif, Awad, Azhar, Ashraf Tashrifullahi, Fasi, Faisal, Jibran, Masood, Omeir Momin, Riaz Ahmed, Eng.Sarfaraz, Syed Zabiullah.

Last but not least, I owe my beloved family an expression of gratitude for their patience, encouragement and moral support which made this work possible and made me achieve this important goal of my life.

TABLE OF CONTENTS

ACKNOWLEDGEMENTS ..... **v**

TABLE OF CONTENTS ..... **vii**

LIST OF TABLES ..... **x**

LIST OF FIGURES ..... **xi**

LIST OF ABBREVIATIONS ..... **xvii**

ABSTRACT (ENGLISH) ..... **xxi**

ABSTRACT (ARABIC) ..... **xxii**

CHAPTER 1 INTRODUCTION **1**

1.1 Research Background 1

1.2 PV Technology 4

1.2.1 Advantages of Photovoltaic Systems 7

1.2.2 Disadvantages of Photovoltaic Systems 8

1.2.3 PV Applications 8

1.2.4 Photovoltaic effect 10

1.3 PV/T Technology 11

1.4 Thesis Objectives 15

1.5 Thesis Outline 16

CHAPTER 2 LITERATURE REVIEW 17

2.1 PV Modeling 17

2.1.1 Electrical Modeling 17

2.2 PV/T Modeling 23

2.2.1 PV/T Modeling (Air cooled) 23

2.2.2 PV/T Modeling (Water cooled) 29

CHAPTER 3 NUMERICAL MODELING 33

3.1 Electrical Modeling 33

3.1.1 NOCT Conditions 39

3.2 Thermal Model 40

3.2.1 PV/T Air Cooled Model 40

3.2.2 PV/T Water Cooled Model 46

CHAPTER 4 EXPERIMENTAL STUDY 51

4.1 Experimental setup 52

4.1.1 PV system 52

4.1.2 Integrated PV and Cooling system 58

CHAPTER 5 RESULTS AND DISCUSSION 66

5.1 PV Module Performance 67

5.2 PV-air and water cooled model 73

5.3 PV water cooling: Experimental results 84

5.4 Validation 89

5.4.1 Air cooled model 89

5.4.2 Water cooled model 94

5.4.3 PV Water Cooling: Numerical Results 100

CHAPTER 6 CONCLUSIONS AND FUTURE WORK 105

6.1 FUTURE WORK 107

REFERENCES 108

VITAE 115

LIST OF TABLES

Table 1: Conditions known at three I-V points on the curve. 36

Table 2: Specifications of the PV module used. 56

Table 3: Accuracy/sensitivity of the instruments used 56

Table 4: Specifications of the PV module used for air and water cooled model 75

Table 5: Specifications of the PV/T collector used for air and water cooled model 76

LIST OF FIGURES

Figure 1.1: World energy demands [2] 2

Figure 1.2: Photovoltaic Panels [6] 5

Figure 1.3: Photo-voltaic effect [6] 5

Figure 1.4: Typical layers of construction of a photovoltaic module 6

Figure 1.5: PV in buildings [7]. 9

Figure 1.6: PV cell, module, array [7] 11

Figure 1.7: PV Panel along with a solar collector [7] 12

Figure 1.8: Module temperature comparison between a bare PV panel and water cooled panel [7] 13

Figure 1.9: Comparison between various PV/T systems. 14

Figure 3.1: Equivalent circuit for an individual PV cell 34

Figure 3.2: I-V and P-V curves for a PV module. 36

Figure 3.3: (a) Cross sectional view of a PV/T air cooled system 41

Figure 3.3: (b) Thermal resistance circuit diagram for a PV/T air cooled system 42

Figure 3.4: (a) Cross sectional view of a PV/T water cooled system 47

Figure 3.4: (b) Thermal resistance circuit diagram for a PV/T water cooled system. 48

Figure 3.4: (c) Schematic view of an integrated Photovoltaic/thermal water collector [51]. 49

Figure 4.1: Experimental test setup showing the testing of PV module. 53

Figure 4.2: Back view of the test setup. 53

Figure 4.3: Sun Saver MPPT controller 55

Figure 4.4: Hygro-Thermo Anemometer 55

Figure 4.5: Pyranometer 57

Figure 4.6: Schematic diagram of the experimental setup. 57

Figure 4.7: PV module integrated with the cooling panel and back insulation 59

Figure 4.8: The back side of the PV panel, before placing the SDM100 solar collector on the panel [63] 59

Figure 4.9: Alignment of the SunDrum collector with the PV panel frame [63] 60

Figure 4.10: SDM100 collector and all four brackets in position, with both insulation panels in place, and clamps and wing nuts installed [63] 60

Figure 4.11: Thermal collector with water inlet/outlet ports [63] 61

Figure 4.12: Front view of the PV(integrated with cooling) test setup 62

Figure 4.13: Side view of the experimental setup 62

Figure 4.14: Back view of the experimental setup showing the cooling panel along with the flow arrangement 63

Figure 4.15: Electrical setup showing the connections to load, MPPT and batteries. 63

Figure 4.16: Sundrum SDM 100 collector used for cooling the panel 64

Figure 4.17: Back view of the hybrid PV with cooling panel. 64

Figure 4.18: Schematic view of the hybrid PV with cooling setup 65

Figure 5.1: Hourly variation of ambient temperature and solar radiation intensity..... 68

Figure 5.2: Hourly variation of measured wind speed, front and back surface temperature of the PV module. 69

Figure 5.3. Hourly variation of measured and computed module back surface temperature. ..... ……..70

Figure 5.4 (a). Hourly variation of measured and computed maximum power point current. 70

Figure 5.4 (b): Hourly variation of measured and computed maximum power point voltage. 71

Figure 5.5: Hourly variation of measured and computed maximum power output..... 72

Figure 5.6: Hourly variation of measured and computed maximum power point efficiency..... 73

Figure 5.7: Comparison of PV cell temperature for air cooling and without cooling 74

Figure 5.8: Comparison of PV cell temperature for water cooling and without cooling……....77

Figure 5.9: Comparison of outlet fluid temperature for air cooling and water cooling... 77

Figure 5.10: Comparison of power output for water cooling and without cooling 78

Figure 5.11: Comparison of power output for air cooling and without cooling..... 79

Figure 5.12: Comparison of power output for air, water cooling and without cooling 80

Figure 5.13: Comparison of electrical efficiency for air, water and without cooling..... 81

Figure 5.14: Variation of power output with irradiance 81

Figure 5.15: Comparison of thermal efficiency for air cooling and water cooling 82

Figure 5.16: Comparison of thermal gain for air cooling and water cooling 83

Figure 5.17: Measured thermal efficiency data for an air cooled PV model and a straight line fit to the collected data. 83

Figure 5.18: Measured thermal efficiency data for a water cooled PV model and a straight line fit to the collected data. 84

Figure 5.19: Hourly variation of irradiance and ambient temperature during the test day (02-02-2012). ..... …..85

Figure 5.20: Hourly variation of module temperatures (front and back) and wind speed during the test day (02-02-2012)……..... 85

Figure 5.21: Comparison of energy collection as a function of irradiance for PV system and hybrid system …….. 87

Figure 5.22: Module temperature as a function of solar irradiance……...87

Figure 5.23: Variation of outlet water temperature throughout the day at different flow rates. 88

Figure 5.24: The Effect of mass flow rate on water temperature rise at different levels of irradiance …..... 89

Figure 5.25: Hourly variations of irradiance, ambient and inlet air temperature during the test day [41]..... 90

Figure 5.26: Experimental Validation of hourly variation of power output with PV air cooled model. 91

Figure 5.27: Experimental Validation of hourly variation of cell temperature with PV air cooled model. 92

Figure 5.28: Experimental Validation of hourly variation of back surface temperature with PV air cooled model. 92

Figure 5.29: Experimental Validation of hourly variation of outlet air temperature with PV air cooled model..... 93

Figure 5.30: Experimental Validation of hourly variation of maximum power point efficiency with PV air cooled model. 93

Figure 5.31: Hourly variation of irradiance and ambient temperature during the test day (08-02-12)... 95

Figure 5.32: Hourly variation of module temperatures (front and back) and wind speed during the test day (08-02-12)..... 95

Figure 5.33: Comparison of numerical and experimental data for module surface temperature with water cooling.. 96

Figure 5.34: Comparison of numerical and experimental data for back surface temperature with water cooling.. 97

Figure 5.35: Comparison of numerical and experimental data for water outlet temperature. 98

Figure 5.36: Comparison of numerical and experimental data for thermal gain with water cooling..... 98

Figure 5.37: Comparison of numerical and experimental data for maximum power output with water cooling..... 99

Figure 5.38: Comparison of numerical and experimental data of maximum power point efficiency..... 100

Figure 5.39: Comparison of cell temperature throughout the day with cooling and without cooling..... 101

Figure 5.40: Comparison of module back surface temperature throughout the day with cooling and without cooling..... 102

Figure 5.41: Comparison of maximum power output of the module throughout the day with cooling and without cooling.. 103

Figure 5.42: Comparison of maximum power point efficiency throughout the day with cooling and without cooling..... 104

LIST OF ABBREVIATIONS

A	area (m^2)
a	ideality factor
C_p	specific heat capacity of air (kJ/kg-K)
D	diameter of the tube (m)
e	root mean square percent deviation
f	Darcy friction factor
F	standard fin efficiency
F_R	Collector heat removal factor
F'	Collector efficiency factor
G	Incident radiation (W/m^2)
G_T	Total incident radiation on a tilted surface (W/m^2)
h	Heat transfer coefficient (W/m^2K)
hp_1	penalty factor due to the presence of solar cell material, glass and EVA
hp_2	penalty factor due to the interface between tedlar and working fluid
I	circuit current (A)
$I–V$	current–voltage
k	Stefan-Boltzmann's constant (W/m^2K^4)
K	thermal conductivity (W/m K)
$K_{\tau\alpha}$	incidence angle modifier
L	dimensions of solar module, duct length, the length of PV/T air collector, thickness (m)
M	air mass modifier

N	number of cells in series
Nus	Nusselt number
$\dot{m}$	mass flow rate (kg/s)
n	number of experiments
P	power (W)
Pr	Prandtl number
PV	photovoltaic
q	elementary charge
Q	heat transfer rate (W)
R_b	geometric factor
R	Resistance
Re	Reynolds number
RMS	Root mean square percentage deviation (%)`
r	correlation coefficient
S	solar absorbed flux (W)
T	temperature (K)
U_L	an overall heat loss coefficient from the PV/T air collector to the environment ($W/m^2 K$)
U_t	an overall heat transfer coefficient from solar cell to ambient through glass cover ($W/m^2 K$)
U_T	an overall heat transfer coefficient from solar cell to flowing air through tedlar ($W/m^2 K$)
U_{tT}	an overall heat transfer coefficient from glass to tedlar

	through solar cell (W/m^2 K)
U_{tf}	an overall heat transfer coefficient from glass to air through solar cell and tedlar (W/m^2 K)
V	circuit voltage (V)
v	wind speed (m/s)
W	Width of the collector(m)
X	experimental or simulated value of parameter

Greek Symbols

α	absorptivity, current temperature coefficient ($mA/^oC$)
$(\tau\alpha)_{eff}$	product of effective transmittivity and absorptivity
β	slope
η	efficiency (%)
ε	emissivity, semiconductor band gap energy (eV)
μ	viscosity at average fluid temperature (Pa-s)
μ_w	viscosity at back surface temperature (Pa-s)

Subscripts

a,amb	ambient
a,NOCT	ambient at NOCT
b	beam component
bs	back surface
c,cell	solar cell
conv	convection
el	electrical

exp	experimental
f	fluid flow
g	glass
in	inlet
m	module
mp	maximum power point
out	outlet
rad	radiative
ref	reference
sh	shunt
sky	sky
t	top
T	Tedlar
th	thermal
u	useful
w	wind

ABSTRACT

Full Name	:	ABDUL SUBHAN
Thesis Title	:	NUMERICAL AND EXPERIMENTAL ANALYSIS OF PHOTOVOLTAIC PANEL COOLING
Major Field	:	MECHANICAL ENGINEERING
Date of Degree	:	May 2012

Solar energy is one of the most promising energy sources in the world. The amount of sun's radiation reaching the earth's surface can be utilized for producing power. The conversion of solar energy to electrical energy is attainable by the utilization of Photovoltaic (PV) technology. This technology has been used for many years and has proved to be successful for power generation but faces challenges in adaptation to the local environment predominantly due to changes in climatic conditions such as high ambient temperature. From previous studies it has been established that conversion efficiency, which translates to power output of the PV system, falls rapidly as the module temperature increases. Therefore, in order to achieve increased power output, the PV modules are combined with a heat extraction mechanism to cool them effectively. In this thesis, an electrical and thermal model for an air cooled as well as water cooled PV module is developed to predict the performance of the PV/T system. Furthermore, an experimental work is carried out to study the effect of reducing the cell temperature of the PV panel using water cooling technique.

ملخص الرسالة

الاسم ال : عبدالسبحان

عنوان الرسالة : تحليل عددى و تجريبى لألواح الخلايا الضوئية المبردة

التخصص : الهندسة الميكانيكية

تاريخ الدرجة العلمية : مايو٢١٠٢

تعتبر الطاقة الشمسية واحدة من أهم الطاقات الواعدة فى العالم حيث أن كمية الإشعاع الشمسى الذى يصل إلى سطح الأرض يمكن أن يستعمل لإنتاج القدرة. تحويل الطاقة الشمسية الى طاقة كهربائية يمكن أن يتم بإستخدام تقنية الخلايا الضوئية. هذه التقنية تم إستخدامها لسنوات عديدة .حيث أثبتت قدرتها على توليد الطاقة الكهربائية لكنها واجهت عدة تحديات فى التكيف مع البيئة المحلية السائدة وذلك بسبب ظروف التغيير المناخى مثل إرتفاع درجة الحرارة المحيطة. من الدراسات السابقة تم اثبات أن تحويل الكفاءة والذى يحول القدرة الخارجة من نظام الخلايا الضوئية ينخفض بدرجة كبيرة مع إرتفاع درجة الحرارة لذا من أجل تحقيق زيادة فى القدرة الخارجة فإن وحدات الخلايا الضوئية تدمج مع منظومة إستخلاص حرارى لتبريدها بكفاءة. فى هذه الرسالة تم تطوير نموذج كهربائى وحرارى بتبريد هوائى وتبريد مائى لوحدات الخلايا الضوئية لتوقع اداء نظام الخلايا الضوئية - الحرارية . إضافة إلى ذلك أجريت تجارب عملية لدراسة تأثير تخفيض درجة حرارة وحدة الخلية الضوئية بإستعمال تقنية تبريد مائى

CHAPTER 1

INTRODUCTION

1.1 Research Background

Energy is currently an important issue all over the world. The demand for fossil fuel has grown steadily due to increased industrial activities in developing and developed countries. It is estimated that the world energy demand will increase by 45% between 2010 and 2030 [1], and the rate of increase will be 1.6% per year as shown in Fig 1.1. The figure shows the estimated world primary energy demand from 1971 to 2030. In general, fossil fuels such as oil, coal and natural gas can be considered as primary sources of energy, especially, oil which is the most dominant fuel in the world. The increase of the energy demand may be met by utilizing fossil fuel resources but the amount of greenhouse gas emissions in the atmosphere will reach a dangerous level. Enormous usage results in exhaustion of these resources and presents a significant danger to the surroundings, mostly through global warming [2]. The fact that oil is running out fast should be kept in mind and different alternatives should be adopted.

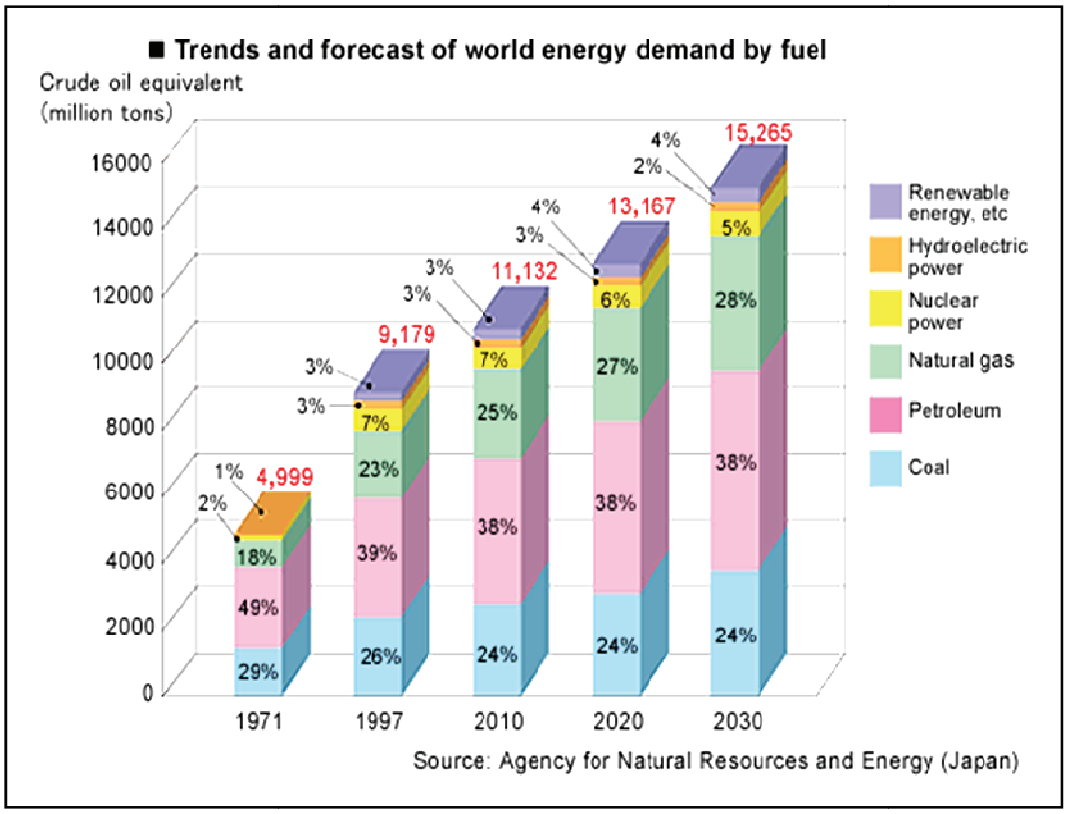

Figure 1.1: World energy demands [1]

Renewable energy includes wind power, solar energy, hydropower, geothermal energy and bio-fuel, are suggested to provide a solution to resolve the global warming problem and alleviate the potential of energy crisis. The demand of fossil fuels will be reduced when renewable energies become popular in the energy market. Furthermore, potential climate change will be mitigated when the renewable energies replace fossil fuels in the future. Solar energy is one of the most promising energy sources with respect to the amount of solar radiation reaching the earth's surface. The fossil fuels we use as the main source of energy needs are rapidly running out and there is a continuous surge to develop or use other sources of energy. Renewable Energy is proving to be the answer for

tomorrow's stable supply of energy. Solar and Wind energy are being considered the biggest sources of renewable energy.

Solar energy is utilized for producing power in two basic methods one by the employment of Photovoltaic (PV) technology and the other by the use of solar/thermal technologies. The use of PV cells to produce electricity has increased in the last few decades and keeps growing as their manufacturing cost decreases and as the world becomes more concerned about energy use. These facilities were basically targeted in remote locations initially, because they do not have access to electrical utility grids. However with time these technologies are being implemented among the local communities where they are connected to the electrical grids to feed in tariff [2].

More than half of the known oil reserves in the world are present in the middle east. The Kingdom of Saudi Arabia is a large country with an area of 2.3 million km^2. The electricity consumption has greatly increased in the Kingdom of Saudi Arabia, about 75% over the past decade. Occupying four-fifths of the Arabian Peninsula, Saudi Arabia is the second largest country in the Middle East. Saudi Arabia is the world's 19th greatest electricity consuming nation and accounts for slightly less than 1% of the world annual electricity generation [3]. The use of PV technology in the Kingdom is about to see its future in the coming years more particularly because the country receives very high solar radiation throughout the year. The use of PV technology is likely to face few challenges in its adaptation to the local environment predominantly because of high ambient temperature and dust.

The power output from the photovoltaic cell depends on the intensity of the sunlight, the cell temperature, the panel's orientation, and its size, among others. The intensity of light affects primarily the amount of current produced, making it proportional, while the cell temperature controls the voltage produced. As the cell temperature increases, the current produced remains the same but the voltage is reduced since the band gap reduces, reducing the output power. Therefore, the power generated in summer does not necessarily increase even if the irradiance increases. Since the conversion efficiency of a PV is not absolutely high, the decrease of the conversion efficiency caused by PV temperature rise cannot be disregarded [4]. Due to the adverse climatic conditions in Saudi Arabia, the PV technology is likely to face the problem of rising cell temperature and hence a study needs to be performed to analyze this problem and come out with effective solutions.

1.2 PV Technology

To convert this available solar energy into electrical energy, photovoltaic (PV) systems are used. Photovoltaic panels (Fig. 1.2) use the photovoltaic effect (Fig. 1.3) in order to directly obtain the above conversion. Typical layers of PV module are shown in Fig. 1.4. PV systems are popularly configured as stand-alone, grid-connected and hybrid systems. The performance of the PV system depends upon several factors, especially the weather conditions such as solar radiation, ambient temperature and wind speed. 'Photovoltaic' mainly means electricity from the energy of sunlight. First used in about 1890, the word has two parts: photo, derived from the Greek 'phos' meaning light, and volt, a unit of

measurement named for Alessandro Volta (1745-1827), a pioneer in the study of electricity [5].

Figure 1.2: Photovoltaic Panels [6]

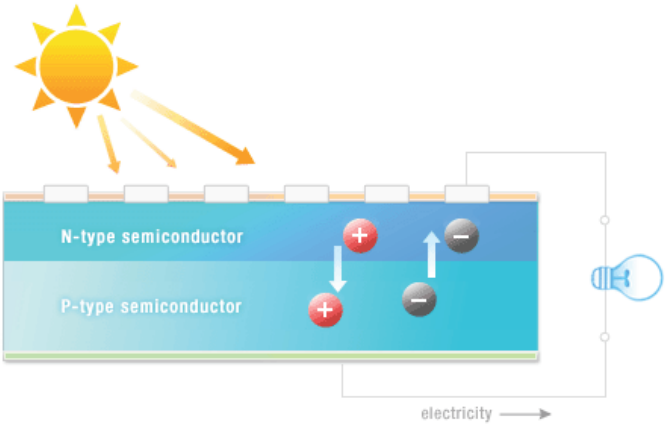

Figure 1.3: Photo-voltaic effect [6]

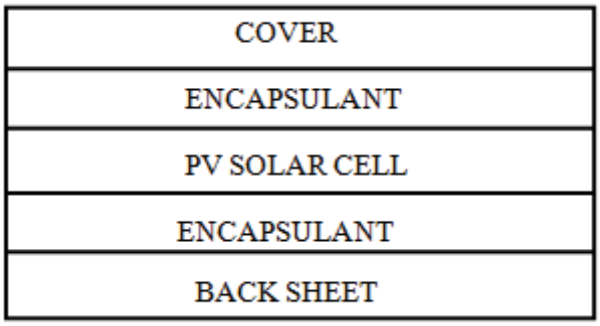

Figure 1.4: Typical layers of construction of a photovoltaic module.

PV systems have a significant advantage over other technologies. Firstly, they can be installed on roofs and can be an integral part of a building. Secondly, even ground-mounted PV collectors are efficient from the perspective of land use. Flat-plate PV technology is the most economical means to produce electricity. Thirdly, adequate sunlight is present in predictable amounts almost everywhere. From environmental viewpoint, PV is the clear choice as it provides sustainable energy, operates silently, produces no toxic emissions or greenhouse gases, and causes no hazardous waste. PV systems generate electricity using the Sun's free energy and moreover, they do not have any rotating components which are prone to wear out with time, hence, low maintenance cost. Photovoltaic production is doubling every 2 years, increasing by an average of 48 percent each year since 2002, making it the world's fastest-growing energy technology. Roughly 90% of this generating capacity consists of grid-tied electrical systems. But the drawback of PV system is its costs. This is because high production cost of silicon from its raw form, silica [7]. Effective ways to reduce the system cost are being studied and analyzed in the research field. There are mainly four general types of PV cells namely, mono-crystalline silicon, poly-crystalline silicon, ribbon silicon and amorphous silicon.

The mentioned advantages and disadvantages of the PV systems are discussed in detail below.

1.2.1 Advantages of Photovoltaic Systems

PV systems offer substantial advantages over standard power sources:

- Reliable: Even in tough conditions, photovoltaic systems have proven their consistency.
- Durable: Many modules available today show no degradation after many years of usage. It is likely that future modules will produce power for 25 years or more.
- Low maintenance cost: Since PV systems require only periodic inspection and occasional maintenance, maintenance costs are usually less than those with conventionally fueled systems.
- No fuel cost: No fuel source is required hence, there is no cost associated with purchasing, storing, or transporting fuel.
- Reduced Sound Pollution: Photovoltaic systems operate silently and with minimal movement.
- Photovoltaic Modularity: PV systems are more cost effective than bulky conventional systems. In order to increase the available power, modules are combined to form arrays.
- Safety: PV systems are very safe when properly designed and installed systems do not require the usage of combustible fuels.

1.2.2 Disadvantages of Photovoltaic systems

PV systems have some disadvantages when compared to conventional power systems:

- Primary Cost: Since the cost of conventional fuel sources increases, the primary cost of PV systems decreases [7].
- Inconsistency of available solar irradiance: Variations in climate conditions require changes in system design. Climatic conditions can affect the power output of any solar-based energy system.
- Energy Storage: PV systems utilize batteries for storing energy, thereby increasing the size, cost, and complexity of a system.
- Improvements in efficiency: A cost-effective use of PV requires a high-efficiency approach to energy consumption.

1.2.3 PV Applications

The electricity from PV systems can be used for a wide range of applications such as:

- PV in power stations: Many solar photovoltaic power stations have been built, mainly in Europe. Most of these plants are integrated to national grids as a supplementary power source.

- PV in satellites: PV has traditionally been used for auxiliary power in space. The International space station uses multiple solar arrays to power all the equipment on board.

- PV in buildings: Building integrated photovoltaic's (BIPV) are increasingly incorporated into new domestic and industrial buildings as a principle or ancillary source of electric power, and are one of the fastest growing segments of the photovoltaic industry. (Fig. 1.5)

Figure 1.5: PV in buildings. [7]

- PV in standalone and grid connected systems: PV has been used for many years to power calculators and novelty devices. In particular, it is used in parking meters, emergency telephones and temporary traffic signs.

- PV in agriculture: PV systems are used effectively worldwide to pump water for livestock, plants or humans. Water pumping appears to be most suitable for solar PV applications as water demand increases during dry days when plenty of sunshine is available.

1.2.4 Photovoltaic effect

Photovoltaic effect refers to a physical phenomenon where the energy carried by electromagnetic radiation is converted into electrical energy. The devices used for carrying out such conversion are known as solar PV cells.

Sunlight consists of photons which are packets of solar energy which contain different amounts of energy that correspond to the different wavelengths of the solar spectrum. The absorbed photons produce electricity when they strike a PV cell.

Certain special electrical characteristics of the PV cell (a built-in electric field) provide the necessary voltage required to pass the current through an external load. The output of these cells is limited by several factors. There is a minimum energy level of photons that can cause the creation of a hole-electron pair. For silicon, the maximum wavelength is 1.15 μm. Radiation at higher wavelengths does not produce hole-electron pairs but heats the cell. Each photon causes the creation of single hole-electron pair, and the energy of photons in excess of which is required to create these pairs is also converted to heat.

Solar cell technology is evolving rapidly, in developing new and more efficient cells and in reducing the cost of manufacture. There are many variations in cell material, design, and methods of manufacture. Amorphous or polycrystalline silicon (Si), cadmium sulfide (CdS), gallium arsenide (GaAs), and other semiconductors are used for cells. Cells are combined to produce modules which in turn combined to produce arrays (Fig. 1.6) are connected in series and parallel to provide convenient currents and voltages.

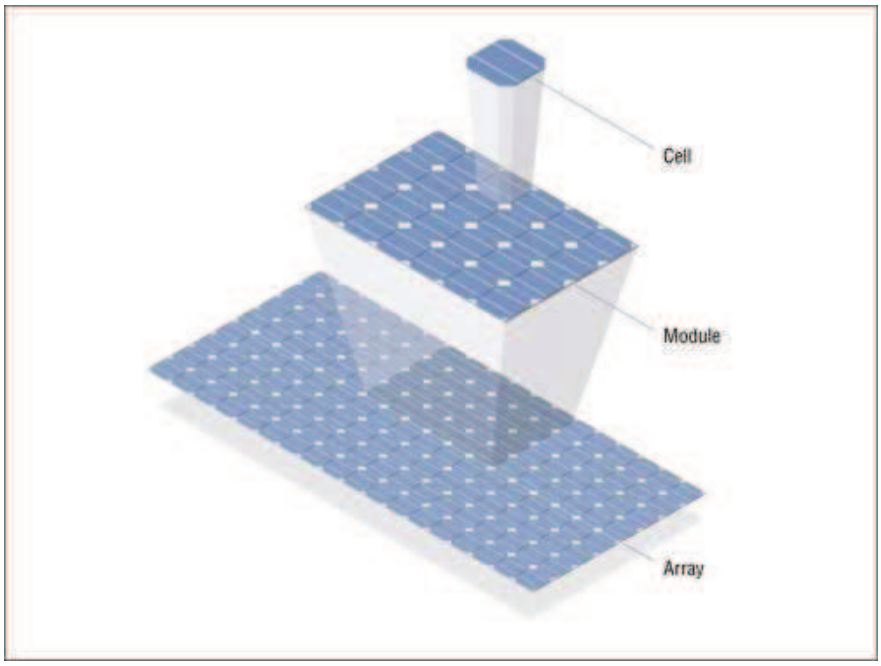

Figure 1.6: PV cell, module, array [7]

1.3 PV/ T Technology

A PV thermal (PV/T) collector is a module in which the PV not only produces electricity but also serves as a thermal absorber. A hybrid PV panel is shown in Fig 1.7. The removal of the heat from the back of the PV modules also enhances the electrical operating efficiency of the panel. In this way, power and heat are produced simultaneously. The cooling medium can be water or air thereby cooling the panel and making it efficient. The most widely used fluid is water and the heat collection systems are flat-plate collectors and solar cells for electrical and thermal applications respectively. When the module temperature is increased, the efficiency drops. This can typically result in an efficiency drop off of 0.5% per °C increase in the cell operating temperature [7]. The operating temperature increases since a large part of the solar radiation is not

converted to electricity but is absorbed by the panel as heat. The easiest way to remove the heat from the panel is using natural circulation of air which consequently increases its efficiency. Another efficient way is to use water as the coolant of the panel. These systems are popularly known as hybrid photovoltaic-thermal system. In these systems, the natural or forced circulation of a heat removing fluid can be used for both PV cooling and heat generation. This heat can be reutilized for hot water applications in residential buildings. Fig. 1.8 shows the module temperature comparison between a conventional panel and water cooled panel.

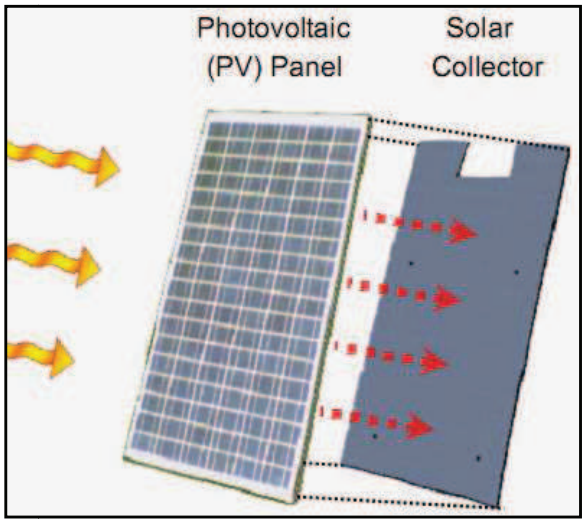

Figure 1.7: PV Panel along with a solar collector [7]

Solar thermal technology is now a mature technology. Widespread utilization of solar thermal technology can reduce a significant portion of the conventional energy. Internationally the market for solar technology has expanded significantly during the last decade. Though the initial investment for these technologies is high compared to

available conventional alternatives, the return on investment has become increasingly attractive with the increase in prices of conventional energy.

There are several reasons which motivate the development of the PV/T system (Fig. 1.9). One of the main reasons is that it can provide higher efficiency than the individual PV and thermal collector system. With increased the efficiency, the payback period of the system can also be shortened.

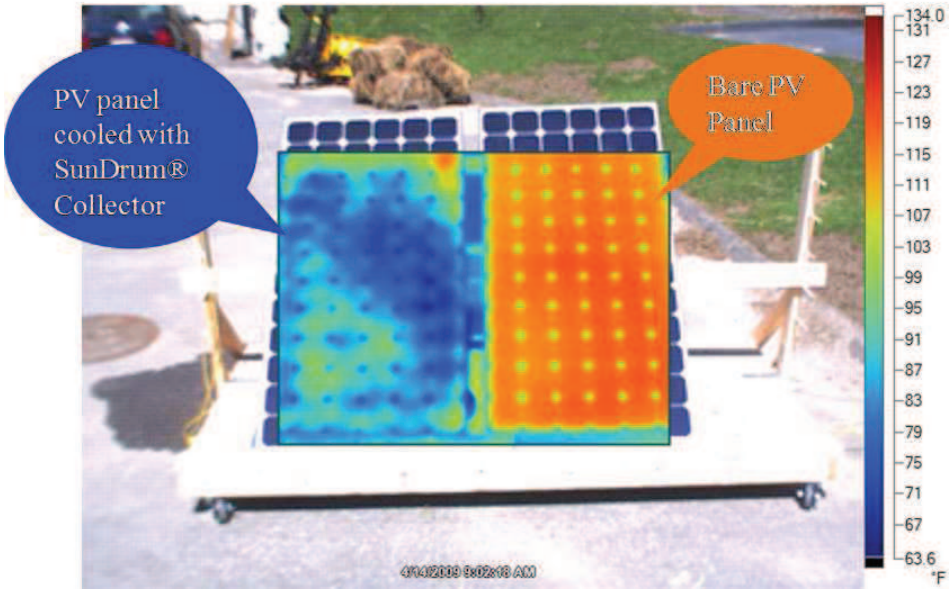

Figure 1.8: Module temperature comparison between a bare PV panel and water cooled panel [7]

The main features of the PV/T system [7] are as follows:

- ❖ It is bi-functional system which can produce both electricity and heat output;
- ❖ It is economical and flexible: the combined efficiency is always higher than using two independent systems and is especially attractive in building integrated photovoltaic when roof spacing is limited;
- ❖ The heat output generated can be used for both heating and cooling applications depending on the season.
- ❖ It can be easily be integrated to building without any major modification making it practically feasible technology

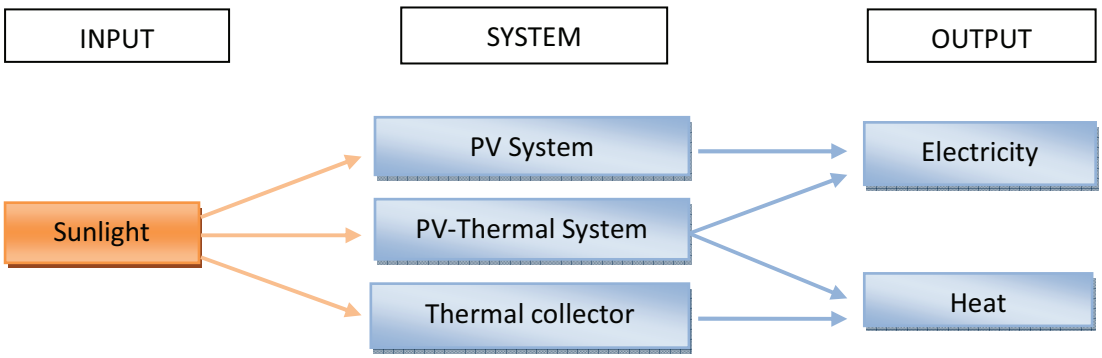

Figure 1.9: Comparison between various PV/T systems.

1.4 Thesis Objectives

The objectives of this thesis work are summarized below:

1. Firstly, to develop an electrical model for PV modules which can predict the performance parameters including cell temperature, maximum power point current and voltage, module efficiency using EES software and validate with the experimental tests conducted for the climate of Dhahran.

2. Secondly, to develop a thermal model for PV/T air and water cooled panel to predict the thermal parameters including back surface temperature, solar cell temperature, thermal energy absorbed and thermal efficiency using EES software and validate their results as well.

3. Finally, an experimental investigation will be made to analyze the effect of reducing the cell temperature (by water cooling the panel) on power output and a comparison of the output of the module without and with cooling would be made. The mechanism of cooling is done by incorporating a heat exchanger behind the PV module and circulating water to achieve the thermal energy gain from the module.

1.5 Thesis Outline

Chapter 1 introduces the subject of PV technology followed by the research objectives of this study.

Chapter 2 reviews the literature related to PV electrical and thermal modeling. The first part reviews different numerical models for estimating the electrical parameters of PV modules. The second part presents the review of thermal modeling and experimental studies (both air and water cooled) of PV modules.

In Chapter 3, the numerical modeling of the PV and PV/T systems is discussed. The modeling involves 3 parts. The first part is the electrical model which predicts the module parameters with climatic data and the data supplied by the manufacturer. The second part involves the modeling of a PV-air cooled model, which predicts the thermal parameters and the last part describes the modeling of PV-water cooled model.

Chapter 4 describes the experimental study carried out for studying the heat transfer characteristics of the PV panel. This chapter has two sections, the first part deals with the experimental evaluation of the conventional PV module. The second part deals with the integrated PV module with the water cooling system.

Chapter 5 is the results and discussion part which presents all the results obtained from this work. In Chapter 6, the conclusions of this study are presented. The directions in which this study can be extended in future are also discussed.

CHAPTER 2

LITERATURE REVIEW

The literature presented in this chapter is divided into two sections. The first section presents the research work done for PV modeling alone. In the second section, the research work accomplished for PV/T (air and water cooling) is presented. The last section of this chapter presents summary of literature review.

2.1 PV Modeling

In the past two decades, extensive research has been done on the parameters which relate to PV electrical modeling. A significant amount of theoretical as well as experimental studies on PV systems have been carried out to optimize their use in the past years.

2.1.1 Electrical Modeling

Brano et al. [8] presented an improved 5 parameter model for PV modules which describes the current-voltage (I-V) characteristics for each condition of solar irradiance and operating temperature. The application of this method allowed an accurate estimation of output current of the PV panel. The consistency of the model was validated by comparing with the results obtained using models given by other authors.

Ahmad et al. [9] introduced a theoretical analysis of the performance of PV modules under different design parameters and meteorological conditions. They used FORTRAN and TRNSYS program to evaluate various parameters of PV modules. The developed program was capable of predicting the temperature, I-V and power-voltage (P-V) curves, and other output parameters of PV modules at different conditions.

Ikegami et al. [10] presented a method to estimate the parameters of the electrical circuit a PV module and for optimal operation of the PV system a quantitative diagnostic method is introduced. The parameters were calculated using a least-square fitting technique on the I-V curve. A new maximum power point tracking (MPPT) method using the model parameters, insolation and cell temperature was shown. The proposed MPPT method using equivalent parameters was verified to show better performance than other methods in the simulation.

Kurnik et al. [11] have performed outdoor testing of PV module performance under different mounting and operational conditions. They examined open rack mounted and unventilated roof integrated cases of PV module installation theoretically and experimentally. In the light of energy balance model, the impact of the PV module conversion efficiency on the module temperature was also shown. The results demonstrated that the module's relative temperature difference was almost equal to the conversion efficiency, regardless of the given irradiance, wind speed and mounting conditions.

Carr and Pryor [12] compared the performance of five different PV module types in temperate climate of Perth, Western Australia. I-V characteristics and maximum power at standard test conditions were measured for each module at regular intervals. The energy production in real operating conditions has been measured for each module. These values were compared to the manufacturers' values, and monitored over time for the modules in the field.

Wang et al. [13] have developed a method to estimate high accuracy MPPT for PV arrays. The proposed method involves simple approach that takes the resistance effect of the solar cells into consideration. The performance of the proposed method is evaluated by examining the characteristics of maximum power point of PV arrays depending on both cell temperature and irradiation intensity. From the experimental results, they concluded that change in temperature mainly affects the PV output voltage while changes in irradiation influence the output current.

Alonso and Balenzategui [14] estimated the performance of PV module throughout the year based on Nominal Operating Cell Temperature (NOCT) condition. The objectives of the study were to verify the feasibility of the procedure with varying module designs to determine the NOCT in a country such as Spain and to apply the NOCT values for yearly analysis of temperature and energy yields. These standards were applied to various module configurations such as glass-glass, thin film technologies etc. NOCT values are obtained based on the fact that difference between the ambient and the module temperature is independent of ambient temperature and linearly proportional to irradiance

above 400 W/m^2. They have given an expression to estimate yearly module temperature from ambient temperature, solar irradiance and NOCT values.

Gxasheka et al. [15] evaluated the performance parameters of five PV modules. They investigated the effect of temperature and irradiance on the performance parameters and found the dependence of efficiency on irradiance yields useful information about performance at different irradiance levels and possible effects such as presence of shunt paths in the module cells. They also mentioned that some modules experienced moisture ingress due to poor encapsulation which affected the module performance.

Villalva et al. [16] presented a comprehensive approach to model and simulate the performance of PV arrays. The objective was to find the parameters of the nonlinear I-V equation by adjusting the curve at three points: open circuit, maximum power point (MPP) and short circuit conditions. This method finds the best equation for the single diode model including the effect of series and parallel resistances. They presented two circuit models that can be used to simulate PV arrays with circuit simulators. The model is validated with experimental data of commercial PV arrays.

Houssamo et al. [17] developed a mathematical model aimed at identifying the model parameters of one diode PV model extended to an array. The model was based on the equivalent circuit of a PV cell. Utilizing the data sheet values and the least square fitting approaches the error between the calculated and measured current of the PV array was minimized. They concluded that the method based on the data-sheet values was more appropriate to identify the PV array model parameters.

De Soto et al. [18] evaluated the PV array performance model obtained using the values of short circuit current (I_{sc}), the open circuit voltage (V_{oc}) and the maximum power point voltage (V_{mp}) and current (I_{mp}) at standard rated conditions The resistances R_s and R_{sh} were considered constant, and light generated current (I_L) was assumed to be linearly proportional to the solar irradiance.

Ishaque and Salam [19] proposed an improved modeling method to determine the parameters of photovoltaic (PV) modules using differential evolution (DE) method. The approach used in this technique enables the estimation of model parameters at any value of solar radiation and ambient temperature using the information provided by the manufacturer's datasheet. The performance of the model is evaluated against the popular single diode model with series resistance R_s. It is found that the proposed model gives better results for any irradiance and temperature variations. The modeling method is useful for PV simulator developers who require complete and precise model for the PV system.

Feng and Liang [20] presented an integrated PV model that describes both thermal dynamics and electricity characteristics of a commercial PV module. The cell temperatures and output electricity characteristics of a commercial PV module are calculated through a series of experiments at real time operating conditions.

Zagrouba et al. [21] presented a numerical technique based on genetic algorithms to identify the electrical parameters of PV solar cells and modules. These parameters were used to determine the corresponding maximum power point (MPP) from the current–

voltage (I–V) characteristic. In comparison with other methods, present technique was found to be very efficient to evaluate the electrical parameters of PV solar cells and modules. The identified parameters are then utilized to extract the maximum power working points for both cell and module.

Firtha et al. [22] presented a model of PV system performance and its use in fault detection from a monitoring study of the performance of a sample of UK domestic PV systems. Five-minute average climatic and performance data was recorded for 27 PV systems at two sites for up to 2 years of operation. New analysis techniques were developed to identify the faults which occur during operation and quantify the energy losses due to these faults. The techniques illustrated four categories of faults. The benefits of applying the data analysis techniques described in this work to PV system clusters and other urban micro-generation technologies were discussed.

Huld et al. [23] proposed a performance rating model for crystalline silicon PV modules. The model represented the output power of the module as a function of module temperature and solar irradiance, with a number of coefficients to be determined by fitting to measured performance data from indoor or outdoor measurements.

Chena et al. [24] evaluated the performance of MPPT devices in PV systems with storage batteries. In order to assess the MPPT device benefits under different climate, the theoretical models have been constructed. By simulation, a comparison between two types of PV charge controllers (with and without MPPT device) under different

atmospheric conditions was presented. The results showed that the MPPT device increased the output in winter season for the climate of Beijing to a great extent.

Skoplaki and Palyvos [25] discussed the importance of solar cell/module operating temperature for the electrical performance of silicon based photovoltaic installations. Suitable tabulations were given for most of the explicit and implicit correlations found in the literature which associate the operating temperature with standard weather variables and system-dependent properties.

2.2 PV/T Modeling

2.2.1 PV/T Modeling (Air cooled)

Extensive research has been done focusing on the parameters which relate to the cell efficiency.

The electrical module efficiency is studied by Tonui and Tripanagnostopoulos [26] and they found that the electrical module efficiency of the crystal silicon prototype with natural air flow was 12%. Brinkworth and Sandberg [27] found out that the conversion efficiency of cell degrades by 0.4-0.5% per degree rise in temperature. Kumar and Rosen [28] presented a detail review on the photovoltaic-thermal solar collectors for air heating. These air heaters find application in preheating the air for many applications such as space heating and drying purposes. From the study it has been concluded that the PV/T collectors produce more energy per unit collector area than the separate PV and thermal systems. Zogou and Stapountzis [29] investigated the flow and heat transfer inside a

PV/T air collector which cools the PV panel by circulating air at the backside of it. The cooling effect of the air increased the conversion efficiency of the panel and the heated air is used for HVAC heating system. A CFD model is also developed to predict the heat transfer coefficients more accurately and also to gain a better understanding of the flow and turbulence inside the air duct under different modes of operation.

Amori and Taqi [30] analysed the thermal and electrical performance of a typical hybrid PV/T air collector for the climatic conditions of Iraq. An improved themal-electrical model is derived to evaluate the performance of the system. The developed model is verified with experimental results as well. The electrical, thermal and overall efficiencies were found to be 12.3%, 19.4% and 53.6% respectively for the winter day and while for the summer day were 9%, 2.8%, 47.8%.

Hegazy [31] and Sopian et al. [32], in studying the performance of PV/T air heaters observed that increase in mass flow rate reduces PV cell temperature and consequently raises the electrical and thermal efficiencies. Zondag et al. [33] performed a study on the electrical and thermal yield of a PV/T collector. In this study four mathematical models have been developed for simulating the thermal yield of a combined PV/T collector. It has been mentioned that combi-panels provide improvement in performance of the system. It also changes the basic characteristics of both PV and thermal collector. The electrical yield of the PV cells is influenced by the collector inflow temperature and the thermal yield is varied by increased heat transfer resistance between the absorber and the fluid. . The efficiency of the combi-panel is measured and compared with that of conventional sheet ad tube thermal collector. In order to study the heat flow through the

panel four models, a 3D dynamic model and three steady state models have been developed. From the results obtained it was concluded that the steady 1D model was the optimum model which performed satisfactorily. This model was hence used for calculation of annual yield of combi-panel design.

Chow [34] presented an explicit dynamic model for operation of PV/T collector. The model was developed based on the control-volume finite difference approach. The proposed model can provide a detailed analysis of the transient energy flow through different types of collector components and the instantaneous energy output can also be monitored. Aste et al. [35] presented the performance of a PV/T air collector. Numerical and experimental results related to the performance of the air collector were presented. The developed simulation model was capable of predicting various thermal and electrical performance parameters. The model was also generalized for testing in any set of design parameters for evaluating the performance of PV/T air collector. Jong and Zondag [36] have conducted a series of comparison between different types of PV/T design and different types of thermal systems. They investigated the covered and uncovered PV/T and thermal system with and without heat pump. The studies indicated that an uncovered PV/T shows improved efficiency for the case which the PV/T is utilized for low-temperature ground storage integrated with a heat pump. However, the net electrical efficiency of the system turns into negative because of the energy consumption of the heat pumps. Both experimental and numerical studies were conducted by Tiwari and Sodha [37] to evaluate the overall performance of PV/T air collector. In this study, different kind of configurations of PVT air collector (like unglazed, glazed, with and

without tedlar) were used to investigate the electrical and thermal performance. It was shown that the glazed PV/T air collector provides the best performance.

A PV/T-air collector was investigated by Garg and Adhikari [38] using a computer simulation model. It was concluded that the thermal efficiency of the absorber without solar cell is higher than that when the absorber is covered with the solar cell. This is because that some of the incidence irradiance is converted into electrical energy.

Dubey et al [39] reported the efficiency of different configurations of PVT-air collector (Case A-Glass to glass PV module with duct, Case B-Glass to glass PV module without duct). The highest efficiency was shown by case A among the all cases. The annual average efficiency of case A and B was 10.41% and 9.75%, respectively. Tonui and Tripanagnostopoulos [40] reported an improvement of heat extraction achieved by modifying the channels of PV/T air system in low cost. Three different configurations of air ducts (simple air channel, thin aluminum sheet and rectangular fin) were investigated by experiment and numerical simulation. Some parameters (channel length, channel depth and mass flow rate) were used to study the effect on electrical and thermal efficiency. From the result of experiment and simulation, a good agreement has been presented and air duct with fins were shown more effective in enhancing the heat transfer from the wall of the channels to air flow.

Joshi et al [41] carried out an evaluation of a hybrid photovoltaic thermal system. Two types of PV module (glass to tedlar and glass to glass) were utilized to investigate the performance under the climate of New Delhi. Parametric studies also indicated that

thermal efficiency decreases with the increase of length of the duct. The highest thermal efficiency obtained from the experiment was 46.28%. Thermal efficiency also increases with air velocity. However, as the air velocity exceeds a certain level, thermal efficiency remains at a constant level. This could be explained as the time of contact of air with module reduces and therefore decreases the heat removal from the back of PV module.

Tripanagnostopoulos et al [42] presented a hybrid PV/T experimental model to investigate the temperature effect on PV electrical efficiency. A booster diffuse reflector was also utilized to enhance the electrical and thermal performance of the system. It was found that PV electrical efficiency decreases at the rate of 0.1%/^{o}C However, with the diffuse reflector, the electrical efficiency decreased at the rate of 0.0957%/ ^{o} C and 0.0814%/ ^{o} C for concentration factor at 1.3 and 1.5 respectively. In this study, a comparison between air cooled and water cooled PV/T was presented. The PV module with thermal insulation leads to high temperature and incurs an electrical efficiency drop ($\eta_{el/insul}$=0.113), and water cooled PV and air cooled PV with $\eta_{el/water}$=0.128, $\eta_{el/air}$=0.126, respectively.

Tripanagnostopoulos [43] also showed that the electrical efficiency of PV module increases by 2% with using the diffuse reflector and without incurring significant penalty in temperature rise. The decreasing rate of temperature effect in electrical efficiency was also found to be 0.1%/^{0}C. Sarhaddi et al [44] evaluated the performance of solar PV/T air collector. They further developed an expression for overall energy efficiency. The effect of climatic, design and operating parameters on overall energy efficiency is analyzed.

The parameters studied upon are solar cell temperature, back surface and outlet air temperature, open circuit voltage and short circuit current, maximum power point current and voltage etc. The predicted results are verified through Joshi et al. [41]. The overall energy efficiency reduced when inlet air temperature, wind speed, duct length is increased. Upon increasing the solar intensity, the overall energy efficiency and electrical efficiency of the air collector increases initially and then decreases after attaining maximum point of solar intensity.

Alonso and Balenzategui [45] estimated the performance of PV module along the year based on NOCT calculations. The objectives of the study were (1) To verify the feasibility of the procedure with varying module designs to determine the NOCT in a country such as Spain. (2) To apply the NOCT values for yearly analysis of temperature and energy yields. These standards were applied to various module configurations such as glass- glass, thin film technologies etc. They also gave an expression to estimate yearly module temperature from ambient temperature, solar irradiance and NOCT values.

Armstrong and Hurley [46] proposed a thermal model for photovoltaic panels under various atmospheric conditions. The present model provides a means of predicting the thermal time constant of a PV panel. This can be achieved by considering the thermal properties of the panels in terms of their electrical equivalents by means of an R-C circuit and investigating the heat transfer from the surface of the panel under varying wind conditions. The model has been validated by experimental measurements. The model incorporates atmospheric conditions, the material composition and the mounting structure of the PV panel.

A hybrid photovoltaic/thermal (PV/T) solar system was experimentally investigated by Teo et al. [47] In order to cool the cells effectively, a parallel array of ducts with inlet/outlet manifold designed for uniform airflow distribution was attached to the back of the PV panel. The module was operated under active cooling condition and the module temperature dropped significantly leading to an increase in efficiency of solar cells to between 12% and 14%.

2.2.2 PV/T Modeling (Water cooled)

Tiwari et al. [48] developed an analytical expression for water temperature of a combined PV/T water heater under constant flow rate of water based on energy balance of the components of the collector system. Exergy analysis of the system has also been carried out. Further analysis of hot water withdrawal at constant collection temperature resulted in an increase in the thermal efficiency with decrease in the collection temperature and increase in flow rate. An optimum flow rate of 0.006 kg/sec which yields maximum thermal efficiency and overall exergy is established.

Chow et al. [49] studied the suitability of using a glass cover on a thermosyphon-based with glazed or unglazed PV/T system based on numerical data and validated the same with experimental results.. A glazed PV/T system was found suitable if the quantity of the overall energy output was to be maximized. From studies they found that the unglazed system gave better results for cell efficiency, packing factor, water mass to collector area ratio. A study by Kaora and Yutaka [50] on performance evaluation of PV

system equipped with a cooling device utilizing siphonage shows that PV energy production increases when the cooling start temperature is kept at a predetermined value. The modules are cooled with cooling water flowing through a narrow gap in a cooling panel, and hot water discharged from the cooling panel can be reused. The reuse of hot water from cooling systems contributes very much to reducing energy consumption of hot-water-supply system.

Tiwari and Sodha [51] developed a thermal model of integrated PV/T system. They also validated their results through another model developed by Huang et al. [52]. Further the expression for the instantaneous thermal efficiency was compared with the well known Hottel-Whiller's characteristic equation for flat plate collector and the difference being the presence of penalty factors introduced They observed an increase in water temperature of about 17ºC with respect to an ambient temperature in the evening. The hourly variation of the fluid temperature with different module lengths, film heat transfer coefficients and mass flow rate was shown. The study indicates that the overall thermal efficiency increased from 24% to 58% due to additional thermal energy due to the water flow.

The thermal modeling of a combined system of PV/T solar water heater is developed by Dubey and Tiwari [53]. This model has been considered and tested for climate of New Delhi. In this paper, a mathematical expression for combined PV/T flat plate collector has been developed and also validated for different configurations. The performance of water heating system has also been studied. The instantaneous thermal efficiency for different cases is studied by covering the absorber by PV module fully and partially. It is

concluded that the present system is self sufficient one and can be installed at remote areas for fulfillment of hot water requirements and electrical energy saved can hence be utilized for other purposes. To improve the PV performance, much research effort has been done on development of hybrid PV/T collector technology using water as a coolant.

Krauter [54] investigated a method of reducing reflection which also provided cooling replacing the front glass surface with a thin (1mm) film of water flowing over the face of the panel. He notes that the refractive index (1.3) of water is superior to that of glass. Reflective losses in glass can lead to losses in yield of 8-15%. The water decreased cell temperatures up to 22^0C. The improved optics and cell temperatures increased electrical yield 10.3% over the day (8-9% after accounting for pumping energy). He also noted an unexpected aesthetic benefit.

Saad and Masud [55] et al. provided an effective way to improving the PV module efficiency using water cooling using long term performance tests. The experimental results indicated that due to the heat loss by convection between water and the PV panel's upper surface, an increase of about 15% in system output is achieved at peak radiation conditions. Kordzadeh [56] studied the effects of nominal power of array and system head on operation of PV system by cooling the PV cells with a thin film of water. The method was based on supplying water for cooling cells by the pump itself. From the results it was concluded that the electrical power output increased noticeably and increasing the system head produced a significant improvement in the array efficiency.

Abdolzadeh and Ameri [57] improved the operation of a PV water pumping system by spraying water over the front of photovoltaic cells as a result of decreasing cell temperature and cell's reflection. The results were compared with traditional systems and the results showed that the cell power increased due to the spraying of water as the modules worked closely at the temperature of maximum power generation.

Rosa et al [58] studied the behavior of PV panel submerged in water and observed a considerable amount of increase in electrical power output. They conducted the tests for 4 months on 3 identical panels. An average increase of 11% in the electrical efficiency was observed. Hosseini et al [59] conducted an experimental study to compare the performance of a PV system combined with a cooling system consisting of a thin film of water running on the top surface of the panel with an additional system to use the hot (or warm) water produced by the system. The results indicated that the combined system yielded higher power output and electrical efficiency and lower module temperature and reflection losses when compared to the conventional PV system.

CHAPTER 3

NUMERICAL MODELING

3.1 Electrical Modeling

The work done here has been focused on modeling and analyzing modern photovoltaic module. Water cooled panels can provide higher efficiencies than conventional ones. The study initially involves the electrical modeling of the PV module. To describe a PV module as a power source, it is necessary to determine the main parameters that assist in studying its performance. The present five parameter model estimates the main electrical parameters such as short circuit current, open circuit voltage, maximum power output and electrical efficiency. A PV module is a non linear device and can be represented by its I-V characteristic curve. There are many mathematical models which describe I-V curve. One of them is the famous five parameter photovoltaic model proposed in [18]. Fig. 3.1 represents the equivalent circuit for an individual PV cell.

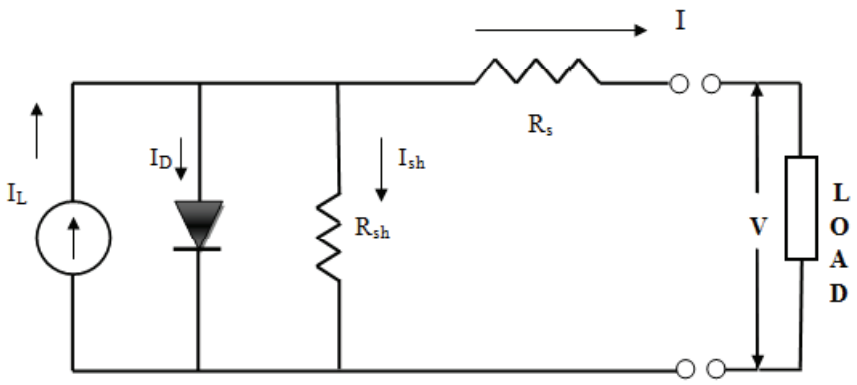

Figure 3.1: Equivalent circuit for an individual PV cell

At a fixed temperature and solar radiation, the I-V characteristic of this model is given by,

$$I = I_L - I_o\left[\exp\left(\frac{V + IR_s}{a}\right) - 1\right] - \frac{V + IR_s}{R_{sh}} \qquad (3.1.1)$$

Where, I and V represent the current and voltage respectively at the load condition. The circuit requires that five parameters be known and they are: light generated current (I_L), diode reverse saturation current (I_0), series resistance (R_s), shunt resistance (R_{sh}), ideality factor (a). The five parameters in the model are obtained using I-V characteristics of a module at reference condition supplied by the manufacturer and other known PV characteristics. Measurements of PV electrical characteristics are made at standard reference condition: incident radiation of 1000 W/m^2, a cell temperature of 25^0 C, and a spectral distribution corresponding to an air mass of 1.5. Since the five parameters are to be determined, five different conditions need to be known. The methodology adopted here is to know three I-V points on the I-V curve (i.e. short circuit current, open circuit

voltage and maximum power point) as shown in Fig. 3.2. The information needed is defined in Table 1 [61].

At short circuit conditions, the current is $I_{sc,ref}$ and the voltage is zero

$$I_{sc,ref} = I_{L,ref} - I_{o,ref}\left[\exp\left(\frac{I_{sc,ref}R_{s,ref}}{a_{ref}}\right)-1\right]-\frac{I_{sc,ref}R_{s,ref}}{R_{sh,ref}} \tag{3.1.2}$$

At open-circuit conditions the current is zero and the voltage is V_{oc} so that

$$I_{L,ref} = I_{o,ref}\left[\exp\left(\frac{V_{oc,ref}}{a_{ref}}\right)-1\right]+\frac{V_{oc,ref}}{R_{sh,ref}} \tag{3.1.3}$$

The measured I-V pair at maximum- power conditions can be substituted into Eq. (3.1.1), resulting in

$$I_{mp,ref} = I_{L,ref} - I_{o,ref}\left[\exp\left(\frac{V_{mp,ref}+I_{mp,ref}R_{s,ref}}{a_{ref}}\right)-1\right]-\left[\frac{V_{mp,ref}+I_{mp,ref}R_{s,ref}}{R_{sh,ref}}\right] \tag{3.1.4}$$

At short circuit conditions the derivative of current with respect to voltage is given by,

$$\left[dI/dV\right]_{sc} = -\frac{1}{R_{sh,ref}} \tag{3.1.5}$$

At maximum power point conditions the derivative of power with respect to voltage is zero.

$$\frac{I_{mp,ref}}{V_{mp,ref}} = \frac{\left(\frac{I_{o,ref}}{a_{ref}}\right)exp\left(\frac{V_{mp,ref}+I_{mp,ref}R_{s,ref}}{a_{ref}}\right)+\frac{1}{R_{sh,ref}}}{1+\left(\frac{I_{o,ref}R_{s,ref}}{a_{ref}}\right)exp\left(\frac{V_{mp,ref}+I_{mp,ref}R_{s,ref}}{a_{ref}}\right)+\left(\frac{R_{s,ref}}{R_{sh,ref}}\right)} \tag{3.1.6}$$

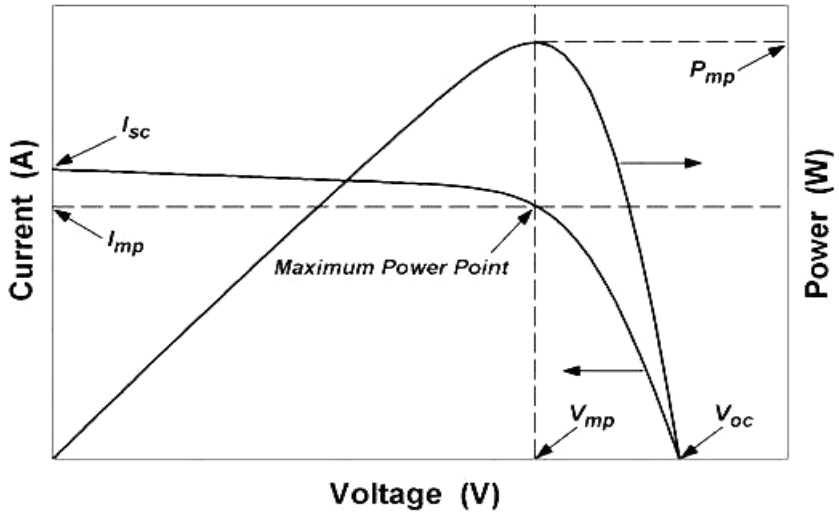

Figure 3.2: I-V and P-V curves for a PV module

Firstly solving these simultaneous equations from (3.1.2) to (3.1.6) gives the value of five parameters (a_{ref}, $I_{L,ref}$, $I_{o,ref}$, $R_{s,ref}$ and $R_{sh,ref}$), at the reference conditions. The ideality factor which is assumed to be dependent on the cell temperature is related to reference condition by,

$$\frac{a}{a_{ref}} = \frac{T_c}{T_{c,ref}} \tag{3.1.7}$$

Table 1: Conditions known at three I-V points on the curve.

Conditions	Parameters
At short circuit current	$I = I_{sc,ref}, V = 0$
At open circuit voltage	$I = 0, V = V_{oc,ref}$
At short circuit condition	$[dI/dV]_{sc} = -1/R_{sh,ref}$
At the maximum power point	$I = I_{mp,ref}, V = V_{mp,ref}$
At the maximum power point	$[d(IV)/dV]_{mp} = 0$

The light current for any operating conditions is related to its reference conditions by,

$$I_L = \frac{S}{S_{ref}}[I_{L,ref} + \mu_{I_{sc}}(T_c - T_{c,ref})] \tag{3.1.8}$$

Where $\frac{S}{S_{ref}}$ is the ratio of absorbed radiation S to the absorbed radiation at reference condition S_{ref}, given by,

$$\frac{S}{S_{ref}} = M\left(\frac{G_b}{G_{ref}} R_b K_{\tau\alpha,b} + \frac{G_d}{G_{ref}} K_{\tau\alpha,d}\left(\frac{1+\cos\beta}{2}\right) + \frac{G}{G_{ref}} \rho_g K_{\tau\alpha,g}\left(\frac{1-\cos\beta}{2}\right)\right) \tag{3.1.9}$$

The diode reverse saturation current is related to reference conditions by,

$$I_0 = I_{oref}\left(\frac{T_c}{T_{c,ref}}\right)^3 \exp\left(\frac{\varepsilon}{kT_{c,ref}} - \frac{\varepsilon}{kT_c}\right) \tag{3.1.10}$$

The following relationship is used to relate the shunt resistance (R_{sh}), (which is assumed to be finite and independent of temperature but varies with the absorbed radiation) at reference conditions to that at operating conditions:

$$\frac{R_{sh}}{R_{sh,ref}} = \frac{S_{ref}}{S} \tag{3.1.11}$$

The model is now complete. These equations are a set of nonlinear equations that cannot be solved unless good initial guesses and variable limits are used. The following guess values are used for determining the parameters.

$$a_{ref,guess} = 1.5KT_{c,ref}N / q \tag{3.1.12}$$

$$I_{o,ref,guess} = I_{sc,ref} \exp(-V_{oc,ref} / a_{ref,guess}) \tag{3.1.13}$$

$$I_{L,ref,guess} = I_{sc,ref} \tag{3.1.14}$$

The series resistance is assumed to be independent of both temperature and solar radiation so that,

$$R_s = R_{s,ref} \tag{3.1.15}$$

Once the values of reference parameters are obtained, Equations (3.1.7-3.1.15) are used to find the parameters at any operating condition. In order to estimate the maximum power point (MPP) from the model, the following equations are used.

$$\frac{I_{mp}}{V_{mp}} = \left[\frac{\frac{I_o}{a} \exp\left(\frac{V_{mp} + I_{mp} R_s}{a} \right) + \frac{1}{R_{sh}}}{1 + \frac{R_s}{R_{sh}} + \frac{I_o R_s}{a} \exp\left(\frac{V_{mp} + I_{mp} R_s}{a} \right)} \right] \tag{3.1.16}$$

The general I-V equation at the MPP must also be satisfied:

$$I_{mp} = I_L - I_o \left[\exp\left(\frac{V_{mp} + I_{mp} R_s}{a} \right) - 1 \right] - \left[\frac{V_{mp} + I_{mp} R_s}{R_{sh}} \right] \tag{3.1.17}$$

The simultaneous solution of the equations (3.1.16 and 3.1.17) yields the MPP current and voltage, further, the maximum power output can be obtained as.

$$P_{mp} = I_{mp} V_{mp} \tag{3.1.18}$$

In estimating the PV module performance, the temperature dependance of the maximum power point efficiency (η_{mp}) is an important parameter and is given by,

$$\eta_{mp} = \frac{I_{mp} V_{mp}}{G_T A_m} \tag{3.1.19}$$

The back surface temperature of the module is calculated using the relation [60];

$$T_{bs} = G_T \left[\exp(x + yv)\right] + T_a \tag{3.1.20}$$

Where x and y are empirically determined coefficients which depend on the type of mounting.

For rack mounted modules the values of x and y are taken as -3.47 and -0.0594 respectively.

3.1.1 NOCT Conditions

The module efficiency will vary from zero to the maximum module efficiency depending on how close to the maximum power point the module is operating. NOCT is defined as the cell or module temperature that is reached when the cells are mounted in a normal way at a incident solar radiation level of 800 W/m^2, a wind speed of 1m/s, an ambient temperature of 20^{o}C and no-load operation (that is, with η_c=0).

The cell temperature at any ambient temperature for a PV module is found from

$$\frac{T_C - T_a}{T_{NOCT} - T_{a,NOCT}} = \frac{G_T}{G_{NOCT}} \frac{U_{L,NOCT}}{U_L} \left(1 - \frac{\eta_c}{(\tau\alpha)}\right) \tag{3.1.21}$$

The ($\tau\alpha$) in the last term of Eq.17 is estimated to be 0.9. An approximation of the ratio $\frac{U_{L,NOCT}}{U_L}$ is given by $\frac{9.5}{(5.7 + 3.8v)}$

3.2 Thermal Model

3.2.1 PV/T Air Cooled Model

One way of cooling the photovoltaic unit is by using air. The heat absorbed by the air could be used for providing warm air inside the residential building.

Figure 3.3(a) shows the cross sectional view of PV system along with the associated air flow for a PV/T system. The system includes a transparent cover i.e. glass followed by the solar cells, tedlar and a well insulated rear plate. The latter has a gap between the tedlar for air to pass through the channel. The heat is transferred from the back surface of the PV module to the flowing air.

The governing equations of the PV/T air collector are formed by writing the energy balance equation for each component of a PV/T air collector (i.e, module, back surface, air flowing below tedlar) gives the thermal parameters and thermal efficiency of a PV/T air collector [44].

An expression for a solar-cell temperature in terms of back surface temperature of the PV module and climatic parameters can be written as:

$$T_{cell} = \frac{(\alpha\tau)_{eff} G + U_T T_{amb} + U_T T_{bs}}{U_t + U_T} \tag{3.1.22}$$

Fig 3.3 (b) shows the equivalent thermal resistance diagram for an air cooled system. The resistances include convective and radiative resistance from the glass to the ambient, conductive resistance of the glass and tedlar, convective resistance of the fluid (air) flowing inside the duct. The absorbed radiation gets converted to electricity through the

cell and gets cooled by the air flowing beneath the cell through an air channel which gives hot air as the heat output which can be utilized for domestic space heating applications.

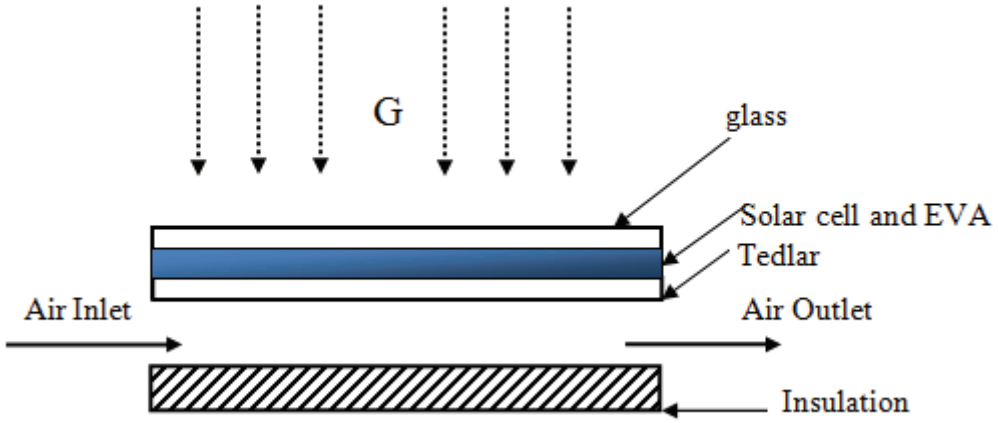

(a)

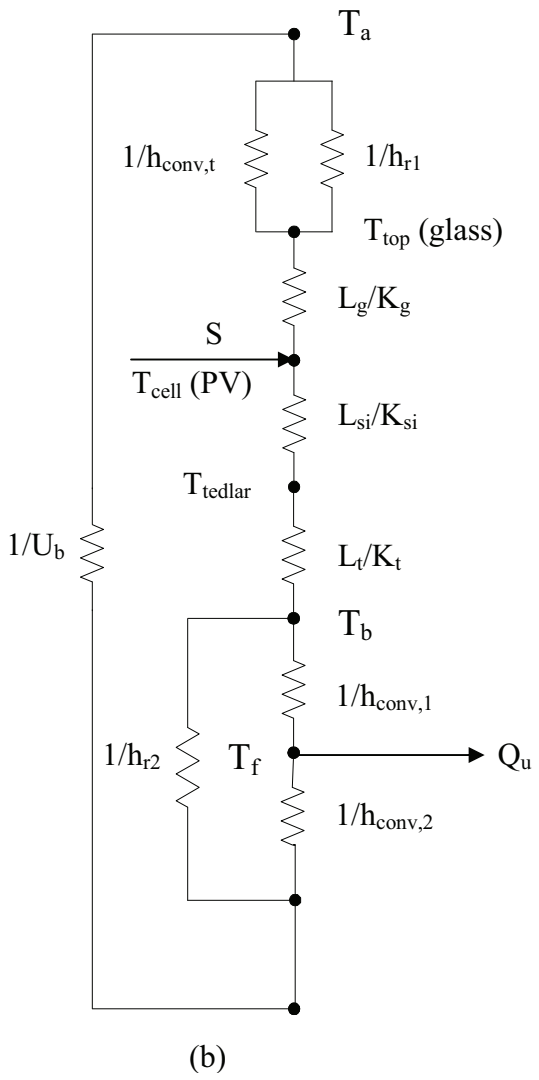

Figure 3.3: (a) Cross sectional view of a PV/T air cooled system, (b) Thermal resistance circuit diagram for a PV/T air cooled system.

The back surface temperature of a PV module is given by

$$T_{bs} = \frac{h_{p1}(\alpha\tau)_{eff} G + U_T T_{amb} + h_f T_f}{U_{tT} + h_f} \tag{3.1.23}$$

The outlet air temperature of the flowing air below the tedlar of a PV module is given by

$$T_{f,out} = \left(T_{amb} + \frac{h_{p1} h_{p2} (\alpha\tau)_{eff} G}{U_L} \right) \left(1 - \exp\left(\frac{-WU_L L}{mC_p} \right) \right) + T_{f,in} \exp\left(\frac{-WU_L L}{mC_p} \right) \quad (3.1.24)$$

The average air temperature of the flowing air is obtained as:

$$\bar{T}_f = \left(T_{amb} + \frac{h_{p1} h_{p2} (\alpha\tau)_{eff} G}{U_L} \right) \left[1 - \left(1 - \exp\left(\frac{-WU_L L}{mC_p} \right) \right) \Big/ \left(\frac{WU_L L}{mC_p} \right) \right] + T_{f,in} \left(1 - \exp\left(\frac{-WU_L L}{mC_p} \right) \right) \Big/ \left(\frac{WU_L L}{mC_p} \right) \quad (3.1.25)$$

From knowing an average air temperature of the flowing air below the tedlar from the above equation, the back surface temperature of a PV module can be obtained from Eq. (3.1.23). Once the back surface temperature of a PV module is known, the solar-cell temperature can be evaluated from Eq. (3.1.22) for given climatic parameters of a solar intensity and an ambient air temperature. Various performance parameters which can be calculated are as follows:

The rate of useful thermal energy obtained from the PV/T air collector is obtained as

$$Q_u = mC_p (T_{f,out} - T_{f,in}) \quad (3.1.26)$$

The thermal efficiency of the PV/T air collector is given by,

$$\eta_{th} = \frac{Q_u}{WLG} \quad (3.1.27)$$

The heat transfer coefficients mentioned in the above equations are defined as follows:

$$(\alpha\tau)_{eff} = \tau_g \left[\alpha_c \beta_c + \alpha_T (1 - \beta_c) - \beta_c \eta_{el} \right] \quad (3.1.28)$$

$$h_{p1} = U_T \big/ \left(U_T + U_t\right) \tag{3.1.29}$$

$$h_{p2} = h_f \big/ \left(U_{tT} + h_f\right) \tag{3.1.30}$$

$$U_{tf} = \left[1/h_f + 1/U_{tT}\right]^{-1} \tag{3.1.31}$$

Where h_{p1} and h_{p2} are the penalty factors due to the glass and tedlar of a PV module respectively.

The improvements made in the heat loss coefficients in predicting the thermal parameters are given as follows:

- The conductive resistance term L_{si}/K_{si} has been added to conductive heat transfer coefficient from cell to flowing air through tedlar (U_T).

$$U_T = \left[\frac{L_{si}}{K_{si}} + \frac{L_T}{K_T}\right]^{-1} \tag{3.1.32}$$

- The radiation heat transfer coefficient term (h_{rad}) is added to the overall heat transfer coefficient from cell to atmosphere through glass (U_t). The convective heat transfer coefficient on the top surface of air collector ($h_{conv,t}$) is given by Eqn. (3.1.34)

$$U_t = \left[\frac{L_g}{K_g} + \frac{1}{h_{conv,t}} + \frac{1}{h_{rad}}\right]^{-1} \tag{3.1.33}$$

$$h_{conv,t} = 2.8 + 3v \tag{3.1.34}$$

$$h_{rad} = \varepsilon_g \sigma \left(T_{sky} + T_{cell} \right) \left(T_{sky}^2 + T_{cell}^2 \right) \tag{3.1.35}$$

Where v is wind speed on the top surface of PV/T air collector. The effective temperature of the sky (T_{sky}) is calculated from the following empirical relation [41]

$$T_{sky} = T_{amb} - 6 \tag{3.1.36}$$

- In the estimation of overall back loss coefficient from flowing air to ambient (U_{bs}), the convective heat transfer coefficient on the back surface of PV/T air collector ($h_{conv,bs}$) has been calculated from Eq. (3.1.34)
- In the previous studies [41], the convective heat transfer coefficient inside the air duct (h_f) has been assumed as a constant factor. However, in this research h_f is calculated according to flow regime and its Nusselt number.
- In the previous studies [41], overall heat transfer coefficient from PV/T air collector to surrounding (U_L) has been assumed as a constant factor, whereas it is not constant. However, in this research this coefficient is considered as a variable. U_L includes all of conduction, convection and radiation losses from the PV/T air collector to the atmosphere. The flow correlation is given by Eq. 3.1.40.

$$U_L = U_{bs} + U_{tf} \tag{3.1.37}$$

The heat transfer correlation used for air is given by [62];

$$Nus = 0.0204 * \mathrm{Re}_{tube}^{4/5} \tag{3.1.38}$$

The average heat transfer coefficient is given by the relation;

$$h_f = \frac{Nus.K}{D_h}\left(\mathrm{Air},\ \ \mathrm{T} = T_f\right) \tag{3.1.39}$$

Since the presence of the electrical efficiency of PV module (η_{el}) in Eq. (3.1.28), the thermal analysis of PV/T air collector and its electrical analysis are dependent.

3.2.2 PV/T Water Cooled Model

This type of system which utilizes fluid as a coolant is known as hybrid system which transforms the sun's radiation to electrical energy and simultaneously absorbs heat from the panel. In this way, the panel is working in lower temperatures (higher efficiency), and the thermal energy gained can be utilized for domestic applications.

Fig. 3.4(a) shows the PV configuration along with the associated water flow for a PV/T system. The system includes a transparent cover i.e. glass followed by the solar cells, tedlar and a well insulated rear plate. The latter has a gap between the tedlar for water to pass through the channel. The heat is transferred from the back surface of the PV module to the flowing water. Fig. 3.4(b) shows the equivalent thermal resistance circuit diagram for the PV/T water cooled system. Fig. 3.4(c) shows the PV configuration along with the associated water flow for a PV/T system.

The governing equations of the water cooled model are defined as follows:

Writing the energy balance equation for each component of a PV/T water collector (i.e, module, back surface, water flowing below tedlar) gives the thermal parameters and thermal efficiency of a PV/T air collector as follows:

Equations 3.1.22 and 3.1.23 are used to estimate the cell temperature and back surface temperature. The outlet fluid temperature is calculated using the equation below [51]:

$$T_{f,out} = \left(T_{amb} + \frac{h_{p1} h_{p2} (\alpha\tau)_{eff} G}{U_L} \right) \left(1 - \exp\left(\frac{-F'WU_L L}{\dot{m} C_p} \right) \right) + T_{f,in} \exp\left(\frac{-F'WU_L L}{\dot{m} C_p} \right) \quad (3.1.40)$$

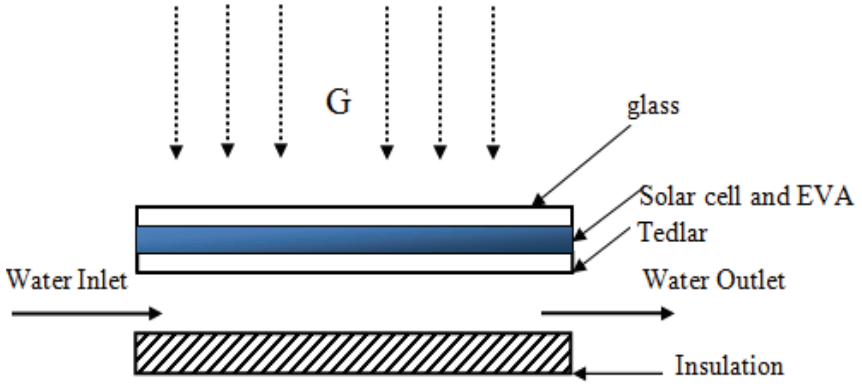

(a)

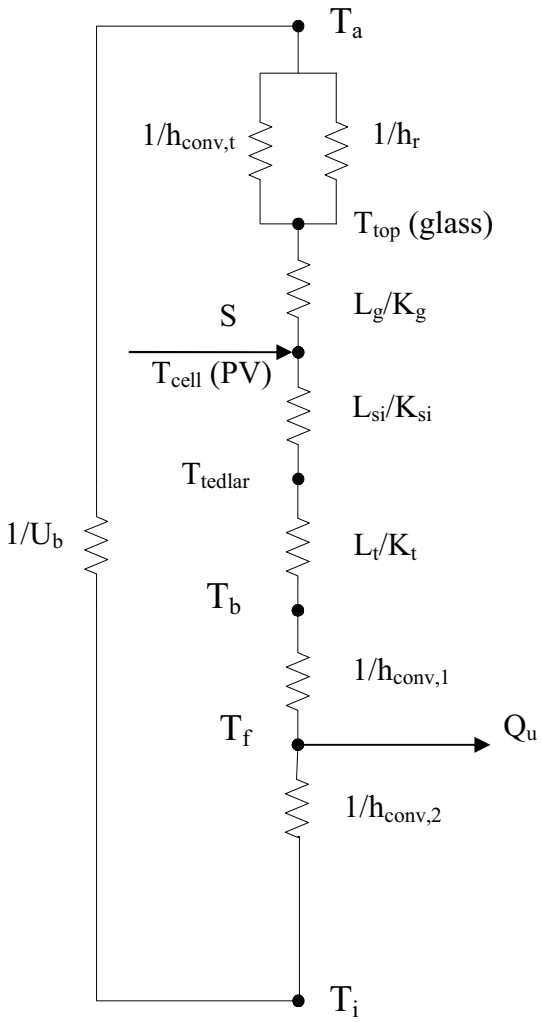

(b)

Figure 3.4 (a) Cross-sectional view of PV /T water cooled system, (b) Thermal resistance circuit diagram for a PV/T water cooled system.

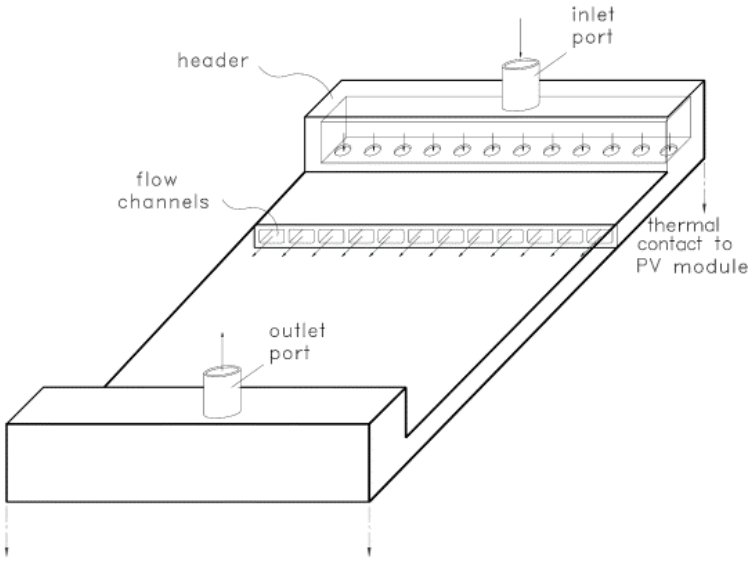

Figure 3.4(c): Schematic view of an integrated photovoltaic /thermal water collector [51].

The heat transfer correlation used for water cooled model is given below [61]

$$Nus = \frac{\left(f_{darcy}/8\right)\cdot\left(Re_{tube}-1000\right)\cdot Pr}{1.07+12.7\cdot\left(f_{darcy}/8\right)^{0.5}\cdot\left(Pr^{2/3}-1\right)}\cdot\left(\frac{\mu}{\mu_w}\right)^{0.11} \tag{3.1.41}$$

The darcy friction factor is given by the following equation

$$f_{darcy} = \left(0.79\cdot ln\left(Re_{tube}\right)-1.64\right)^{-2} \tag{3.1.42}$$

Following Duffie and Beckman [61] neglecting the bond conductance, the collector efficiency factor (F') is given by:

$$F' = \frac{1}{\frac{WU_L}{\pi D_h}+\frac{W}{D+\left(W-D\right)F}} \tag{3.1.43}$$

Where, the standard fin efficiency (F) is given by

$$F = \frac{\tanh\left[\frac{m(W-D)}{2}\right]}{\left[\frac{m(W-D)}{2}\right]} \tag{3.1.44}$$

The rate of useful thermal energy obtained from the PV/T water collector is obtained as

$$Q_u = F_R\left[h_{p1}h_{p2}(\alpha\tau)_{eff}\,G - U_L(T_{wi} - T_{amb})\right] \tag{3.1.45}$$

Where, the collector heat removal factor (F_R) is given by:

$$F_R = \frac{\dot{m}C_{pw}}{A_c U_L}\left[1 - \exp\left(-\frac{A_c U_L F'}{\dot{m}C_{pw}}\right)\right] \tag{3.1.46}$$

The instantaneous thermal efficiency is given by:

$$\eta_{th} = \frac{Q_u}{A_c G_T} \tag{3.1.47}$$

The thermal model incorporates the effect of cooling and results in better performance of the hybrid system. This model is coupled to the electrical model (mentioned in the section 3.1) since the electrical efficiency is utilized in predicting various thermal parameters in the study. The results with air and water cooling are discussed in the chapter 6.

CHAPTER 4

EXPERIMENTAL STUDY

Various experimental procedures have been reported in the previous literature with the aim of finding out the most efficient and cost effective technique in improving the PV module performance. Many such techniques such as front panel cooling, back panel cooling using air/water as the cooling medium have been adopted. Long term monitoring tests have also been carried out in order to have a better understanding of this hybrid system.

In this chapter an experimental evaluation of PV module performance with and without cooling is carried out to study the heat transfer characteristics of the PV/T system. The study involved two phases. In the first phase, the PV module was tested alone and its performance was monitored for a period of 1 month. The performance data was then compared with the results of numerical model mentioned in the previous chapter and results with good agreement were obtained. In the second phase of the study, the PV module is integrated with the cooling panel (heat exchanger) with water as the cooling medium and the behavior of various electrical and thermal parameters is studied.

4.1 Experimental Setup

This section discusses the details of the experimental setup and procedures adopted for the recording the measurements.

4.1.1 PV system

Figure 4.1 shows the experimental test setup with different components to study the PV module performance. Fig. 4.2 shows the back view of the test setup with the thermocouples attached on the backside of the panel. The details of various components used in this setup are given below:

- PV module: The module used in this study is a 230W rated power (72 cell, mono-crystalline silicon type) panel which is commercially available. The module is mounted on a stand at an inclination of 30^0. The panel's reduced voltage-temperature coefficient and exceptional low-light performance attributes provide outstanding energy delivery per peak power watt.

- Load: In order to drive the system producing electricity, a load consisting of DC bulbs (24V, 70W) is used.

- Battery: In order to store the excess electrical energy produced from the PV panel, two batteries (12V, 80 AH connected in series) are used.

Figure 4.1: Experimental test setup showing the testing of PV module.

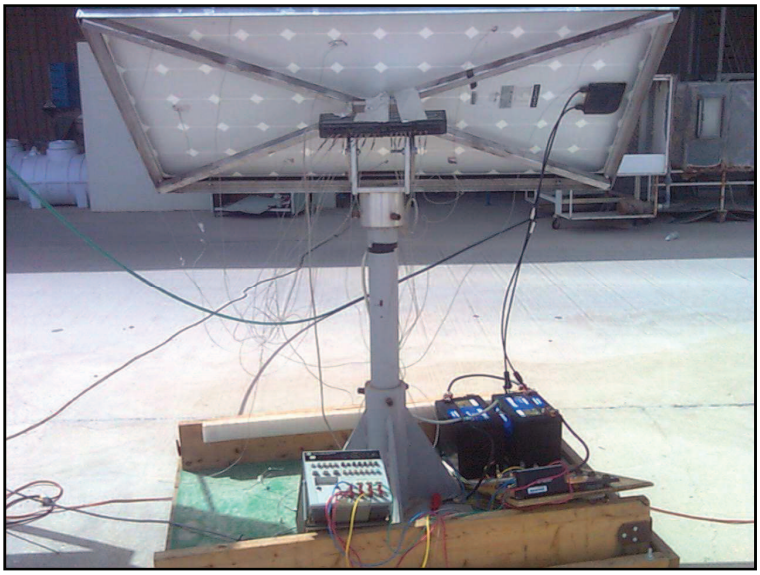

Figure 4.2: Back view of the test setup.

- MPPT(maximum power point tracker): To modulate the power output from the solar panel at a given irradiance to ensure that maximum electrical power is extracted, MPPT (Fig. 4.3) is used. The controller works on an algorithm that utilizes maximum energy from the PV panel and provides load control to prevent over discharge of the battery. The SunSaver MPPT used in this study suits for both professional and consumer PV applications. The device has an optional remote meter and battery temperature sensor.

- Voltage and current measurements: For measuring the maximum current and voltage produced from the panel, an ammeter and voltmeter is used.

- Thermocouples: Temperature measurements are significant in this study, hence standard thermocouples (type K) were used. Using a digital switch the temperatures (front and back) at various points on the module are measured with the help of thermocouple thermometer.

- Anemometer: Wind speed and ambient temperature was recorded through an hygro thermo-anemometer (Fig. 4.4). Figure shows the device used for measuring the same.

Figure 4.3: Sun Saver MPPT controller

Figure 4.4: Hygro-Thermo Anemometer

Table 2 provides the specifications of the module. Table 3 provides the accuracy/sensitivity of the instruments used in the study.

Table 2: Specifications of the PV module used.

Solar PV module parameters	**Value**
Module type	SUN POWER SPR-230WHT-U
Maximum Power (P_{mp})	230 Watts
Maximum Power Voltage (V_{mp})	41 V
Maximum Power Current (I_{mp})	5.61 A
Maximum Power point efficiency(η_{mp})	18.5%
Open Circuit Voltage (V_{oc})	48.7 V
Short Circuit Current (I_{sc})	5.99 A
Area of the module (A)	1.24 m^2
Temperature co-efficient of Short-circuit current (μ_{Isc})	3.5mA/K
Number of solar cells	72 (mono crystalline type)

Table 3: Accuracy/sensitivity of the instruments used.

Instrument Used	**Accuracy/sensitvity**
Sunsaver MPPT	Current: 1%; Voltage: 2%
Pyranometer	30.1μV/(W/m^2)
Hygro Thermo-Anemometer	2% ±0.2 m/sec
Thermocouple Thermometer	±1°C

❖ Pyranometer: To measure the solar radiation flux density (in W/m^2), a standard pyranometer (Fig 4.5) is used.

A schematic diagram of the experimental setup is shown in Fig. 4.6 which shows the components such as battery, load, MPPT controller, measurement devices and the panel.

Figure 4.5: Pyranometer

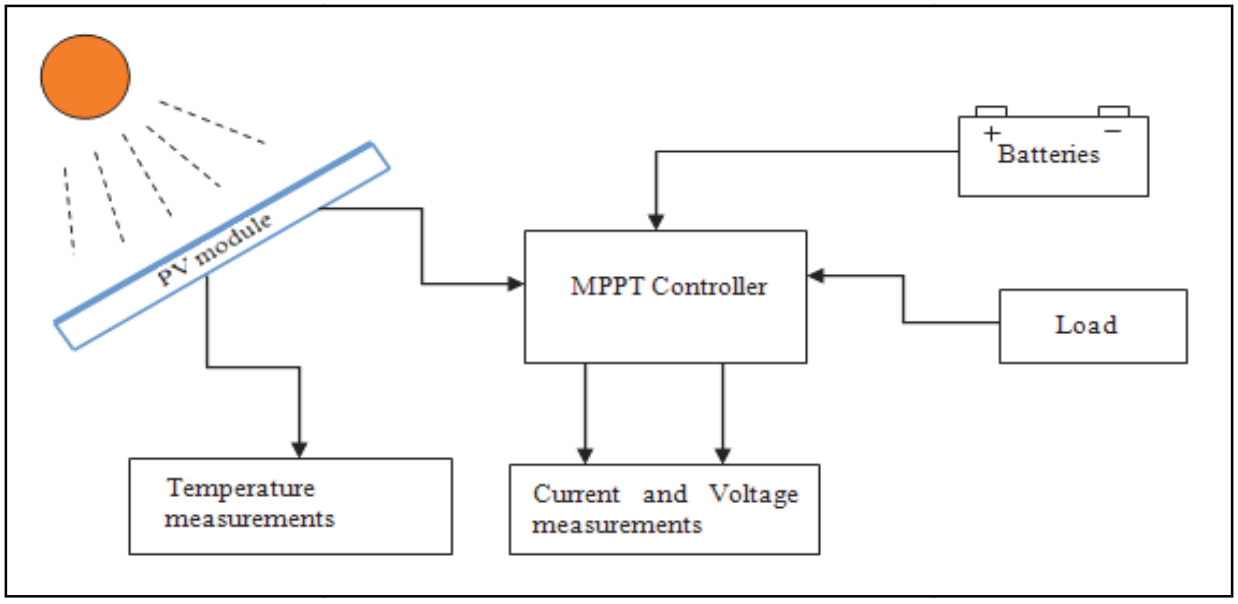

Figure 4.6: Schematic diagram of the experimental setup.

4.1.2 Integrated PV and cooling system

In the second phase of the experimental study, the PV module is integrated with a cooling panel followed by insulation with thickness of about 20mm attached on the rear side of the module. Fig. 4.7 shows the test setup of the combined PV with the cooling panel. Fig. 4.8 shows the back view of the PV panel before placing the SDM100 solar collector on it. Various components used in the integrated setup are mentioned below:

- Storage tank: The water to be supplied to the cooling panel is stored in a well insulted storage tank. The outlet of the tank is connected to a pump for circulating water at the required pressure.
- Pump: The pump delivers the water to the cooling panel only after adjusting the required flow rate and pressure using a bypass system. The maximum pressure allowed for the cooling panel is 6 psi.
- Bypass system: In order to maintain the water pressure to an adequate level, a bypass system is created. The bypass system which regulates the pressure by pumping the water back to the storage tank (with pressure gauge and valve arrangement) ensures the pressure does not exceed 6 psi.
- Flow meter: To regulate the water flow inside the cooling panel, a flow-meter with maximum flow rate of 3.6 lit/min is used.
- Thermocouples: The cooling water flows through the collector, captures the waste heat from the PV module and producing hot water which is collected at the collector outlet. The water temperature is measured using standard type-K thermocouples attached at the inlet and outlet of the cooling panel.

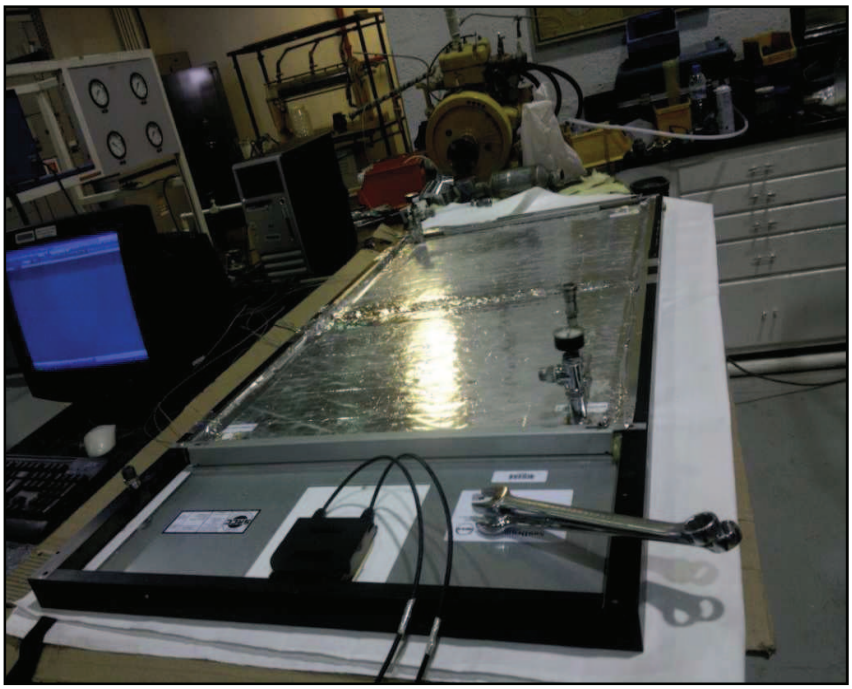

Figure 4.7: PV module integrated with the cooling panel and back insulation.

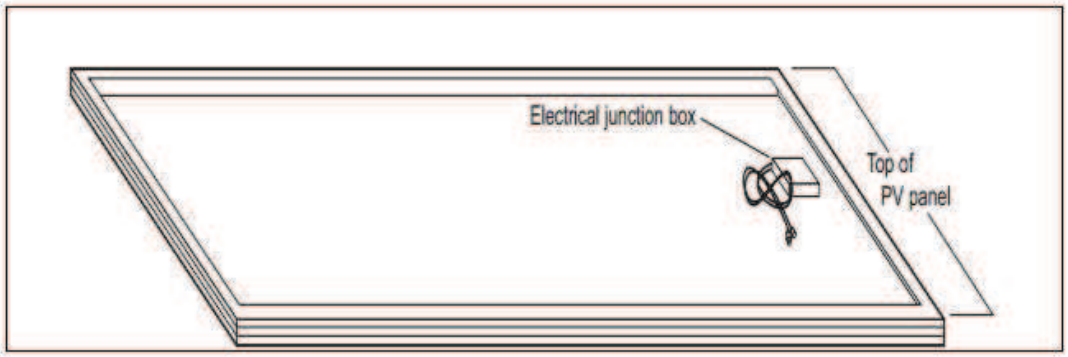

Fig 4.8: The back side of the PV panel, before placing the SDM100 solar collector on the panel [63]

Figs. 4.9 and 4.10 show the assembling of the collector to the panel frame with all the brackets, nuts and clamps installed.

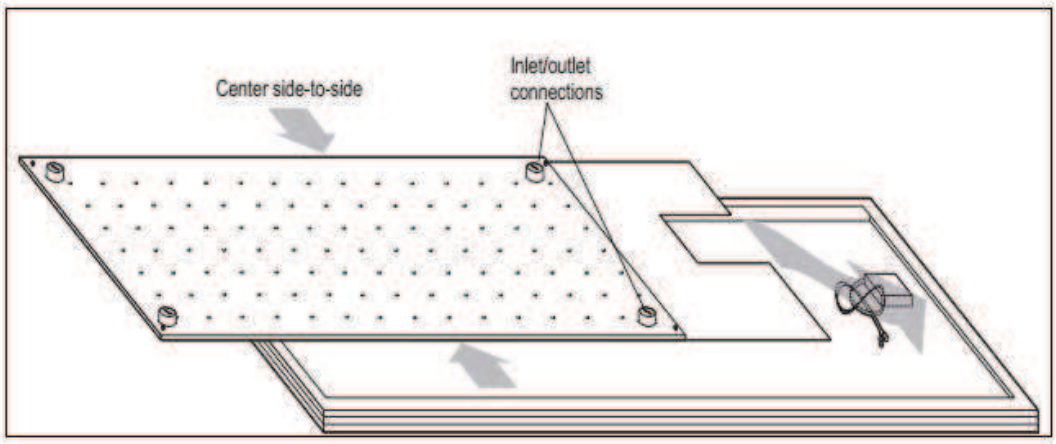

Fig 4.9: Alignment of the SunDrum collector with the PV panel frame [63]

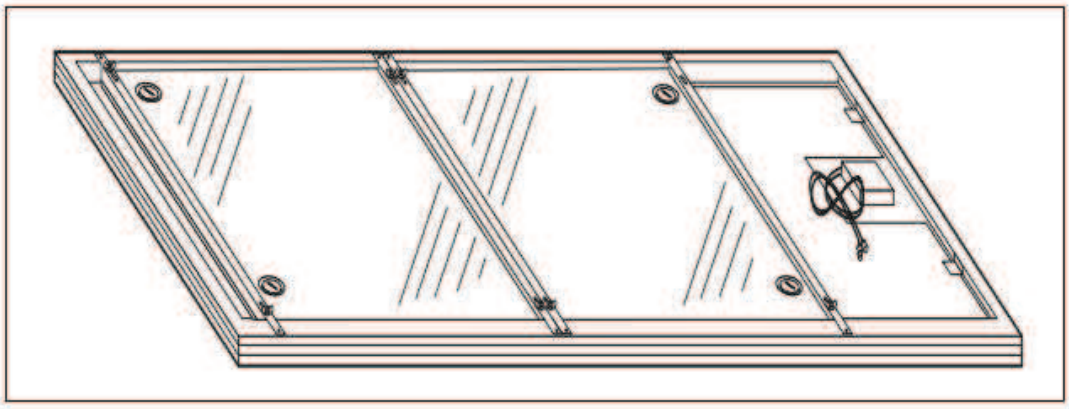

Fig 4.10: SDM100 collector and all four brackets in position, with both insulation panels in place, and clamps and wing nuts installed [63]

The outlet and inlet ports for water flow are shown in Fig 4.11. Various configurations of water inlet/outlet are provided by the manufacturer. Figs. 4.12-4.14 show different views of the integrated PV with cooling test setup. Fig. 4.15 shows the electrical test setup with connections to load, MPPT and batteries. Fig. 4.16 shows the SDM 100 collector with thermo-couples attached on it. The collector after being attached to the panel is mounted

on the stand shown in Fig. 4.17. A schematic view of the whole test setup is shown in Fig. 4.18.

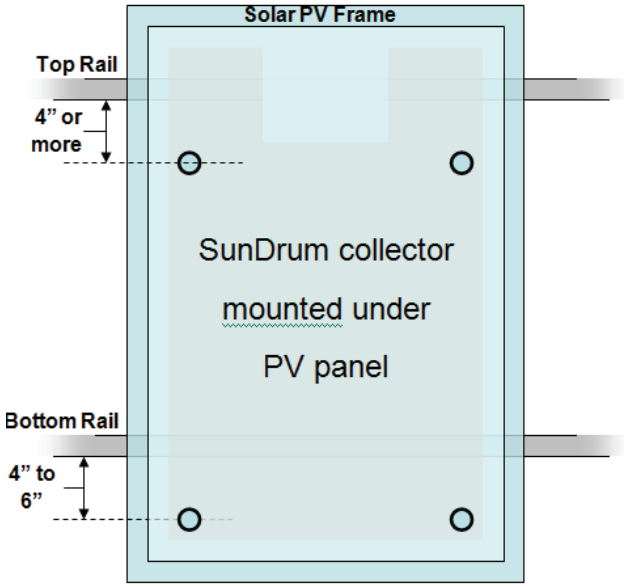

Fig 4.11: Thermal collector with water inlet/outlet ports [63]

Figure 4.12: Front view of the PV (integrated with cooling) test setup

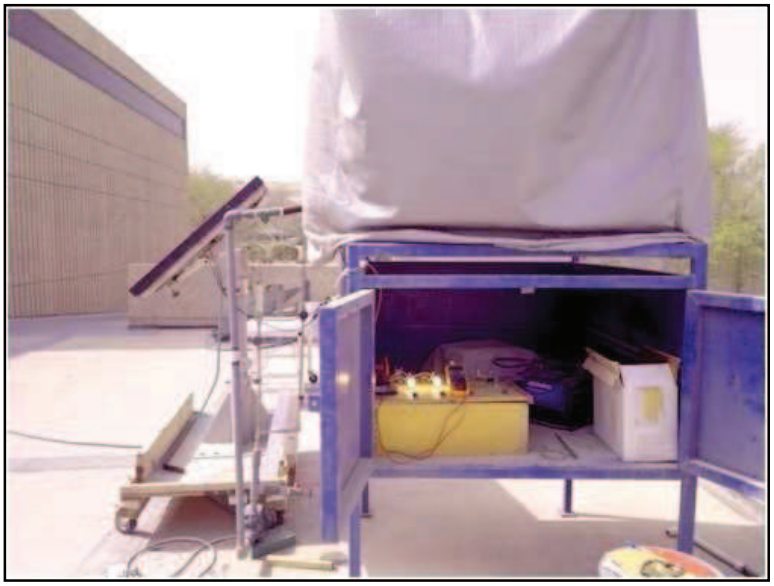

Figure 4.13: Side view of the experimental setup

Figure 4.14: Back view of the experimental setup showing the cooling panel along with the flow arrangement

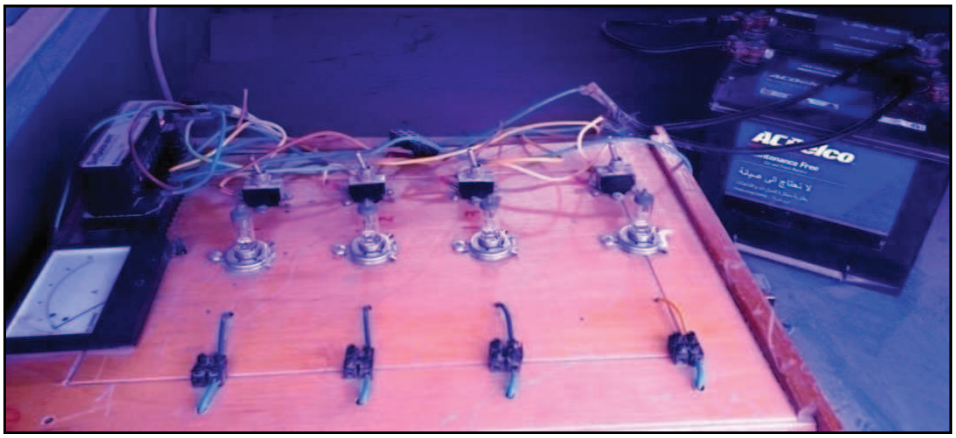

Figure 4.15: Electrical setup showing the connections to load, MPPT and batteries.

Figure 4.16: Sundrum SDM 100 collector used for cooling the panel.

Figure 4.17: Back view of the hybrid PV with cooling panel.

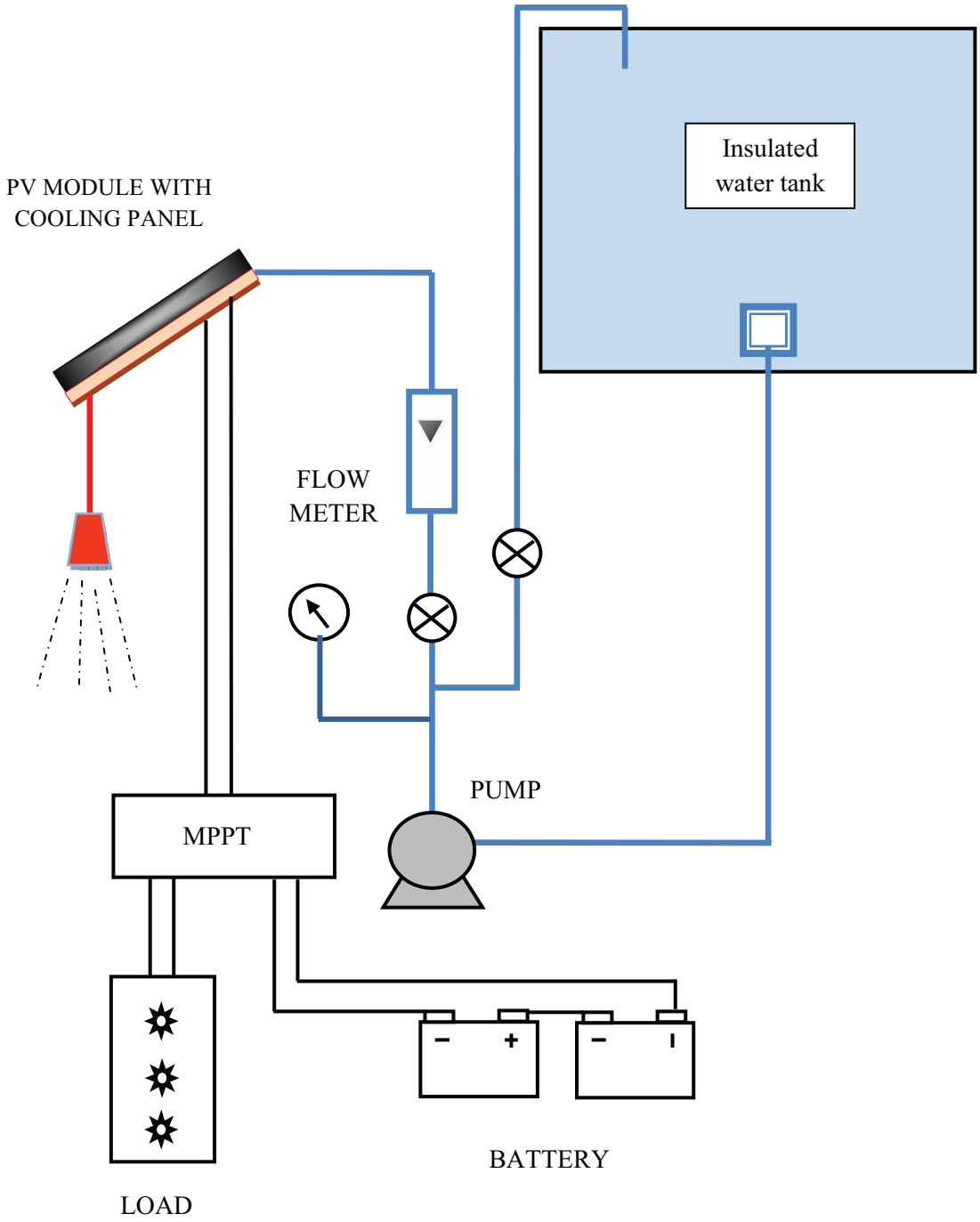

Figure 4.18: Schematic view of the hybrid PV with cooling setup.

CHAPTER 5

RESULTS AND DISCUSSION

This chapter consists of three sections. In each section, results obtained are presented, discussed and pertain to the objectives discussed in the first chapter. The first section presents and discusses the results of PV module performance predicted using the electrical model for the climatic conditions in Dhahran. The modeling results are compared using experimental data recorded in the month of May, 2011. In the second section, the results of numerical study of PV model combined with air cooled and water cooled model is presented. A comparison between the two models is done to optimize the system. Various parameters which relate to the performance of the PV/T system are discussed. The effect of cooling the module is also discussed in detail.

In the last section, experimental results of improved PV panel performance using back panel water cooling technique are discussed. The experimental study was carried out in the month of February, 2012. The performance of the hybrid system is studied using various water flow rates and a comparison between an un-cooled PV system and PV/T hybrid system is also presented. In the next chapter the conclusions obtained from these results are presented.

5.1 PV Module Performance

To verify the electrical model, the results obtained from the simulation program using EES software are compared to that obtained from measurements using the above experimental setup. The data sheet for the PV module used for the study is given in Table 2. Further, in order to compare the computed results with the experimental measurements, a correlation coefficient (r) and root mean square percent deviation (e) have been evaluated by the following equations [37] and depicted in these figures.

$$e = \sqrt{\frac{\sum\left[100 \times \left(X_{sim,i} - X_{\exp.i}\right) / X_{sim,i}\right]^2}{n}} \tag{5.1}$$

$$r = \frac{n\left(\sum X_{\exp} \cdot X_{sim}\right) - \left(\sum X_{\exp}\right) \cdot \left(\sum X_{sim}\right)}{\sqrt{n \cdot \left(\sum X_{\exp}^2\right) - \left(\sum X_{\exp}\right)^2} \cdot \sqrt{n \cdot \left(\sum X_{sim}^2\right) - \left(\sum X_{sim}\right)^2}} \tag{5.2}$$

The results reported here are recorded in the month of May, 2011 which were consistently clear days. Figure 5.1 shows the diurnal variation of solar radiation intensity and ambient temperature throughout the day from 9:00am to 4:00 pm for Dhahran. The effective radiation reaching the module is the function of intensity of direct and diffuse short wave radiation inputs, and the absorptivity of the cell. The intensity of solar radiation also depends on the time of the day, season and latitude of the location. The maximum values of solar radiation intensity and ambient temperature can be noted along noon since the sun's rays have smallest angle of incidence to the earth's surface are spread over the smallest area. They also have to pass through the least amount of

atmosphere, so there is less reflection. The maximum values of ambient temperature and global radiation recorded are 43^0C and 880 W/m^2, respectively, on a clear day. Whereas during cloudy days the incident light reaching the earth is less which further reduces its intensity.

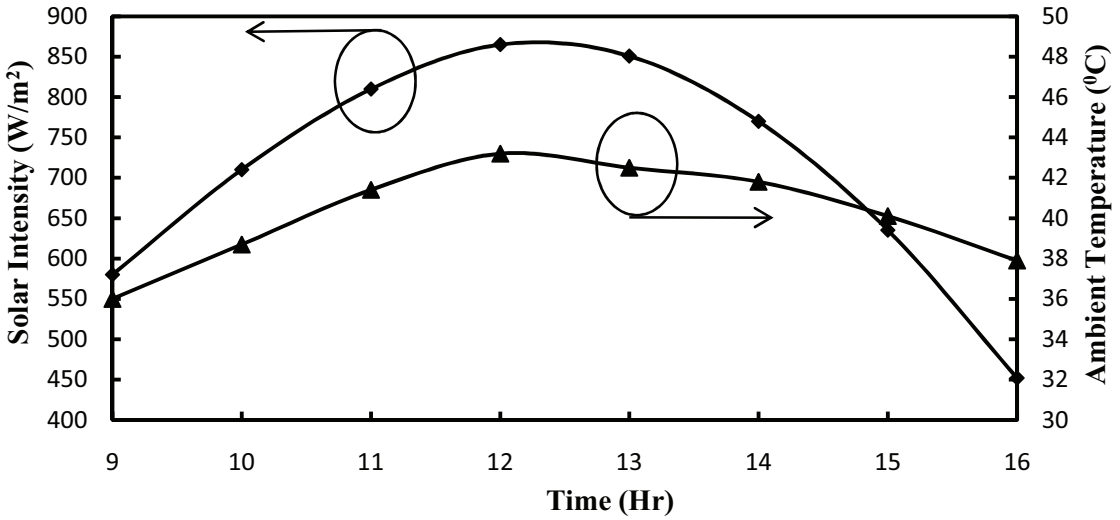

Figure 5.1: Hourly variation of ambient temperature and solar radiation intensity.

For a set of experiments conducted, Fig.5.2 shows the hourly variation of top and back surface temperatures of the PV module as well as the wind speed. The maximum value of wind speed recorded is 2.5 m/s at 11:00 am. Temperature effects are the result of an inherent characteristic of crystalline silicon cell based modules as the front and the back surface gets heated up with the irradiance which results in increase of cell temperature. The operating temperature of the module depends on the equilibrium maintained between the heat generated by the module and the heat lost to surrounding environment. The maximum module temperature in the front and back surface is observed to reach 52.6^0 C and 49.4^0 C respectively at solar noon. This is attributed to the high absorption of solar

irradiation at noon time. The average temperature difference on both surfaces varies around 2.5% throughout the day.

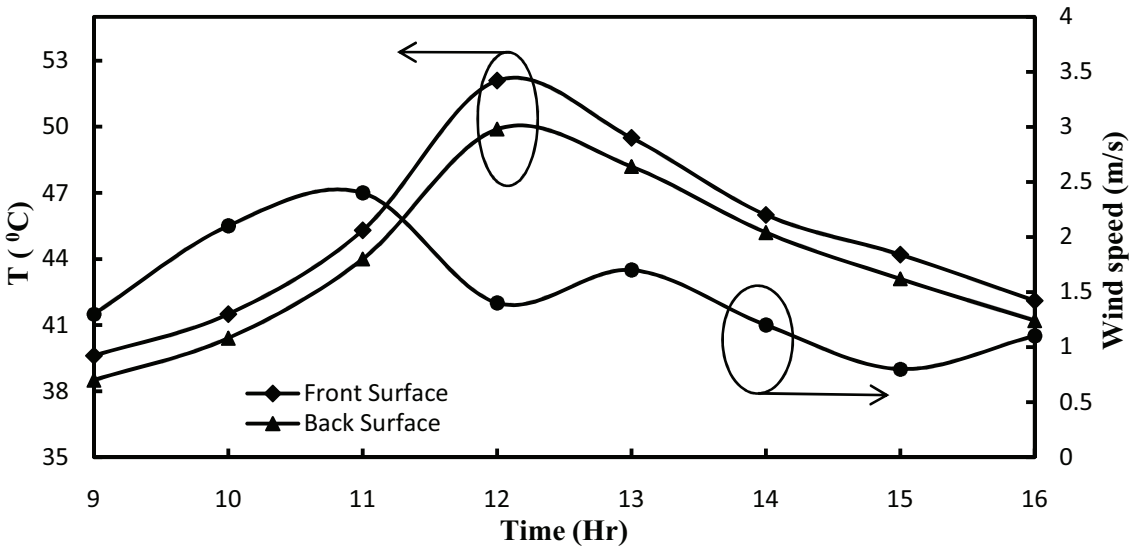

Figure 5.2: Hourly variation of measured wind speed, front and back surface temperature of the PV module.

Figure 5.3 shows the measured and computed back surface temperature of the module. The module temperature shown here is the average of four thermocouples on the back surface. From this Figure, it is observed that there is a fair agreement between the experimental and numerical values with correlation coefficient, r = 0.99 and root mean square percent deviation, e = 2.35%.

Figure 5.4(a) shows the comparison of numerical and experimental values of maximum power point current. There is a fair agreement between them with correlation coefficient, r = 0.98 and root mean square percent deviation, e = 4.05%. Figure 5.4 (b) shows the comparison of numerical and experimental values of maximum power point voltage.

There is a fair agreement between them with correlation coefficient, r = 0.95 and root mean square percent deviation, e = 3.1%.

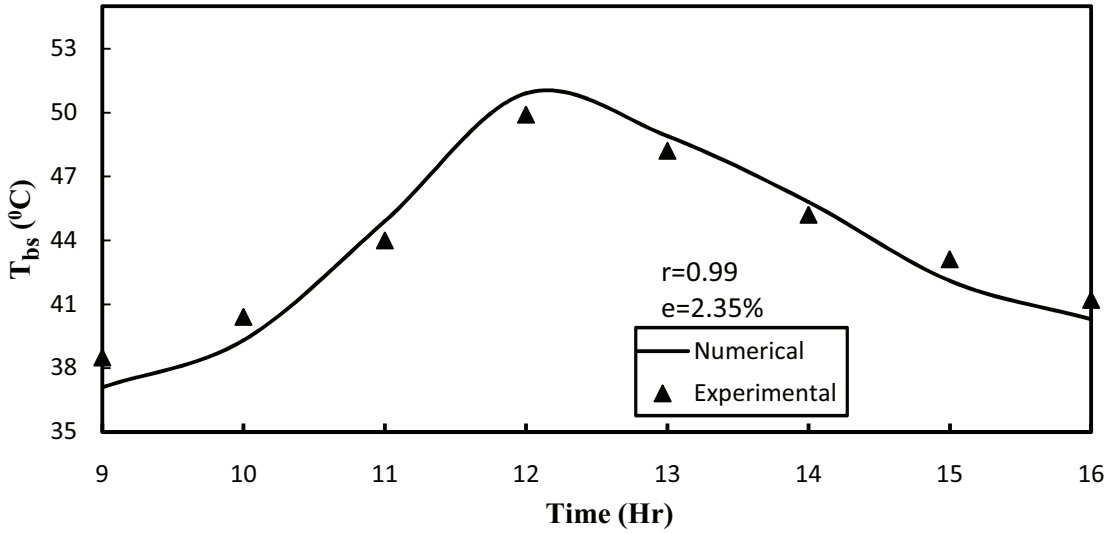

Fig.5.3. Hourly variation of measured and computed module back surface temperature.

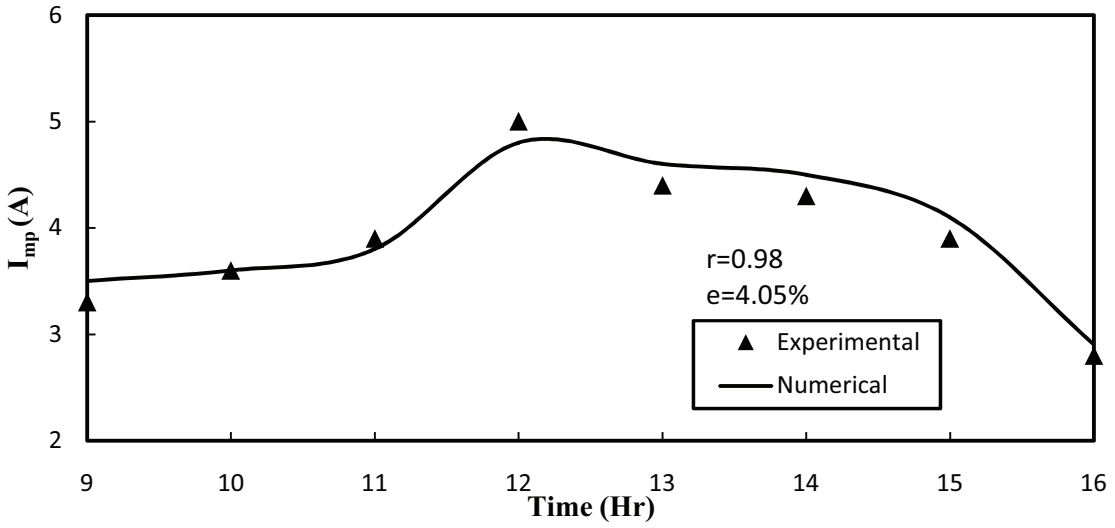

Figure 5.4 (a). Hourly variation of measured and computed maximum power point current.

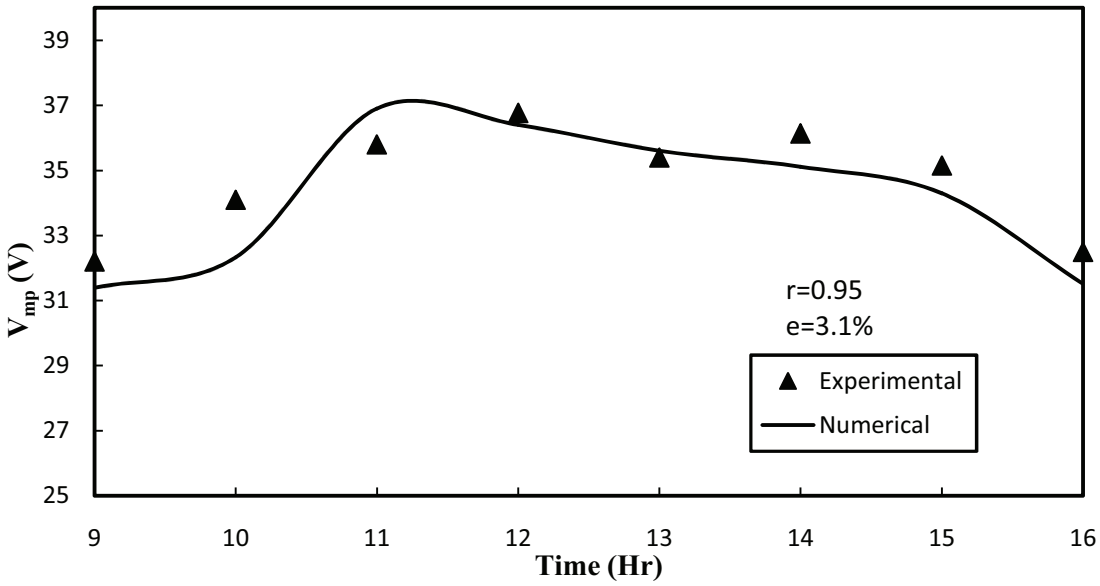

Figure 5.4 (b): Hourly variation of measured and computed maximum power point voltage.

Figure 5.5 shows the comparison between the experimental and numerical results of maximum power output from the module. Solar radiation intensity is a primary factor affecting the output power of the PV module. When the module and the sunlight are perpendicular to each other (i.e., around noon time for Dhahran) the power density of module is always high. The results are in good agreement with each other. Maximum power output is around 12 noon when the sun is at its zenith due to the solar intensity being highest at that time. The maximum power obtained from the module is around 180W at 12 noon when compared to its rated peak power at 230W. The loss in power is due to optical losses, ohmic losses and heat loss from the module to the surroundings. It is observed from Fig.5.5 that there is a fair agreement between the experimental and numerical values with correlation coefficient, r = 0.98 and root mean square percent

deviation, e = 5.22%. Fig. 5.6 shows the comparison between experimental and numerical results of electrical efficiency of the module. The maximum efficiency is observed to be 17.2% of an average intensity of solar radiation and it can be observed that there is a fair agreement between them with a correlation coefficient, r = 0.98 and root mean square percent deviation, e = 5.2%.

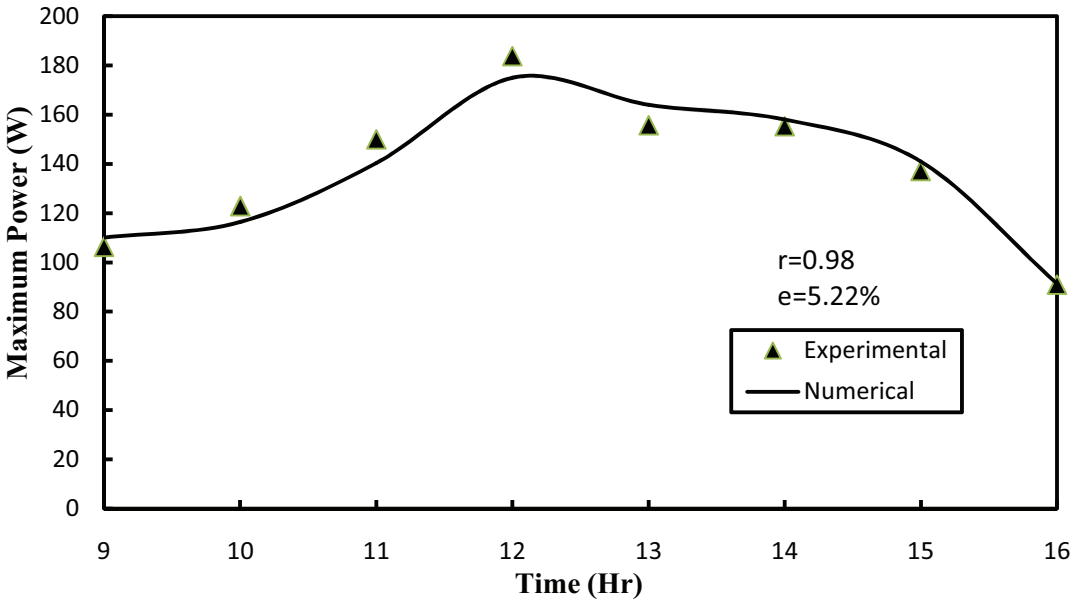

Figure 5.5: Hourly variation of measured and computed maximum power output.

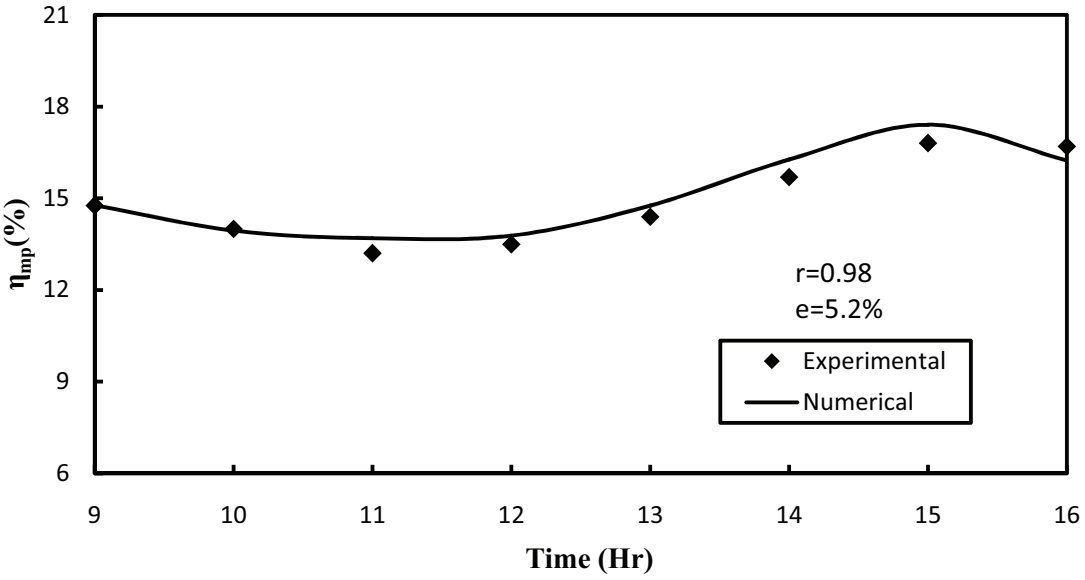

Figure 5.6: Hourly variation of measured and computed maximum power point efficiency.

5.2 PV-air and water cooled model

This section presents and discusses the results of numerical analysis of air cooled and water cooled PV models. The effect of cooling the PV module is analyzed in this study. Since the PV panels interact with the environment and their efficiency is so low, they passively absorb about 80% of the incoming solar irradiance as heat. The electrical efficiency of PV module declines with the increase in temperature of the PV module. This would not be such a problem if not for a 0.5% efficiency loss of the solar PV panels associated with a 1˚K increase of the cell temperature.

Figure 5.7 shows the comparison of cell temperature for an air cooled panel with a conventional (un-cooled panel) throughout the day. The maximum cell temperature without cooling is found to be 63.2^0C, whereas the air cooling technique reduces the cell

temperature to 55^{o}C. Temperature reduction is significant due to heat transfer by water. The percentage reduction in the cell temperature by air cooling is about 14%. This translates to an increase in the module's power output.

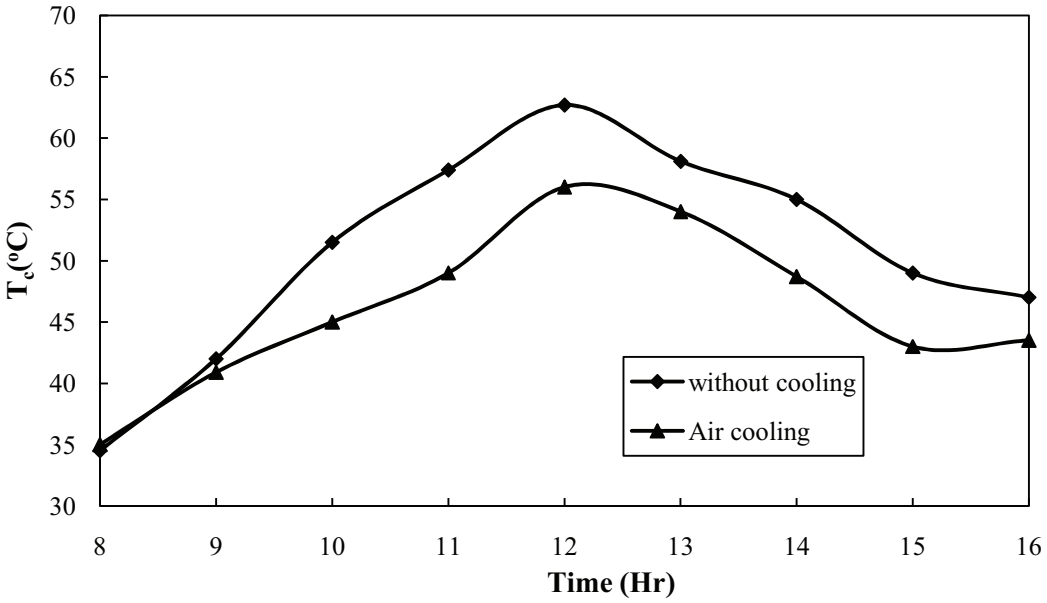

Figure 5.7: Comparison of PV cell temperature for air cooling and without cooling

The details of the PV module used in this study are given below in Table 4. The main module parameters which are utilized in the modeling are shown in the table below. The specification of the collector used for air cooling is given in Table 5.

Table 4: Specifications of the PV module used for air and water cooled model

Solar PV module parameters	**Value**
Module type	Siemens SP75, monocrystalline silicon
Maximum Power (P_{mp})	75 W
Maximum Power Voltage (V_{mp})	17 V
Maximum Power Current (I_{mp})	4.4 A
Maximum Power point efficiency(η_{mp})	17%
Open Circuit Voltage (V_{oc})	21.7 V
Short Circuit Current (I_{sc})	4.8 A
Area of the module (A)	0.6324 m^2
Temperature co-efficient of Short-circuit current (μ_{Isc})	2.06mA/K
Number of solar cells	36 (mono crystalline type)

Table 5: specifications of the PV/T collector used for air and water cooled model

Solar PV/T air/water collector parameters	**Value**
The thickness of glass cover,	0.003 m
The conductivity of glass cover, K_g	1 W/m K
The transmittivity of glass cover, τ_g	0.95
The emissivity of PV/T collector, ε_g	0.88
The absorptivity of solar cell, α_c	0.85
The thickness of silicon solar cell, L_{si}	300×10^{-6} m
The conductivity of silicon solar cell, K_{si}	0.036 W/m K
The length of duct, L	1.2 m
The width of PV/T collector, W	0.45 m
The duct depth, δ	0.05 m
The packing factor of solar cell, β_c	0.83

Figure 5.8 shows the comparison of cell temperature for a water cooled panel with a conventional (un-cooled) panel throughout the day. The maximum cell temperature is around noon time when highest amount of solar radiation strikes the panel. It is observed that the cell temperature reduces by 16% employing the water cooling technique. Figure 5.9 shows the fluid outlet temperature variation throughout the day for air cooling and water cooling models. The outlet temperature for water increases as the waste heat

absorbed by the panel is removed hence, cooling and increasing its power output. After solar noon the water outlet temperature decreases as the panel temperature starts to lower with decrease in solar intensity. The outlet temperature for water is higher than air showing good thermo-physical properties of water, making it a good cooling medium. Modules nearly always produce less than their rated peak power in real-life conditions.

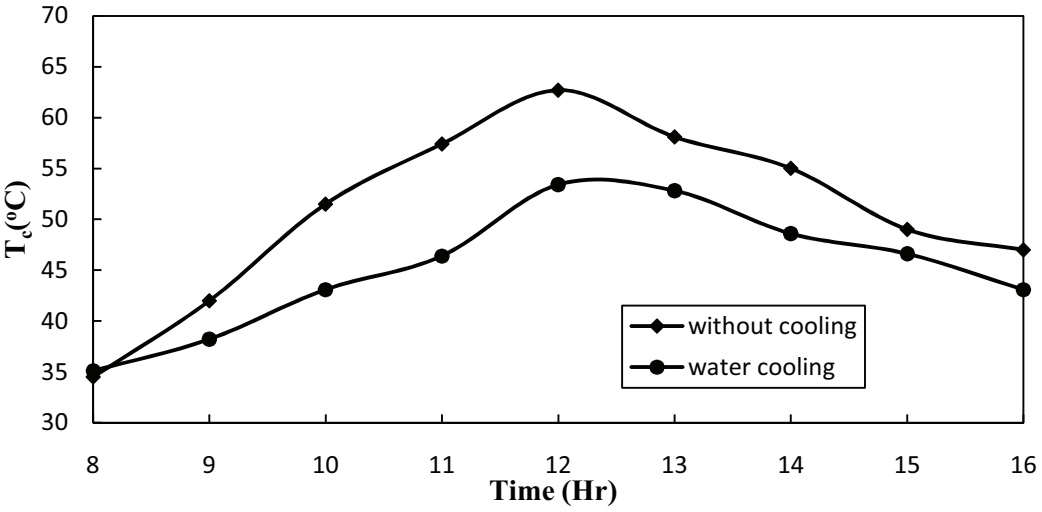

Figure 5.8: Comparison of PV cell temperature for water cooling and without cooling

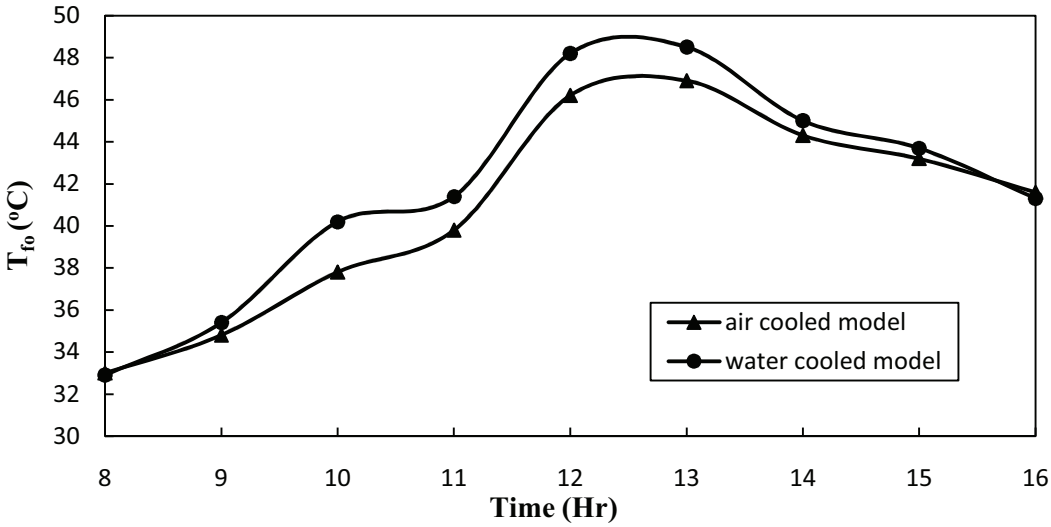

Figure 5.9: Comparison of outlet fluid temperature for air cooling and water cooling

Figure 5.10 shows the power output comparison for an un-cooled and water cooled panel throughout the day. By employing water cooling technique, an average increase of 20% in the power output of the panel is observed hence improving the module performance. Both electrical and thermal energy are generated through the hybrid PV/T system.

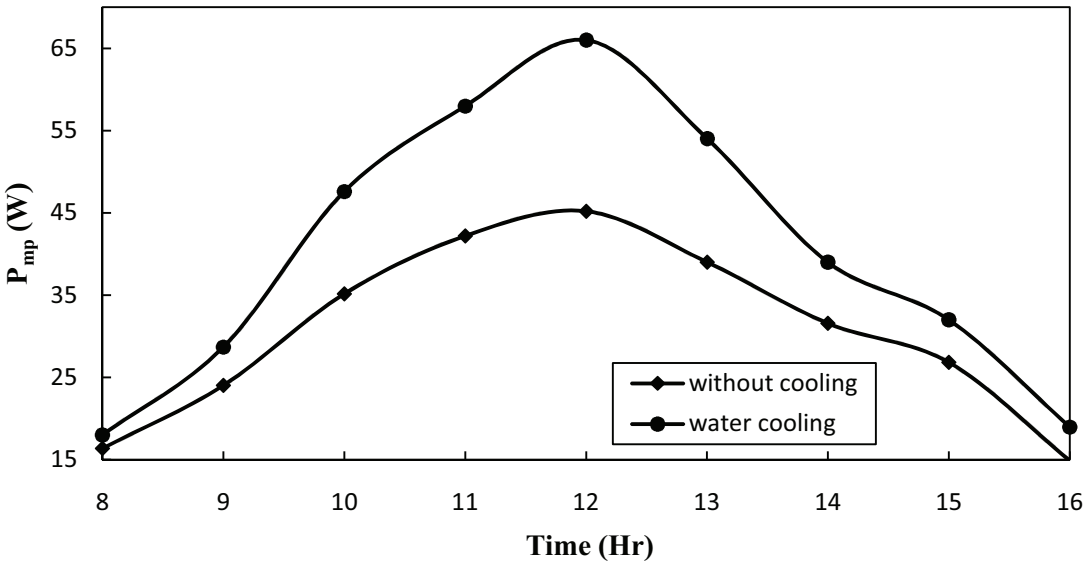

Figure 5.10: Comparison of power output for water cooling and without cooling

Figure 5.11 shows the power output comparison for air cooled panel with an un-cooled panel. The rate power output for the panel is 75W. The remaining power is lost due to optical and reflection losses. The maximum power output for a conventional panel around noon is about 45W whereas for a water cooled panel is 65 W. During early hours of the day, no significant effect of cooling is observed. But as the irradiance increases, the cooling effect plays a major role in increasing the power output.

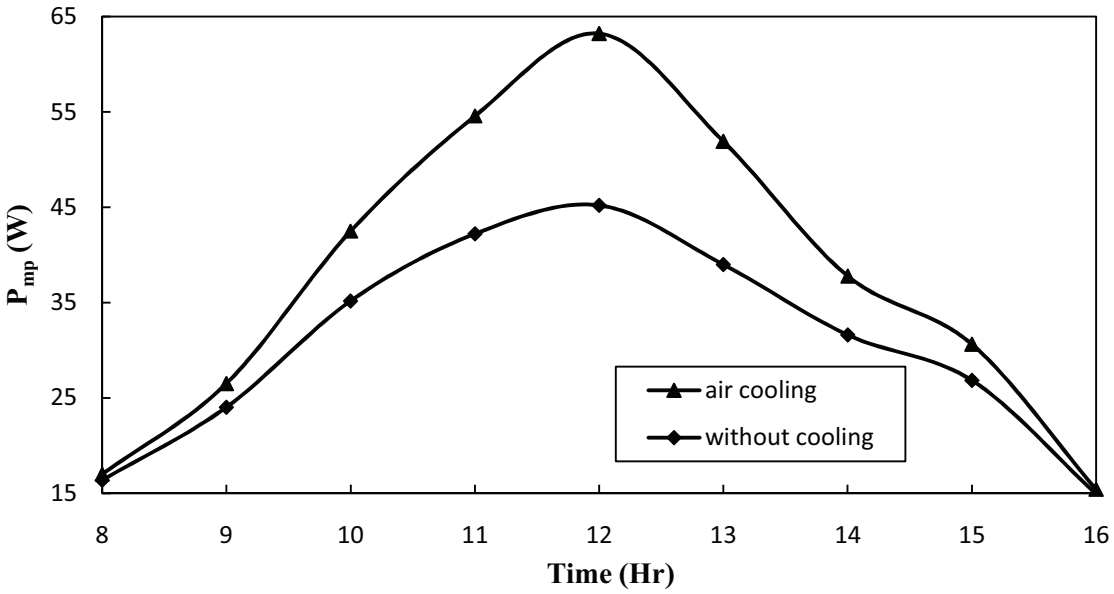

Figure 5.11: Comparison of power output for air cooling and without cooling.

Finally, a comparison of power output for an air cooled, water cooled and un-cooled panel is given in Fig 5.12. The maximum power extracted from the panel is obtained by water cooling. Decreasing the level of electrical power reduces the photovoltaic panel efficiency significantly as temperature exceeds the critical daily limit. Thus in optimum system operation, it is suitable to decrease the module temperature near the ambient temperature. During the working day, the panel efficiency decreases and reaches a minimum at solar noon. By reducing the cell temperature and therefore increasing the power level, efficiency rises. By incorporating the cooling mechanism an increase in the electrical efficiency is observed.

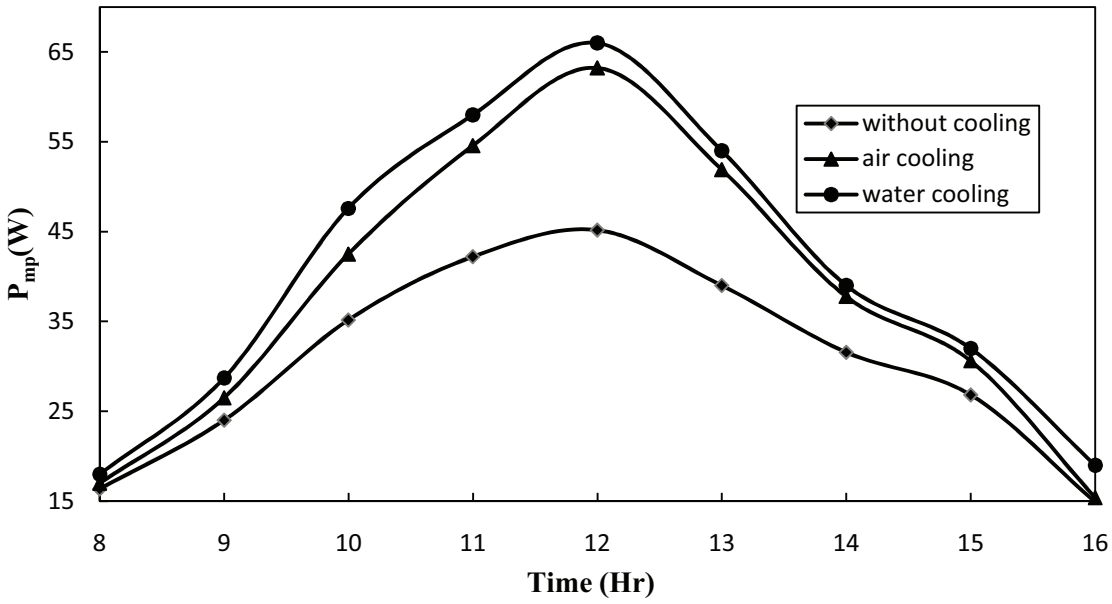

Figure 5.12: Comparison of power output for air, water cooling and without cooling

Figure 5.13 shows the variation of electrical efficiency of a conventional panel throughout the day and a comparison with air and water cooling is also shown. The maximum efficiency of the water cooled and air cooled panel is about 14% and 11% near solar noon. Temperature effects are the result of an inherent characteristic of crystalline silicon cell-based modules. They tend to produce higher voltage as the temperature drops and conversely, to lose voltage in high temperatures. Variation of power output with irradiance is shown in Fig. 5.14. As the irradiance increases, the power output is found to increase. The effect of irradiance on the power output is an important factor in studying the PV panel performance. Decrease in the irradiance levels can seriously affect the power output of the panel.

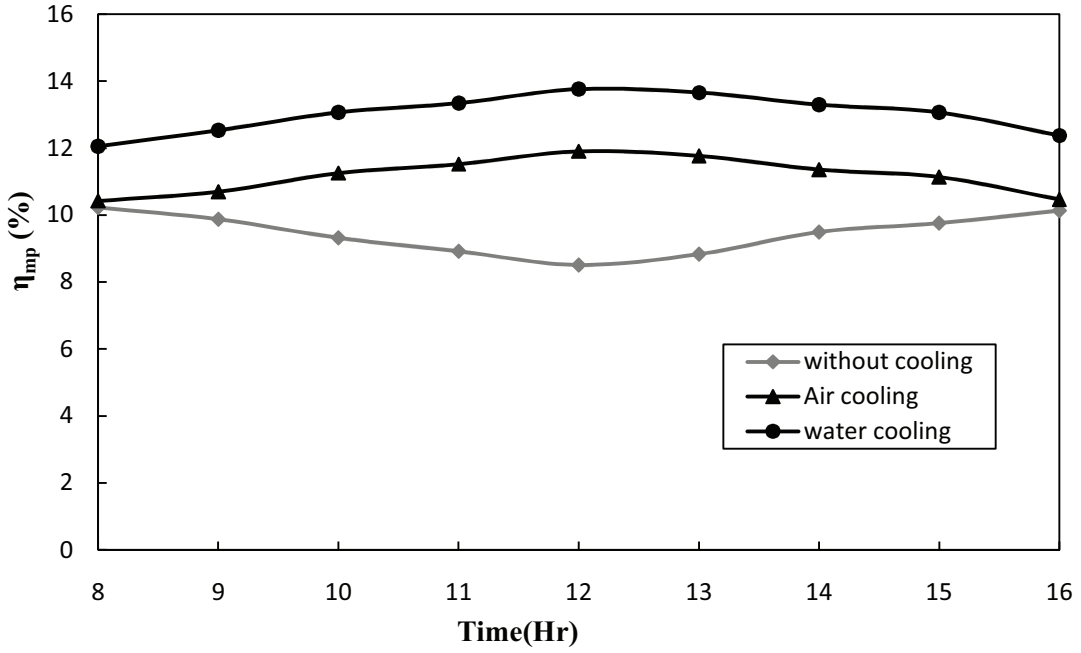

Figure 5.13: Comparison of electrical efficiency for air, water and without cooling

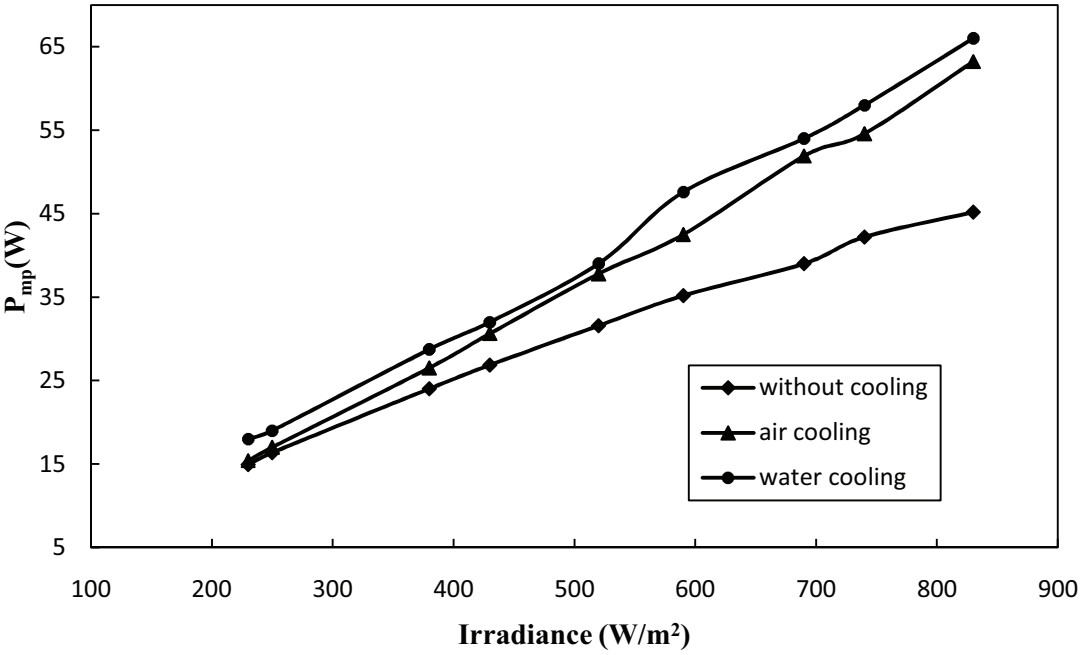

Figure 5.14: Variation of power output with irradiance

The hybrid panel thus produces electrical energy as well as thermal energy. Thermal performance of air cooled and water cooled modules are shown in Fig. 5.15. Maximum thermal efficiency of an air cooled model is found to be 46% around noon time whereas for water cooled model the efficiency is 57%. The percentage difference in the efficiency is about 18%. The variation of thermal gain with air cooling and water cooling is shown in the Fig. 5.15. The maximum gain is 250W with water cooling and 210 W with air cooling because of high heat transfer characteristics of water. The thermal gain for air and water cooling is shown in Fig 5.16. The thermal efficiency as a function of reduced temperature is also presented. The least square fit of the data for thermal efficiency for an air cooled as well as for water cooled panel is shown in Figs. 5.17 and 5.18 respectively. The scatter in the data is expected, because of temperature dependence, wind effect variations.

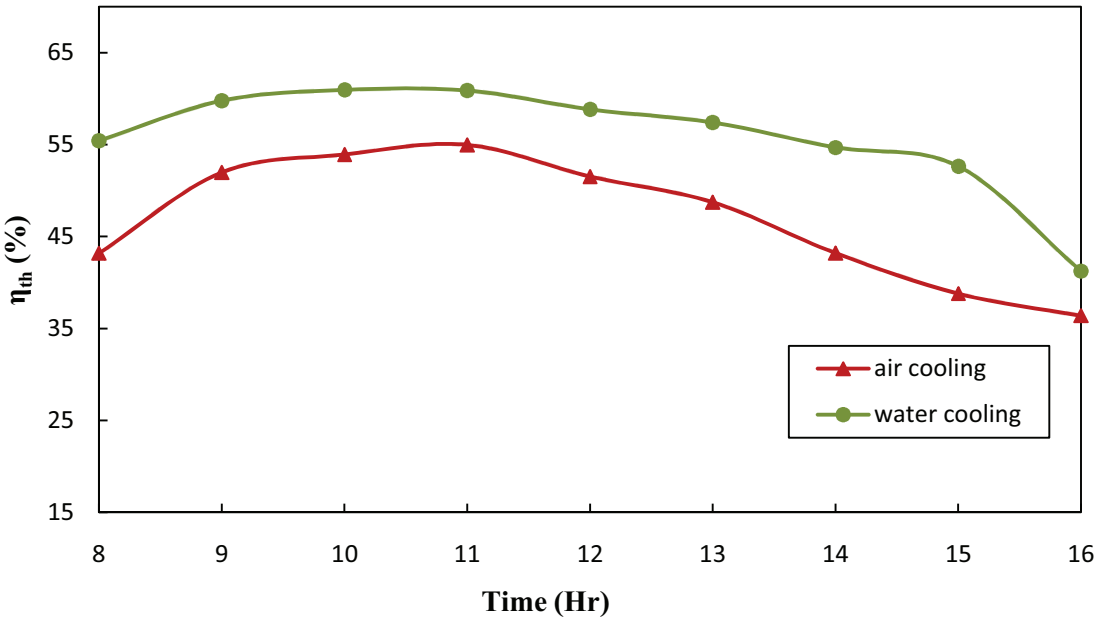

Figure 5.15: Comparison of thermal efficiency for air cooling and water cooling

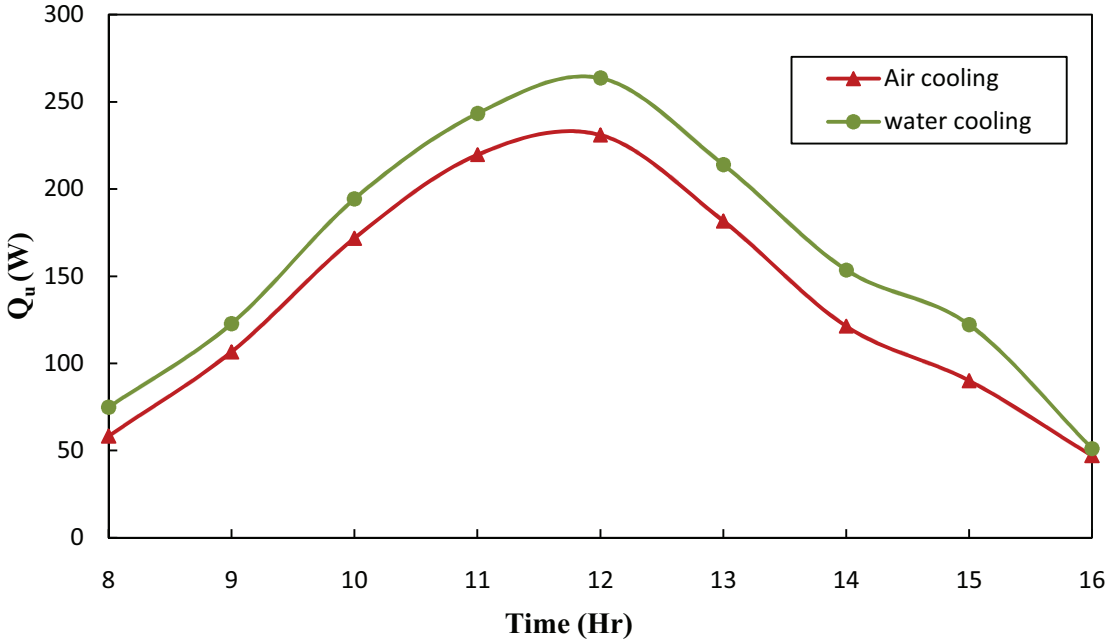

Figure 5.16: Comparison of thermal gain for air cooling and water cooling

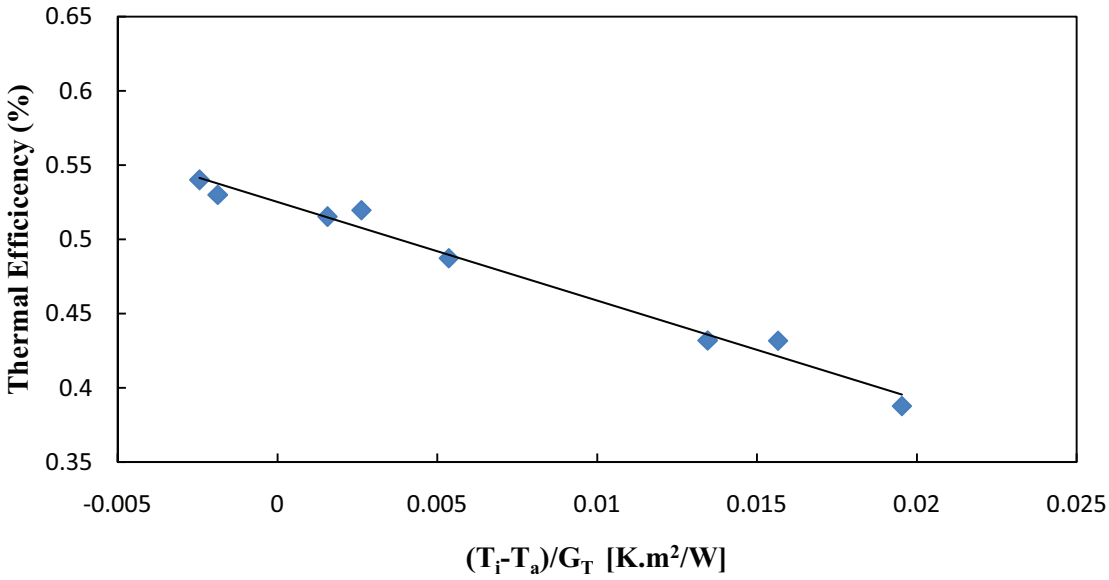

Figure 5.17: Measured thermal efficiency data for an air cooled PV model and a straight line fit to the collected data.

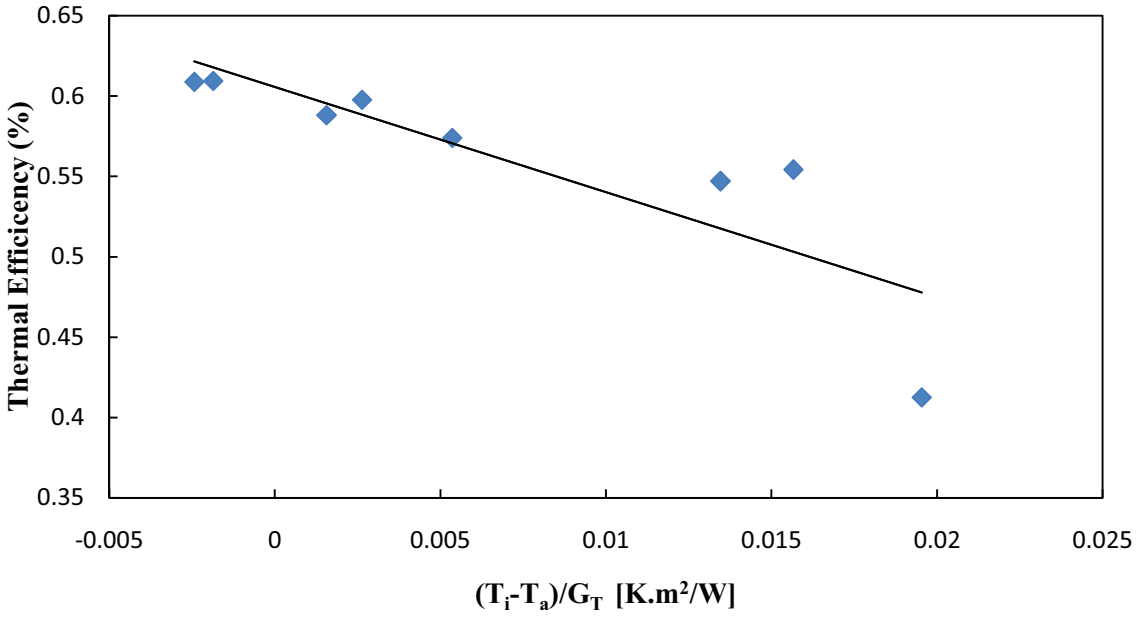

Figure 5.18: Measured thermal efficiency data for a water cooled PV model and a straight line fit to the collected data.

5.3 PV-water cooling: Experimental results

The performance of PV system depends on several climatic factors such as solar radiation, ambient temperature and wind speed since the maximum power point (MPP) on the current-voltage (I-V) performance curve varies with these factors. The tests were conducted with water cooling in the month of Feb. 2012. The variation of irradiance received by the panel surface during the test day is shown in Fig. 5.19 Maximum value of radiation received is 954 W/m^2 at solar noon. The climatic data including ambient temperature, wind speed for the test day is also shown in Figs. 5.19 and 5.20.

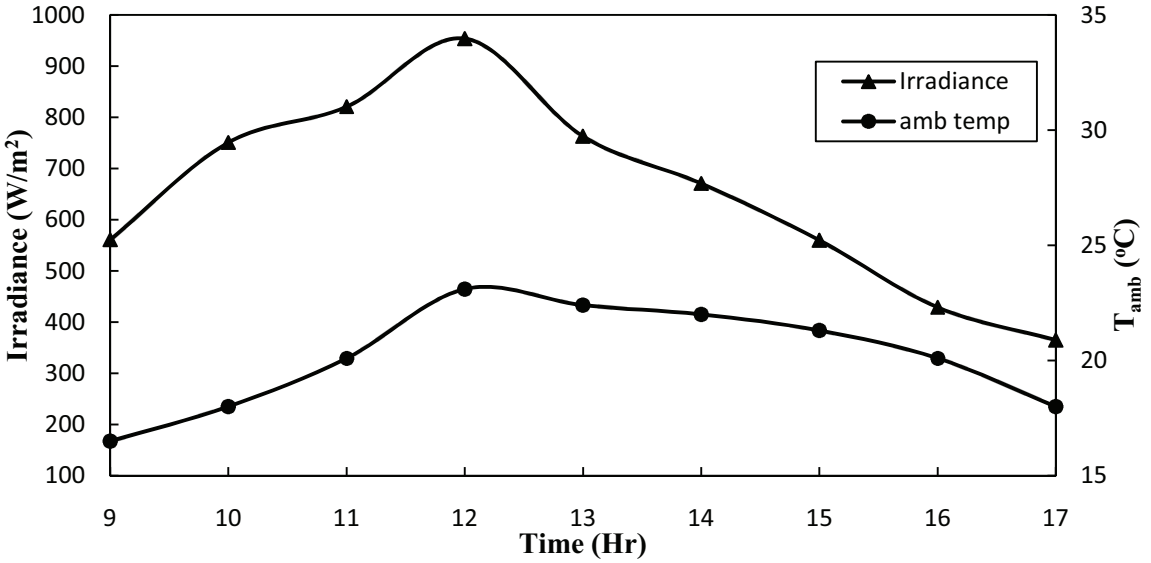

Figure 5.19: Hourly variation of irradiance and ambient temperature during the test day (02-02-2012).

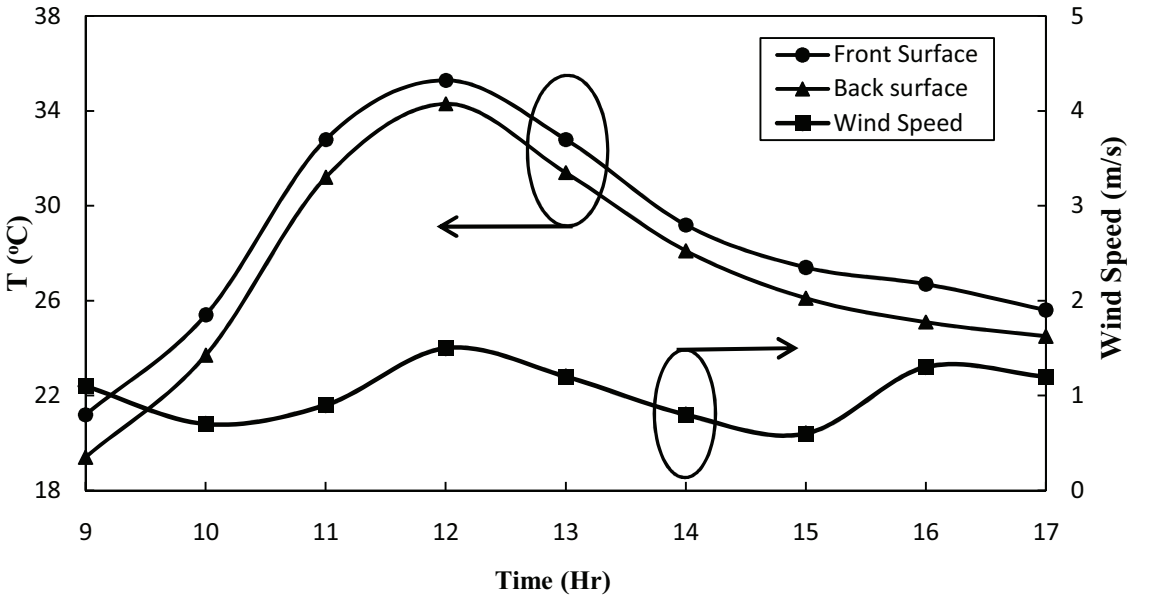

Figure 5.20: Hourly variation of module temperatures (front and back) and wind speed during the test day (02-02-2012).

Increase in the PV module temperature inversely affects the power output. The increase in the module temperature above the ambient temperature initiates the process of heat loss from the module through the mechanisms (conduction, convection and radiation) and results in a decrease of output voltage. The variation of module surface temperatures (front and back) during the test day (02-02-2012) is shown in Fig. 5.20. The maximum module temperatures (front and back) were found to be 35.3^{o}C and 34.3^{o}C at noon time. To boost the electrical efficiency of the PV module, temperature and temperature gradient over the PV module are considered critical. The operating temperature of the PV module directly relates to the module efficiency.

Fig. 5.21 shows the energy collection as a function of irradiance with comparison between the conventional PV system and the hybrid system. From the figure, it is observed that as the irradiance increases the energy collection increases. The maximum energy obtained with PV system is around 190W whereas at the same irradiance level, the hybrid system captures a maximum of 750W which is nearly 4 times higher than the PV system.

Fig. 5.22 shows the PV module temperature as a function of irradiance. From the figure it is observed that the module temperature is linearly proportional to irradiance. The module temperature variation for the case of with and without cooling is presented in the figure. In the case of without cooling, for an irradiance of about 1000 W/m^2 the module temperature reaches to about 45^{0}C, whereas at the same irradiance level, with cooling the module temperature reduces to 34^{0}C showing that the temperature reduction is significant

due to heat absorbed by the water. An overall reduction of 20% in the module temperature throughout the day is observed with the influence of cooling.

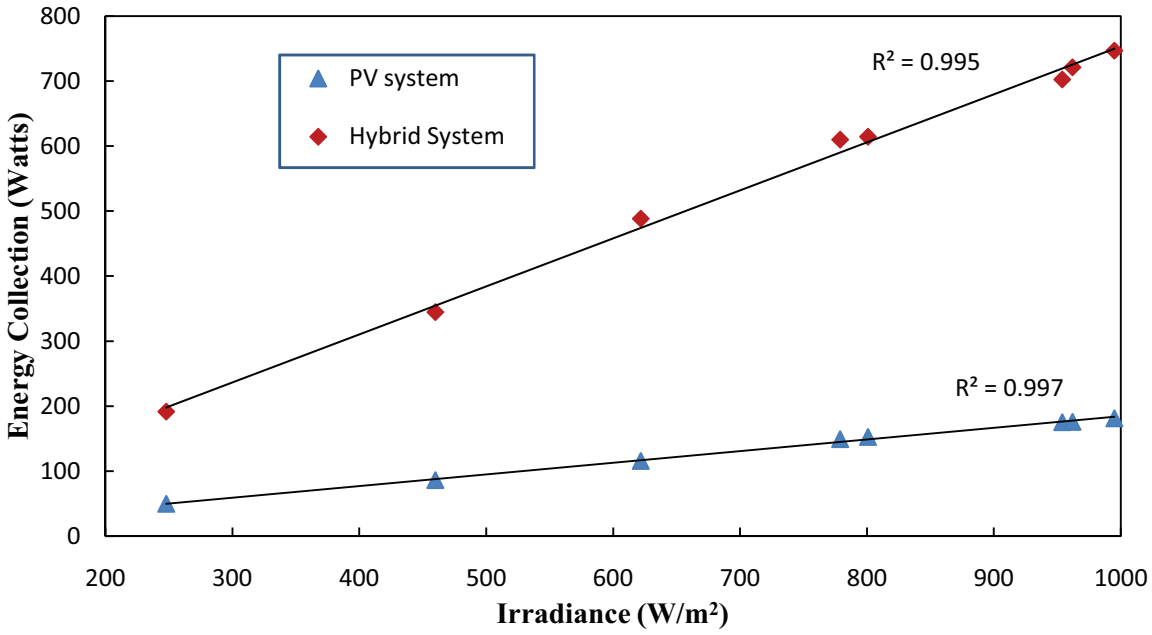

Figure 5.21: Comparison of energy collection as a function of irradiance for PV system and hybrid system.

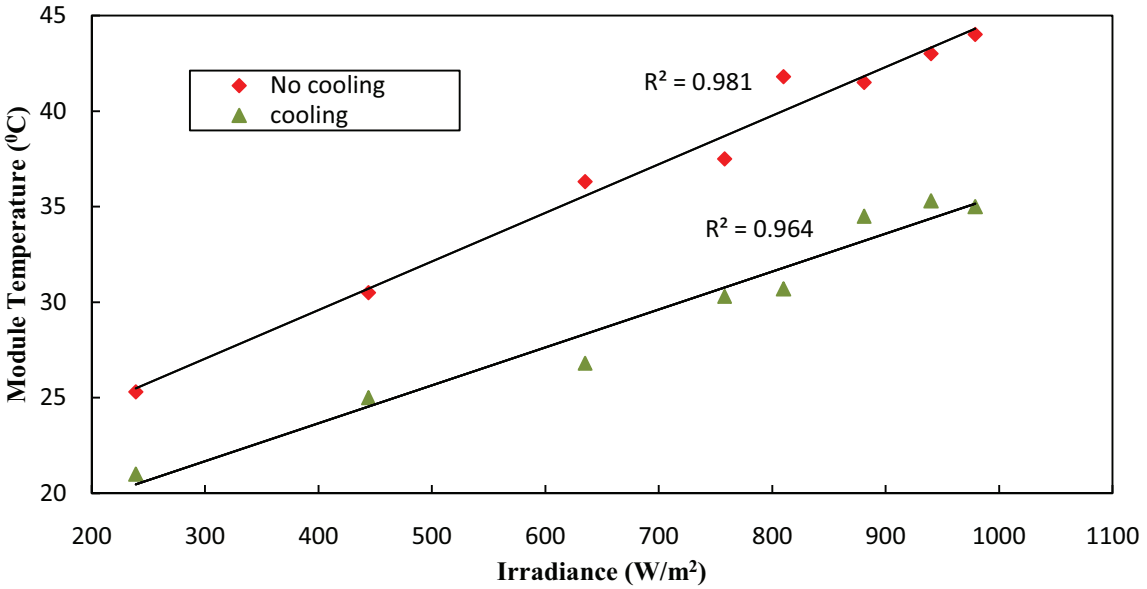

Figure 5.22: Module temperature as a function of solar irradiance.

Variation of outlet water temperature at different flow rates is presented in the Fig. 5.23. From this figure it is observed that at lower flow rates the outlet water temperature is high but as the flow rate increases, the outlet temperature reduces. The effect of mass flow rate on maximum rise in water temperature (T_0-T_i) is shown in Fig. 5.24. It can be seen that the rise in temperature decreases with increase in mass flow rate. The effect of radiation intensity on the temperature rise is seen also in Fig. 5.24 which shows that the temperature rise increases with increase in radiation intensity at same flow rate.

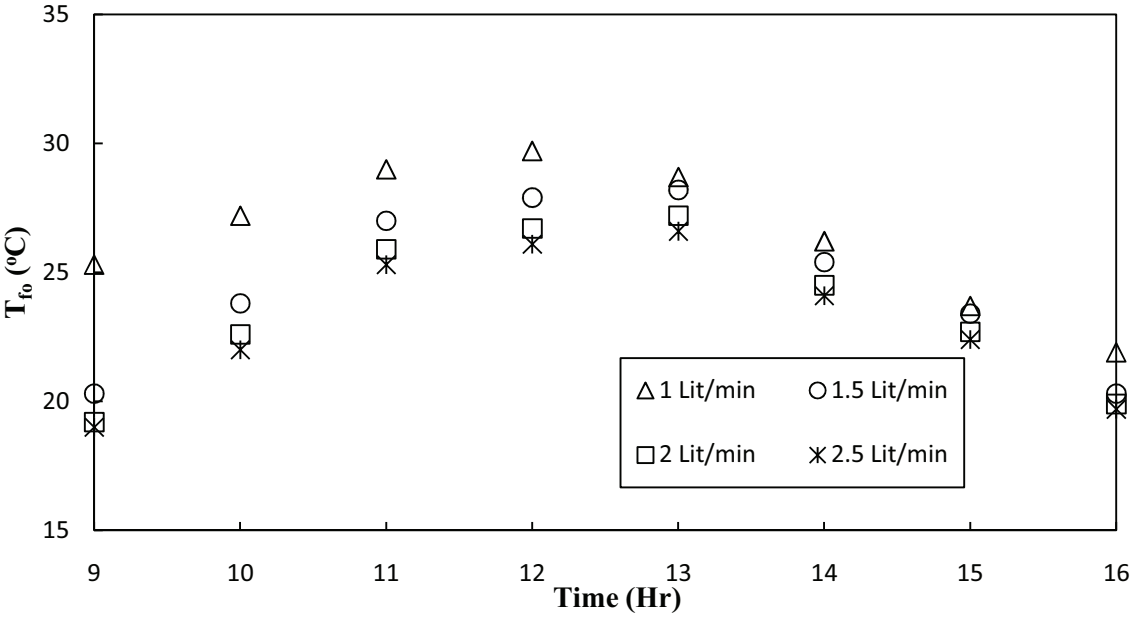

Figure 5.23: Variation of outlet water temperature throughout the day at different flow rates.

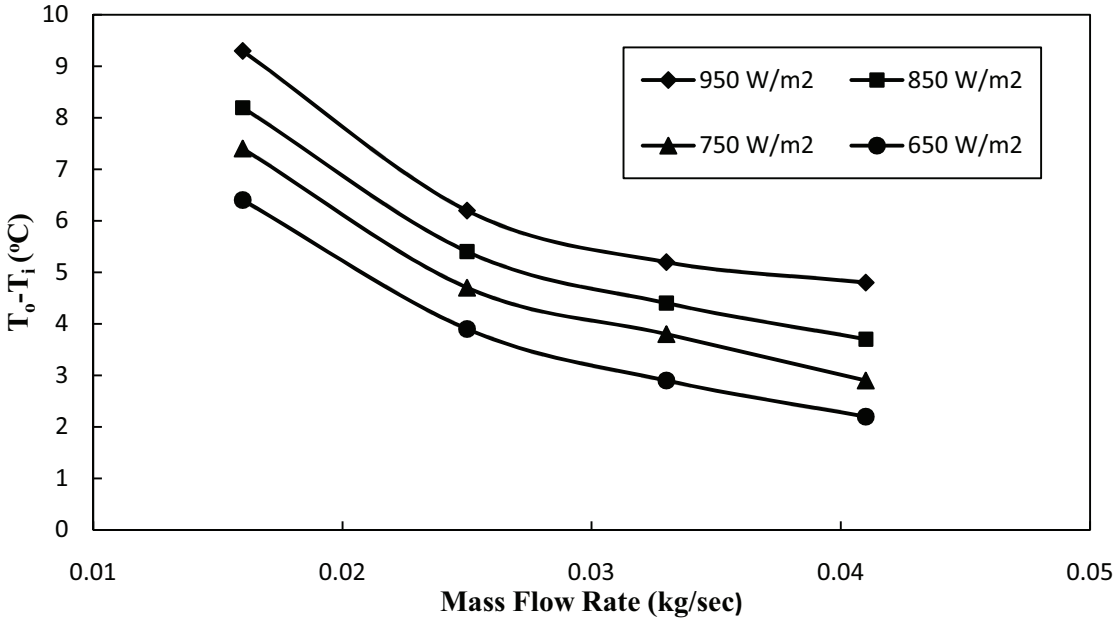

Figure 5.24: The Effect of mass flow rate on water temperature rise at different levels of irradiance

5.4 Validation

5.4.1 Air cooled model

This section presents the results of air cooled model validated with the data available in the literature. Further, to compare the results, a correlation coefficient (*r*) and root mean square percent deviation (*e*) given by Eqns.5.1 and 5.2 have been evaluated and depicted in the figures as well.

Fig 5.25 shows the variation of solar irradiance, ambient temperature and the inlet fluid temperature throughout the day [41].

Fig. 5.26 shows the experimental and numerical results of maximum power output throughout the day. The experimental results show that the maximum power attained is around 85W, whereas the numerical results predict it to be around 95W. A good agreement between the computed results and experimental data is obtained with correlation coefficient, r = 0.98 and root mean square percent deviation, e = 12.4% is obtained.

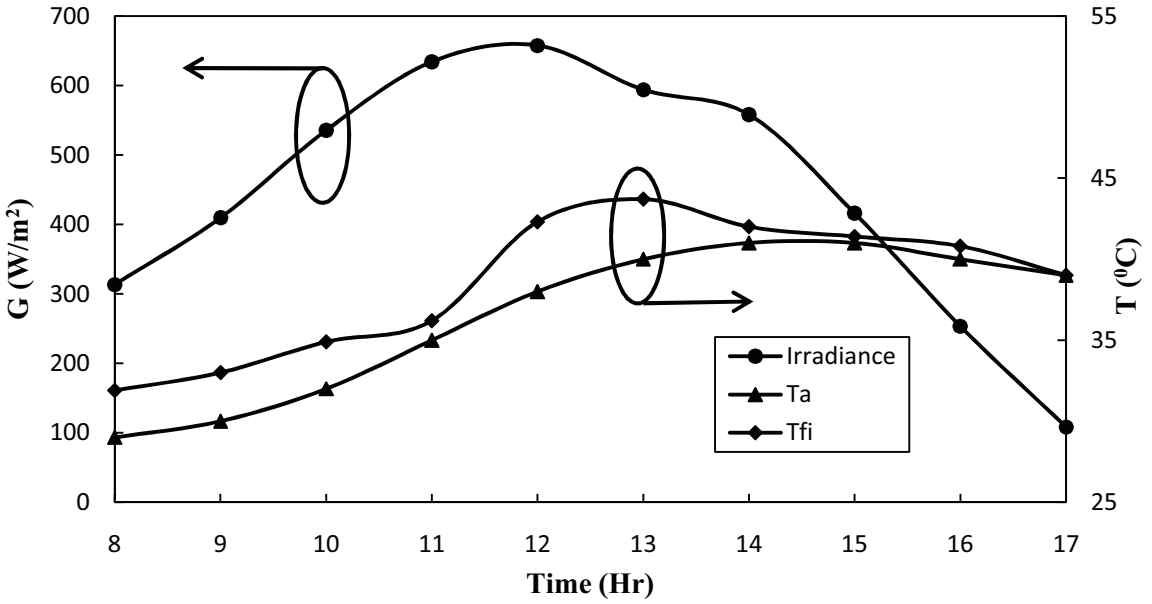

Figure 5.25: Hourly variations of irradiance, ambient and inlet air temperature during the test day [41].

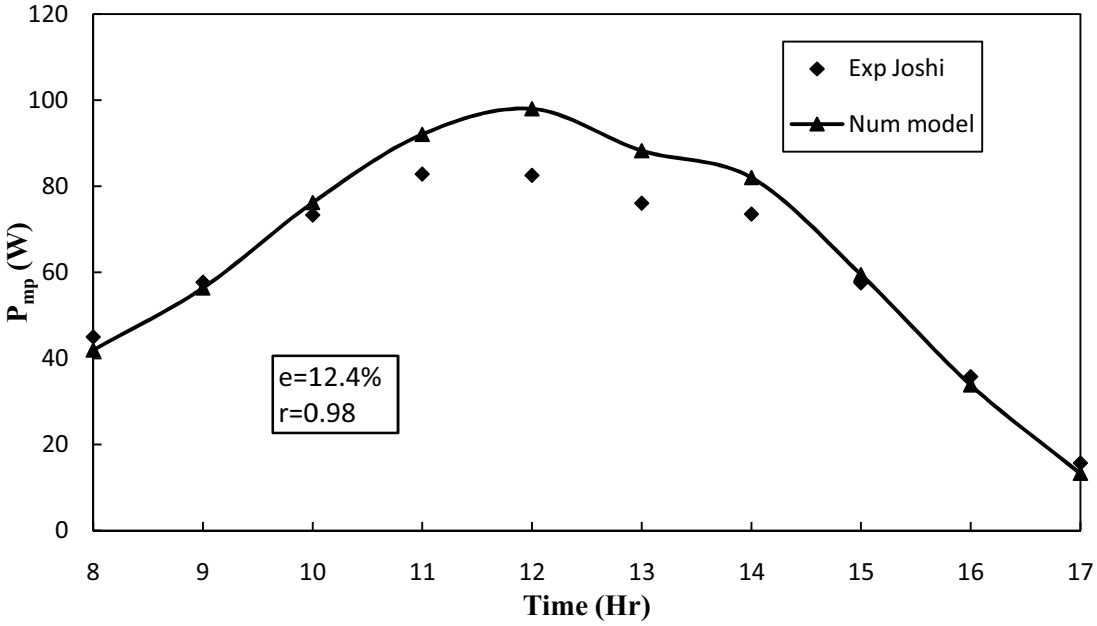

Figure 5.26: Experimental Validation of hourly variation of power output with PV air cooled model

The numerical and experimental results of the cell temperature, back surface temperature and outlet air temperature of joshi et al. [41] are compared with the results of the present model in Figs.5.27, 5.28 and 5.29 respectively. From the figure it is observed that the present model predicts the results more accurately than the model developed by [41], which over predicts the experimental data.

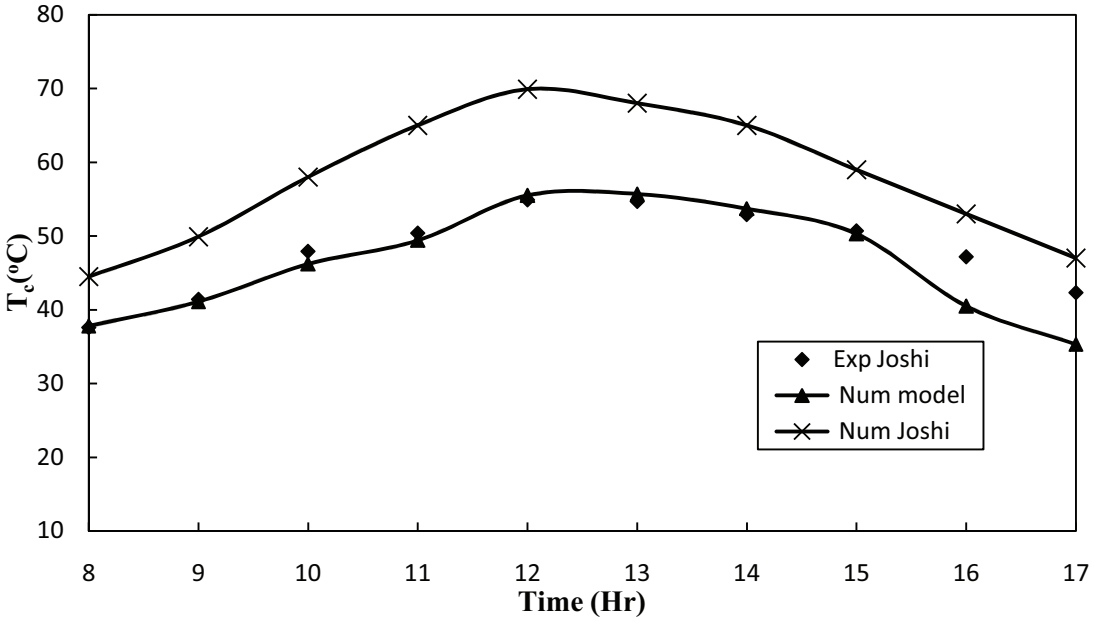

Figure 5.27: Experimental Validation of hourly variation of cell temperature with PV air cooled model

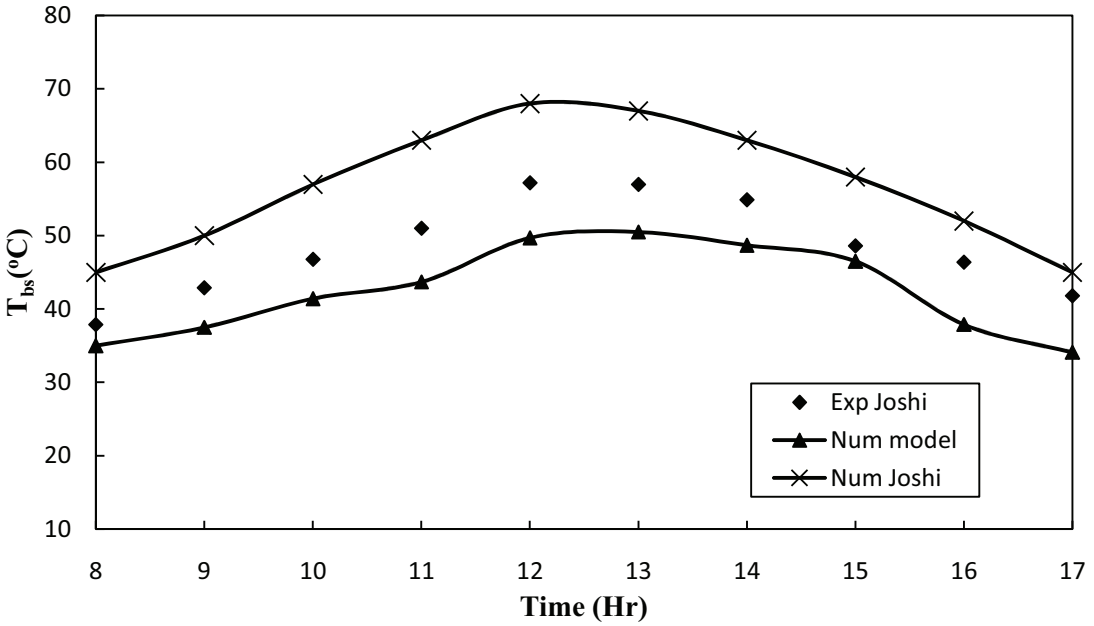

Figure 5.28: Experimental Validation of hourly variation of back surface temperature with PV air cooled model

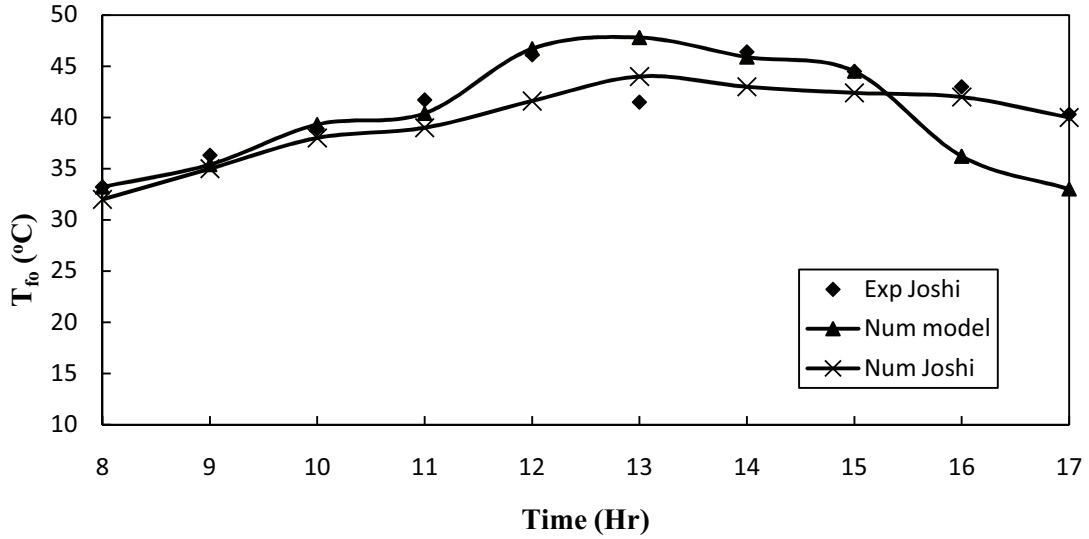

Figure 5.29: Experimental Validation of hourly variation of outlet air temperature with PV air cooled model

Fig. 5.30 shows the comparison of present numerical model and experimental results of maximum power point efficiency throughout the day. A good agreement with correlation coefficient, r = 0.98 and root mean square percent deviation, e = 8.26% is obtained.

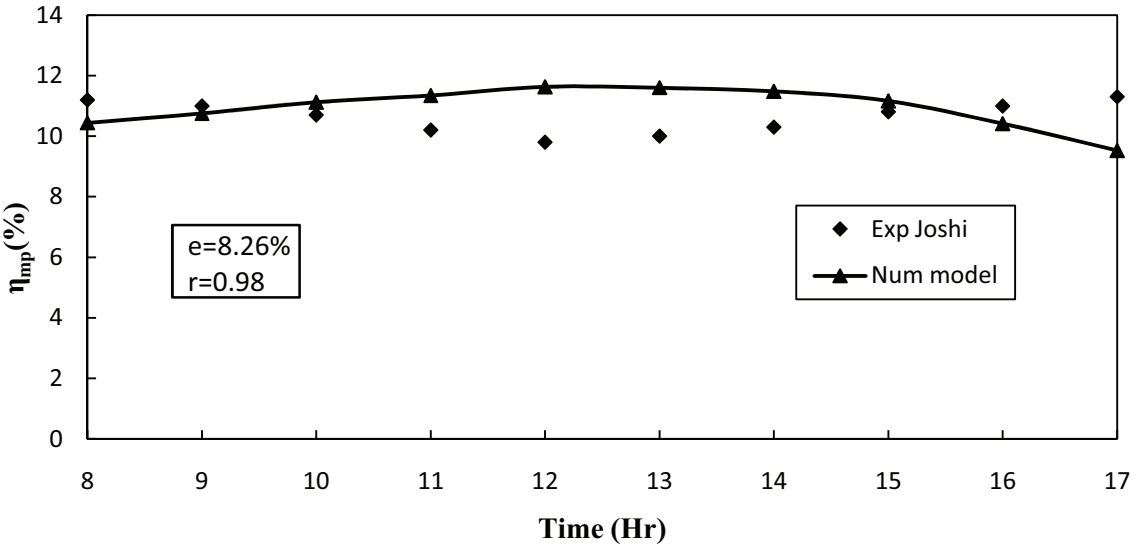

Figure 5.30: Experimental Validation of hourly variation of maximum power point efficiency with PV air cooled model

5.4.2 Water cooled model

The numerical results obtained from the water cooled model are validated with the experimental data from the tests conducted at KFUPM in the month of Feb. 2012. Further, to compare the results, a correlation coefficient (*r*) and root mean square percent deviation (*e*) has been evaluated by the following equations. and depicted in the figures as well. The variation of irradiance received by the panel surface during the test day is shown in Fig. 5.31. Maximum value of radiation received is 979 W/m^2 at 11 am whereas the average radiation throughout the day was 710 W/m^2. The weather data which includes the ambient temperature is also shown in the same figure. Maximum ambient temperature is found to be 21^0C at noon time and the average temperature throughout the day was 20^0C.

Increase in the PV module temperature inversely affects the power output. The increase in the module temperature above the ambient temperature initiates the process of heat loss from the module through the mechanisms (conduction, convection and radiation) and results in a decrease of output voltage. The variation of module surface temperatures (front and back) and the wind speed during the test day is shown in Fig.5.32. The maximum module temperatures (front and back) were found to be 45^oC and 42.8^oC at noon time. The average wind speed throughout the test day was 1.5 m/s.

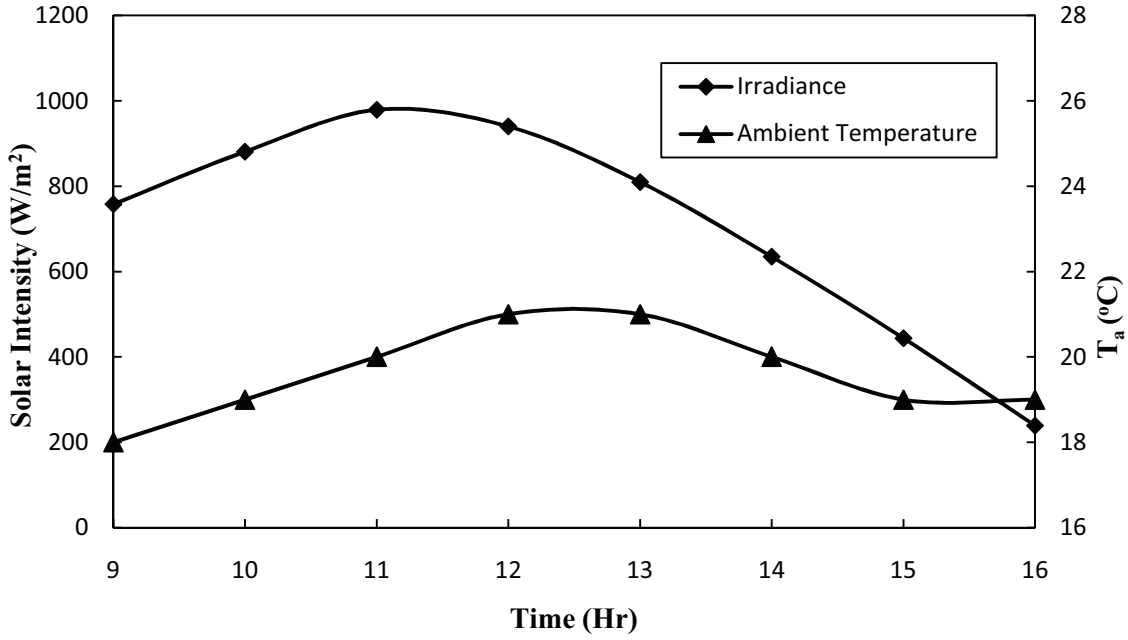

Figure 5.31: Hourly variation of irradiance and ambient temperature during the test day (08-02-12).

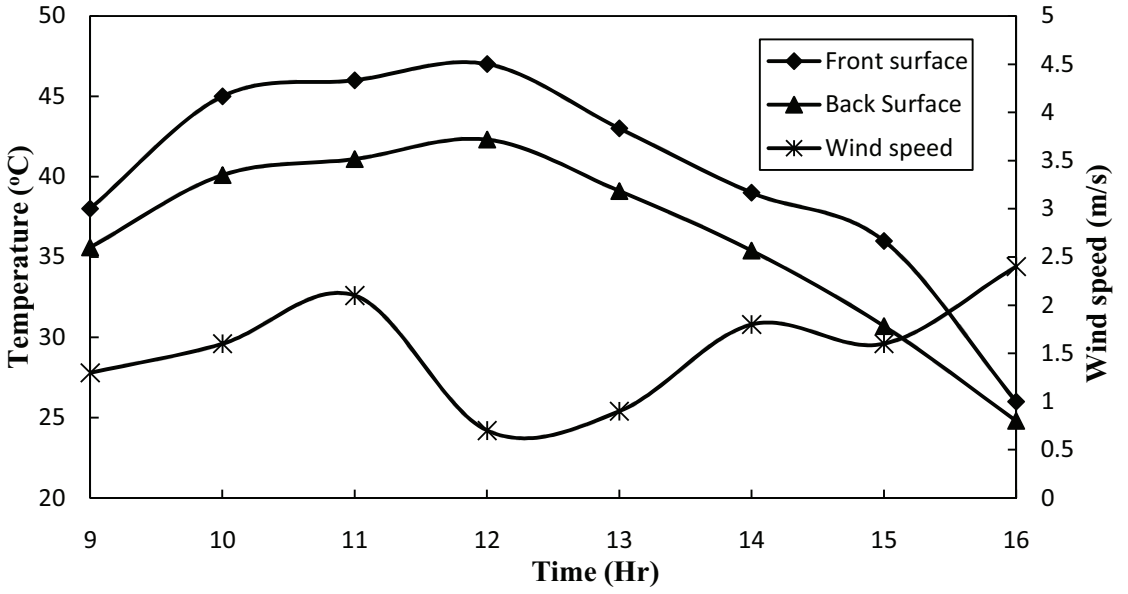

Figure 5.32: Hourly variation of module temperatures (front and back) and wind speed during the test day (08-02-12).

Fig. 5.33 and 5.34 shows the comparison of numerical and experimental result for the module front surface and back surface temperatures throughout the day. The measured surface temperature shown in the figures is the average temperature of 5 thermocouples each at front and back. From Fig. 5.33, a fair agreement between the numerical and experimental results with correlation coefficient, r = 0.98 and root mean square percent deviation, e = 5.43% is obtained. From Fig. 5.34, a fair agreement with correlation coefficient, r = 0.98 and root mean square percent deviation, e = 7.4% is obtained.

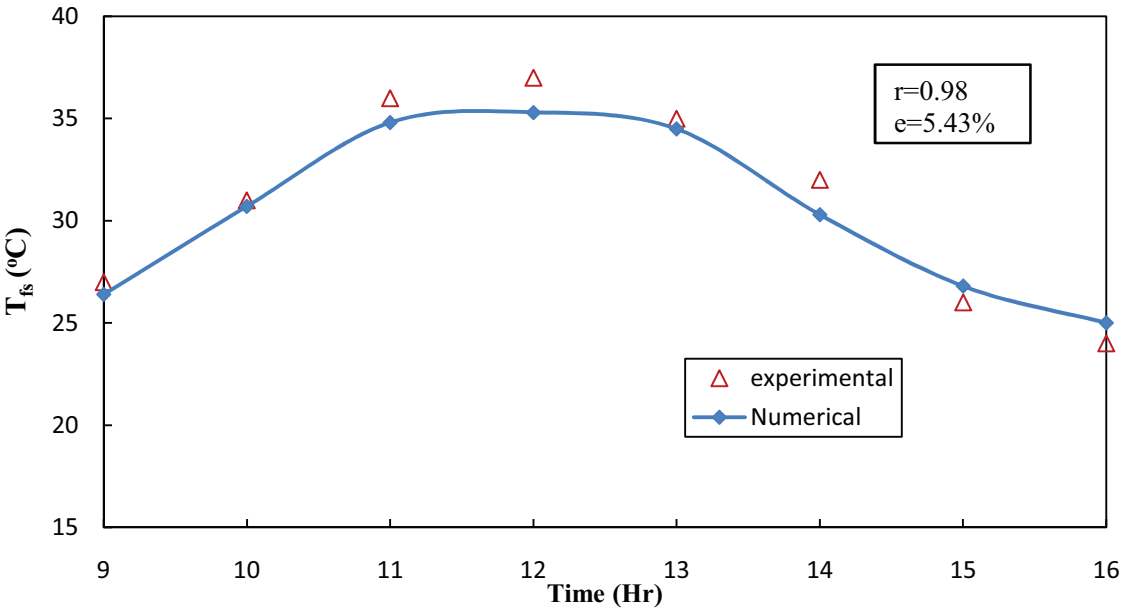

Figure 5.33: Comparison of numerical and experimental data for module surface temperature with water cooling.

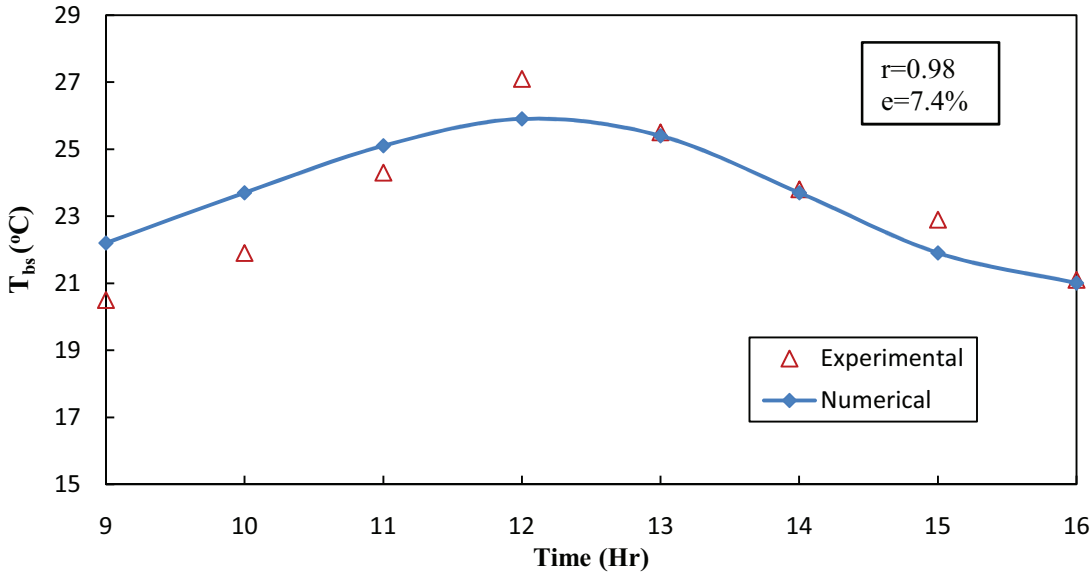

Figure 5.34: Comparison of numerical and experimental data for back surface temperature with water cooling.

Figure 5.35 presents the numerical and experimental results of outlet fluid temperature throughout the test day. Maximum water temperature recorded is 30^0 C around noon time and a good agreement with the numerical results (correlation coefficient, r = 0.99 and root mean square percent deviation, e = 4.56%) is obtained.

Figure 5.36 shows the thermal gain captured throughout the day. Thermal energy output is defined as the increase in the internal energy of the water running over the panel due to the increase in the temperature of the water. Due to high specific heat of water the temperature increase is quite a bit. As the outlet water temperature increases the thermal gain also increases. A fair agreement between the numerical and experimental results (correlation coefficient, r = 0.98 and root mean square percent deviation, e = 6.1%) is obtained.

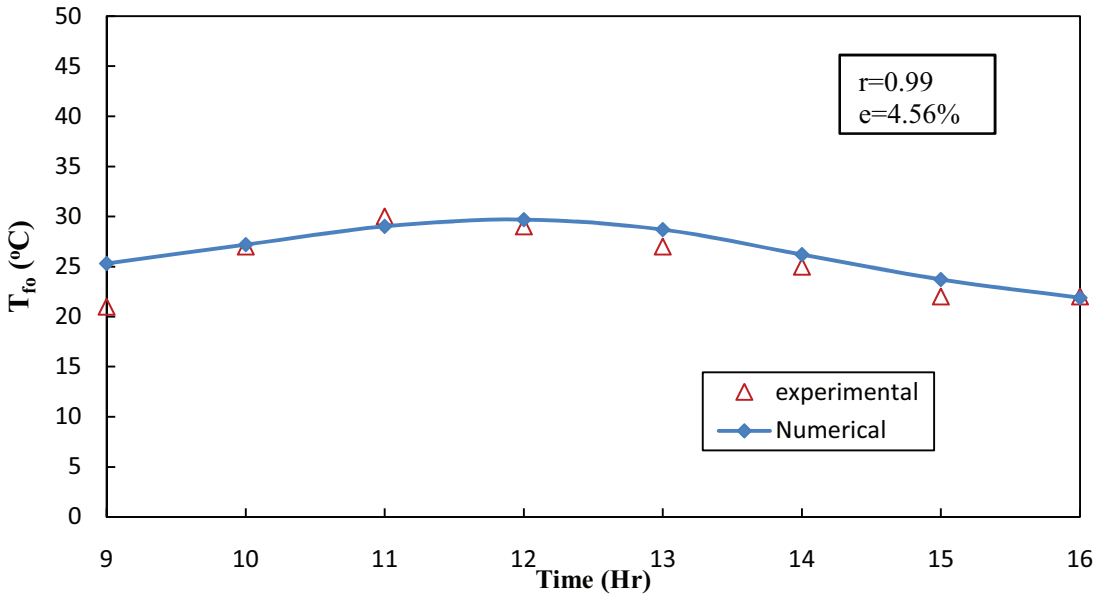

Figure 5.35: Comparison of numerical and experimental data for water outlet temperature.

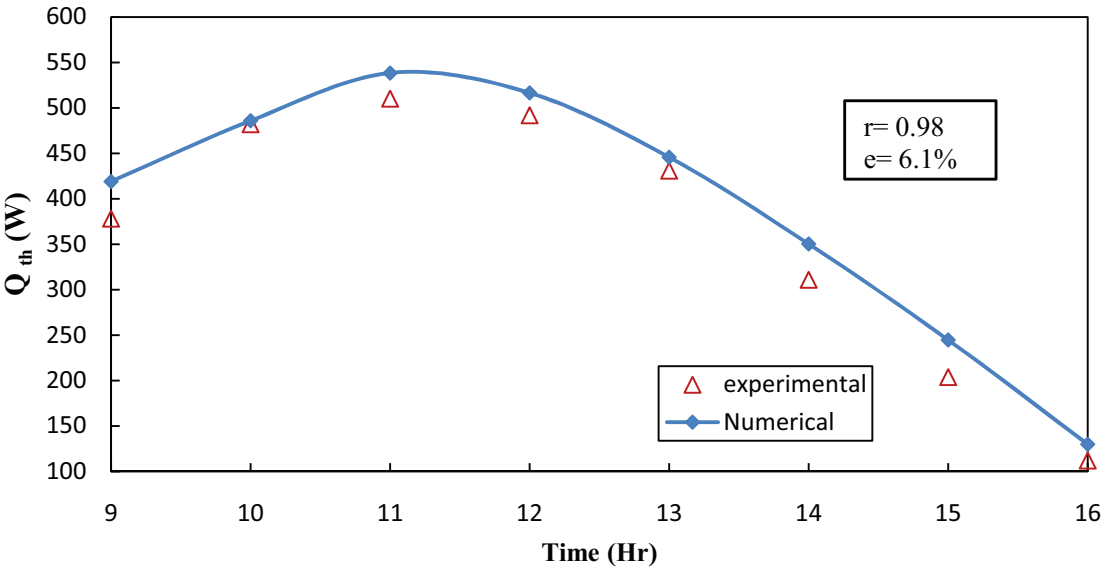

Figure 5.36: Comparison of numerical and experimental data for thermal gain with water cooling.

Figs. 5.37 and 5.38 show the comparison of numerical and experimental results of maximum power and efficiency. The measured power output fairly matches with the numerical result (correlation coefficient, r = 0.99 and root mean square percent deviation, e = 4.1%) and maximum power point efficiency as well with correlation coefficient, r = 0.98 and root mean square percent deviation, e = 5.2%.

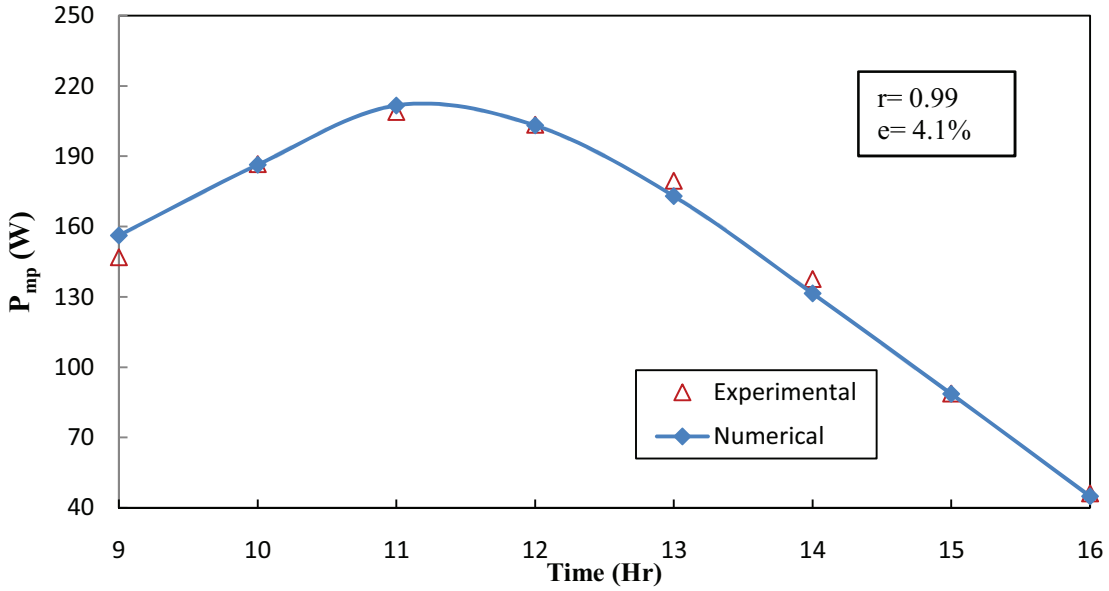

Figure 5.37: Comparison of numerical and experimental data for maximum power output with water cooling.

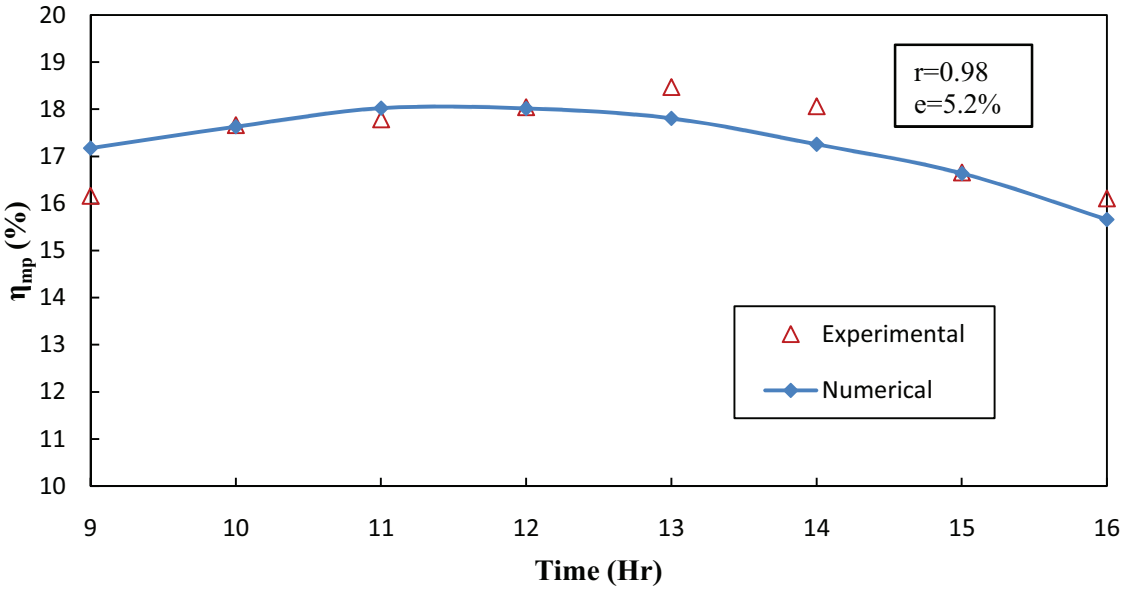

Figure 5.38: Comparison of numerical and experimental data of maximum power point efficiency.

5.4.3 PV Water Cooling: Numerical Results:

In this section, the results from the developed water cooled model in EES software using the specifications of PV module (Table 2) are shown. The impact of water cooling on cell temperature throughout the day is shown in Fig.5.39. The variation of cell temperature for cooling and non-cooling case is presented and average cell temperatures for cooling and non-cooling case are 30.5 ^{0}C and 37.8 ^{0}C. Cooling the module resulted in the reduction of the cell temperature by 19.3%. The variation of back surface temperature throughout the day for the cases mentioned above is presented in Fig.5.40. The maximum temperature for cooling and non-cooling case was 25.9 ^{0}C and 42.8 ^{0}C. The percentage reduction observed in the back surface temperature by employing the cooling technique

was 34%. Since the cooling panel is attached to the rear surface of the module, maximum amount of thermal gain is achieved and hence resulted in a reduced back surface temperature.

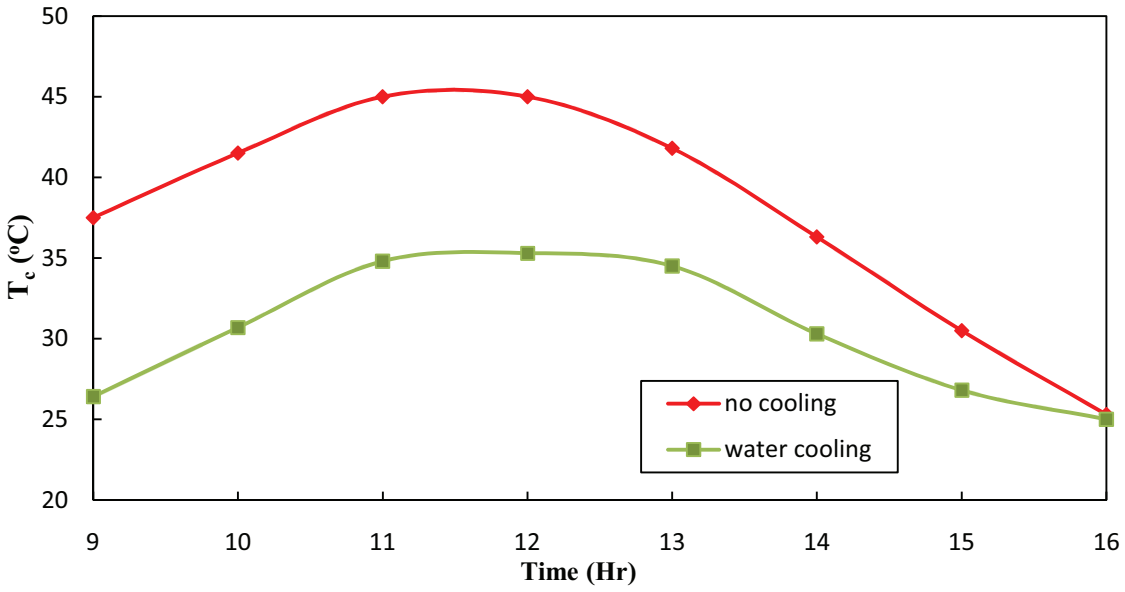

Figure 5.39: Comparison of cell temperature throughout the day with cooling and without cooling.

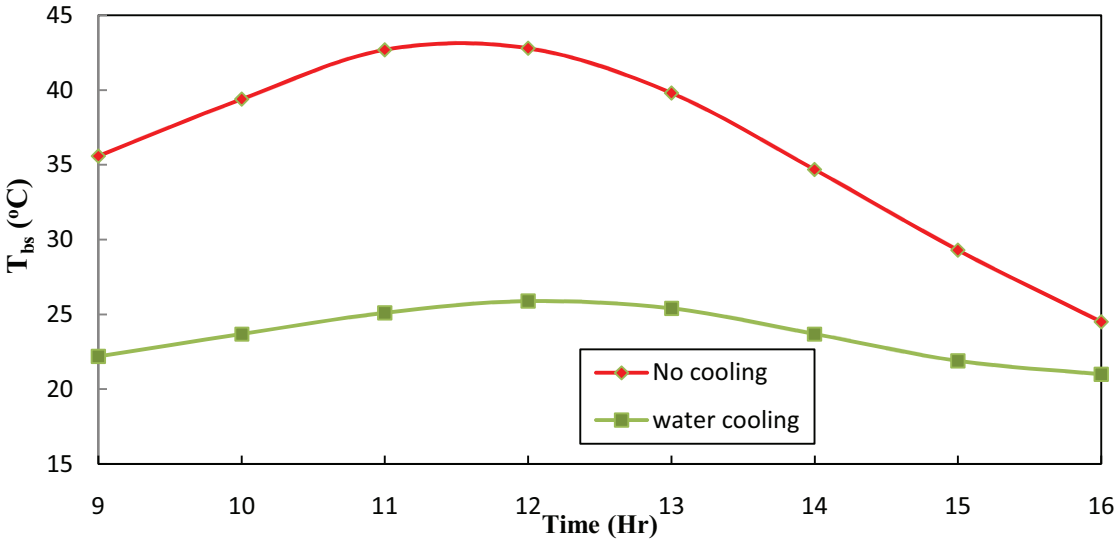

Figure 5.40: Comparison of module back surface temperature throughout the day with cooling and without cooling.

The maximum power output from the panel varies with the intensity of the solar irradiance and the temperature of the cell. The output of a PV module also depends on the number of cells in the module, the type of cells, and the total surface area of the cells. All modules are rated by manufacturers in terms of their peak power (Wp) under standard test conditions: i.e. (Irradiance of 1000 W/m²; air mass of 1.5 and cell temperature 25 ºC). Modules nearly always produce less than their rated peak power in real-life conditions. The output varies depending upon: the amount of solar radiation; the temperature of the module (output decreases as temperature rises); the voltage at which the load (or battery) is drawing power from the module. The comparison of electrical power output of the panel for the two cases are throughout the test day is shown in Fig.5.41. The maximum value of power output of the module for non-cooling case is 185 W at 11am whereas the

maximum power output with cooling is 211 W. An average increase of 10% in the power output of the module was observed in the case of cooling.

The efficiency of the module is a major factor in the PV performance. The conversion efficiency is the percentage of incident solar energy that a PV module converts to electricity. Fig. 5.42 shows the hourly variation of electrical (MPP) efficiency during the test day. As seen from the figure, a significant increase in the efficiency is observed with water cooling. The maximum value of efficiency without cooling is 15.8% observed at 9 am whereas in the case of cooling the maximum value is 18% at 11am. The temperature reduction has caused a noticeable improvement in electrical efficiency in Fig. 5.42. With active cooling, the increase in the electrical energy yield over the day was 9%.

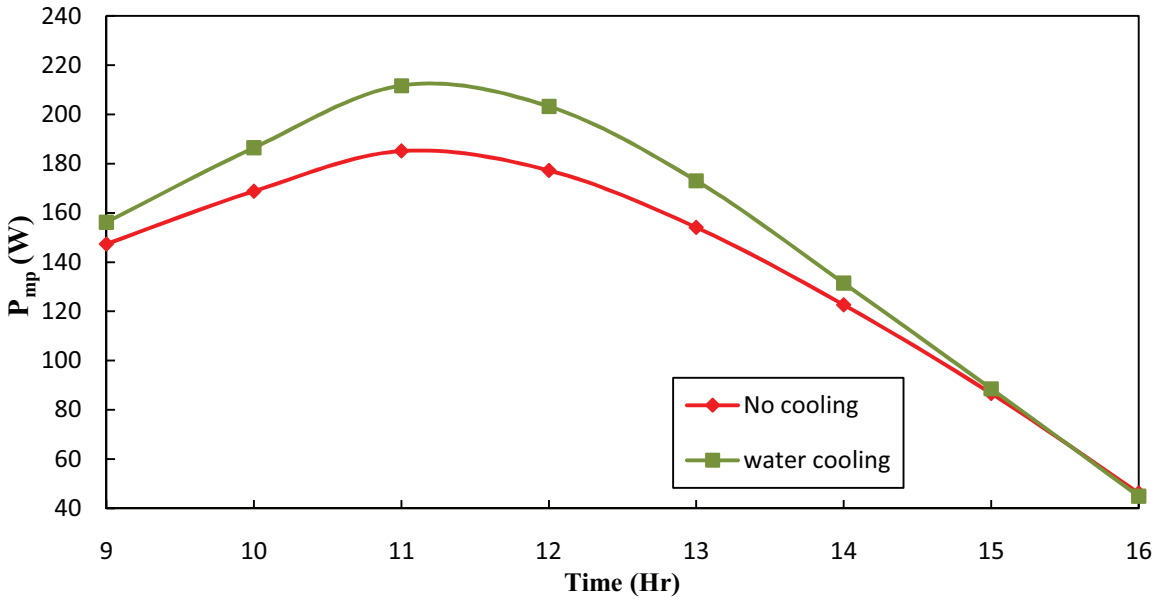

Figure 5.41: Comparison of maximum power output of the module throughout the day with cooling and without cooling.

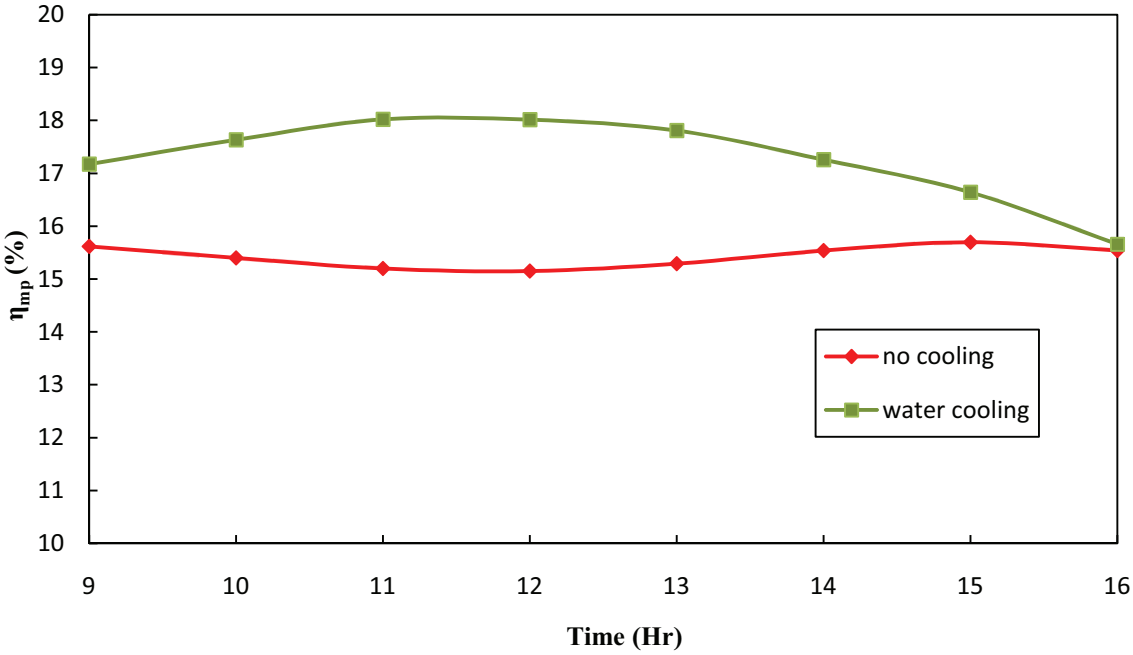

Figure 5.42: Comparison of maximum power point efficiency throughout the day with cooling and without cooling.

CHAPTER 6

CONCLUSION AND FUTURE WORK

This chapter of the thesis discusses the conclusions of the study and the results presented in the previous chapter. In the last section, some of the directions in which this thesis work can be extended are discussed.

All the objectives mention in this thesis have been achieved successfully. The first task was to develop an electrical model which could predict the performance parameters of the PV module with climatic and manufacturers data provided. The program was developed using the engineering equation solver (EES) software. The results of the numerical data have also been validated with the experimental tests conducted at KFUPM campus and a good agreement between them was achieved. The developed model is very much capable of predicting the output parameters such as cell temperature, maximum power point current, voltage, power and efficiency. The following conclusions were drawn after this study.

Increase in the solar irradiance provides higher power output but at the cost of reduction in the module efficiency. Absorption of solar radiation increases the temperature of PV cells resulting in a drop of electrical efficiency.

To increase the operating electrical efficiency of PV systems, an obvious method is to cool (in the form of air cooling and water cooling) the temperature of the cells by incorporating a cooling mechanism. There has been considerable amount of research in this area by employing cooling ducts to the system as well as by creating hybrid PV and thermal (PV/T) systems, which could produce hot water in addition to electricity. In both cases, a heat carrier fluid would remove the heat from the cells thus cooling them and allowing their electrical efficiency to increase.

The second task to develop an air cooled and water cooled thermal model which aimed at improving the performance of the PV system. The two models were developed by coupling the electrical model with the thermal model using EES software. Various thermal performance parameters such as thermal gain and thermal efficiency are shown in the previous chapter.

The third task was to experimentally analyze the performance of a PV system integrated with a water cooling system. The experimental results of with cooling and without cooling are also presented in section 5.3 in the previous chapter. A considerable improvement in the performance of the PV system was obtained when integrated with the cooling mechanism. An increase in power output with reduced cell temperature was achieved and an additional thermal gain which can be utilized for domestic applications as well.

6.1 Future Work

The direction in which this study can be extended further is discussed in this section. The main focus was aimed at reducing the cell temperature which plays a major role in PV system performance.

Another technology utilized to capture solar energy is the concentrator technique. Concentrated solar power (CSP) systems use mirrors or lenses to concentrate a large amount of sunlight onto a small area. One measure of the effectiveness of this approach is the concentration ratio which relates on the amount of concentration a cell receives. Concentrator PV systems have many advantages over flat-plate systems as they reduce the size or number of cells needed and allow certain designs to use more expensive semiconductor materials which would otherwise be cost prohibitive. The reflectors which are placed beside the PV panel focus the solar radiation on the panel with multiple reflections and hence raise the cell temperature significantly. The cooling mechanism will be beneficial in this study since more irradiance gets concentrated at panel surface area.

High concentration ratios also have heating problem. Therefore, the cells must be kept cool in a concentrator system, requiring sophisticated heat sync cooling designs.

REFERENCES

[1] http://www.publicagenda.org/whoturnedoutthelights/world-energy-demand

[2] http://www.onlinemarketing-trends.com/2011/02/world-energy-trend-and-projections.html

[3] http://www.arab.de/arabinfo/saudi.htm

[4] http://photovoltaics.sandia.gov/docs/PVFEffIntroduction.htm

[5] http://www.energydigital.com/renewable_energy/global-pv-installations-reports-2011s-leaders

[6] http://www.esru.strath.ac.uk/Courseware/Solar_energy/index.htm

[7] http://en.wikipedia.org/wiki/Solar_cell

[8] Brano VL, Orioli A, Ciulla G, Gangi AD. An improved five-parameter model for photovoltaic modules. Solar Energy Materials and Solar Cells 2010; 94(8):1358-70.

[9] Ahmad GE, Hussein, HMS, El-Ghetany, HH. Theoretical analysis and experimental verification of PV modules. Renewable Energy 2003;28(8):1159-68.

[10] Ikegami T, Maezono T, Nakanishi F, Yamagata Y, Ebihara K. Estimation of equivalent circuit parameters of PV module and its application to optimal operation of PV system. Solar Energy Materials and Solar Cells 2001;67(1-4):389-95.

[11] Kurnik J, Jankovec M, Brecl K, Topic M. Outdoor testing of PV module temperature and performance under different mounting and operational conditions. Solar Energy Materials and Solar Cells 2011;95(1):373-76.

[12] Carr AJ, Pryor TL. A comparison of the performance of different PV module types in temperate climates. Solar Energy 2001;76(1-3):285-94.

[13] Wang JC, Su YL, Shieh JC, Jiang J.A. High-accuracy maximum power point estimation for photovoltaic arrays. Solar Energy Materials and Solar Cells 2011;95(3):843-51.

[14] Alonso MC, Balenzategui JL. Estimation of photovoltaic module yearly temperature and performance based on Nominal Operation Cell Temperature calculations. Renewable Energy 2004;29(12):1997-2010.

[15] Gxasheka AR, Van Dyk EE, Meyer EL. Evaluation of performance parameters of PV modules deployed outdoors. Renewable Energy 2005;30(4):611-20.

[16] Villalva MG, Gazoli JR, and Filho ER. Comprehensive Approach to Modeling and Simulation of Photovoltaic Arrays. IEEE TRANSACTIONS ON POWER ELECTRONICS, 2009;24(5):1198-1208.

[17] Houssamo I, Sechilariu M, Locment F, Friedrich G. Identification of photovoltaic Array Model Parameters. Modelling and Experimental Verification. International Conference on Renewable Energies and Power Quality (ICREPQ'10) Granada,Spain. 23rd to 25th March 2010.

[18] De Soto W, Klein SA, Beckman WA. Improvement and validation of a model for photovoltaic array performance. Solar energy 2006;80:78–88.

[19] Ishaque K and Salam Z. An improved modeling method to determine the model parameters of photovoltaic (PV) modules using differential evolution (DE). Solar energy 2011;85:2349–2359.

[20] Feng H and Liang H. Implementation and verification of integrated thermal and electrical models for commercial PV modules. Solar Energy 2012;86:654–665.

[21] Zagrouba M, Sellami A, Bouaicha M and Ksouri M. Identification of PV solar cells and modules parameters using the genetic algorithms: Application to maximum power extraction. Solar Energy 2010;84:860–866.

[22] Firtha SK, Lomas KJ, Rees SJ. A simple model of PV system performance and its use in fault detection. Solar Energy 2010;84:624–635.

[23] Huld T, Friesen G, Skoczek A, Kenny R, Sample T, Field M and Dunlop DE. A power-rating model for crystalline silicon PV modules. Solar Energy Materials & Solar Cells 2011;95:3359–3369.

[24] Chena W, Shenc H, Shuc B, Qind H and Deng T. Evaluation of performance of MPPT devices in PV systems with storage batteries. Renewable Energy 2007; 32:1611–1622.

[25] Skoplaki E and Palyvos JA. Operating temperature of photovoltaic modules: A survey of pertinent correlations. Renewable Energy 2009;34:23–29.

[26] Tonui JK and Tripanagnostopoulos Y. Performance improvement of PV/T solar collector with natural air flow operation, Solar Energy 2008,82:1-12.

[27] Brinkworth BJ and Sanderberg M. Design procedure for cooling ducts to minimize efficiency loss due to temperature rise in PV arrays, Solar Energy 2006, 80:89- 103.

[28] Kumar R and Rosen M. A critical review of photovoltaic–thermal solar collectors for air heating, Applied Energy 2011,88:3603–3614.

[29] Zogou O and Stapountzis H. Flow and heat transfer inside a PV/T collector for building application, Applied Energy 2012,91: 103–115.

[30] Amori KE and Taqi HMN. Analysis of thermal and electrical performance of a hybrid (PV/T) air based solar collector for Iraq, Applied Energy 2012;98;384-395.

[31] Hegazy AA. Comparative study of the performances of four solar air PV/T collectors, Energy Conversion &Management 2000;41:861-881.

[32] Sopian K, Liu HT, Kakac S, Veziroglu TN. Performance of a double pass photovoltaic Thermal solar collector suitable for solar drying systems, Energy Conversion & Management 2000;41:353-365.

[33] Zondag HA, de Vries DW, van Helden WGJ, van Zolingen RJC and van Steenhoven, AA. The thermal and Electrical yield of a PV/T collector. Solar energy 2002;72:113-128.

[34] Chow TT. A review on PV/T thermal hybrid solar technology, Applied Energy 2010;87:365-379.

[35] Aste N, Chiesa G and Verri F. Design, development and performance monitoring of a photovoltaic-thermal (PVT) air collector, Renewable Energy 2008;33:914–927.

[36] Jong MJM and Zondag HA. System studies on combined PV/T thermal panels. 9th International conference on solar energy in high latitudes, Northsun, , Leiden, Netherlands. 6th -8th May 2001.

[37] Tiwari A and Sodha MS. Parametric study of various hybrid PV/thermal air collector: Experimental validation of theoretical model, Solar Energy material & Solar Cells 2007;91:17-28.

[38] Garg HP and Adhikari RS. System performance studies on photovoltaic/thermal (PV/T) air heating collector, Renewable Energy 1999;16:725-730.

[39] Dubey S, Sandhu GS and Tiwari GN. Analytical expression for electrical efficiency of PV/T hybrid air collector, Applied Energy 2009;86:697-705.

[40] Tonui JK, Tripanagnostopoulos Y. Air-cooled PV/T solar collectors with low cost performance improvements. Solar Energy 2007;81:498-511.

[41] Joshi AS, Tiwari A, Tiwari GN, Dincer I, Reddy BV. Performance evaluation of a hybrid photovoltaic thermal (PV/T) (glass-to-glass) system, International Journal of Thermal Science 2009;48:154-164.

[42] Tripanagnostopoulos Y, Nousia TH, Souliotis M and Yianoulis P. Hybrid Photovoltaic/Thermal Solar Systems, Solar Energy 2002;72:217-234.

[43] Tripanagnostopoulos Y, Aspects and improvements of hybrid PV/T solar energy systems, Solar Energy 2007;81:1117-1131.

[44] Sarhaddi F, Farahat S, Ajam H, Behzadmehr A, Mahdavi Adeli M, An improved thermal and electrical model for a solar photovoltaic thermal (PV/T) air collector, Applied Energy 2010;87:2328-2339.

[45] Alonso GMC, Balenzategui JL, Estimation of photovoltaic module early temperature and performance based on Nominal Operation Cell Temperature Calculations, Renewable Energy 2004;29:1997-2010.

[46] Armstrong S and Hurley W.G. A thermal model for photovoltaic panels under varying atmospheric conditions. Applied Thermal Engineering 2010;30(11-12):1488-1495.

[47] Teo HG,. Lee PS, Hawlader MNA. An active cooling system for photovoltaic modules. Applied Energy 2012;90:309–315.

[48] Tiwari A, Dubey S, Sandhu GS, Sodha MS and Anwar SI. Exergy analysis of integrated photovoltaic thermal Solar water heater under constant flow rate and constant collection temperature modes, Applied Energy 2009;86(5):2592–2597.

[49] Chow TT, Pei G, Fong KF, Lin Z, Chan ALS, Ji J. Energy and Exergy analysis of Photovoltaic-thermal collector with and without glass cover. Applied Energy 2009; 86(3):310-316.

[50] Kaora F and Yutaka. Performance Evaluation of Photovoltaic Power-Generation System Equipped With a Cooling Device Utilizing Siphonage, Journal of Solar Energy Engineering 2006;128:146-151.

[51] Tiwari A, Sodha MS. Performance evaluation of solar photovoltaic/thermal system: An experimental validation. Solar energy 2006;80:751-759.

[52] Huang BJ, Lin TH, Hung WC, Sun FS, Performance evaluation of solar photovoltraic/thermal systems. Solar energy 2001;70:443-448.

[53] Dubey S, Tiwari GN, Thermal modeling of a combined system of PV/T solar water heater. Solar energy 2008;82:602-612.

[54] Krauter S. Increased electrical yield via water flow over the front of photovoltaic panels. Solar Energy Materials & Solar Cells 2004;82:131–137.

[55] Saad O and Masud B. Improving Photovoltaic Module Efficiency Using Water Cooling. Heat Transfer Engineering 2009;30(6):499–505.

[56] Kordzadeh A. The effects of nominal power of array and system head on the operation of photovoltaic water pumping set with array surface covered by a film of water. Renewable Energy 2010;35:1098–1102.

[57] Abdolzadeh M and Ameri M. Improving the effectiveness of a PV water pumping system by spraying water over the front of photovoltaic cells. Renewable Energy 2009;34:91–96.

[58] Rosa CM, Rosa CP, Tina GM, Scandura PF. Submerged photovoltaic solar panel: SP2. Renewable Energy 2010;35(8):1862-1865.

[59] Hosseini R, Hosseini N, Khorasanizadeh H, An experimental study of combining photovoltaic system with a heating system. World Renewable Energy Congress 2011 Sweden, 8-13th May 2011.

[60] King DL, Boyson WE, Kratochvil JA. Photovoltaic Array Performance Model. Sandia National Laboratories Report: SAND2004-3535.2004.

[61] Duffie JA, Beckman WA. Solar engineering of thermal processes.3rd ed. New York: John Wiley and Sons; 2006.

[62] Brinkworth BJ. Estimation of flow and heat transfer for the design of PV cooling ducts. Solar Energy 2000;69(5):413-420.

[63] http://www.sundrumsolar.com/SDM100/collectorassemblyguide

Vitae

Name : Abdul Subhan

Nationality : Indian

Date of Birth : 23/12/1987

E-mail : nadeemkfupm@gmail.com

Address : H.No:16-2-41/9, Akber Bagh, New Malakpet, Hyderabad, A.P, India, Pin 500036.

Telephone : 0091-40-24553875 (India)

: 0536344315 (Saudi)

Academic Background: Received Bachelor of Engineering degree in Mechanical Engineering from Muffakham Jah College of Engineering & Technology, Affiliated to Osmania University, Hyderabad, India in 2009. Joined Mechanical Engineering Department of King Fahd University of Petroleum and Minerals, Dhahran as Research Assistant in September 2009-present.